Height variation in the canine species as a model to identify new targets in bone regenerative medicine.

Michelle Teunissen
Honours Programma 2012/2013

Supervisors: Dr. Marianna Tryfonidou
Frank Riemers

16-10-2013

Table of contents

Chapter 1: Aim and Scope of the project

Introduction

Bone formation is a complicated process orchestrated by systemic and local factors that instruct the progenitor cells to differentiate towards the osteogenic lineage and produce bone. It is therefore not surprising that, despite the many developments in the field of bone regenerative medicines, there are still many challenges left in the treatment of large bone defects or complicated fractures. At this moment, the state of the art treatment is the use of autologous bone grafts. [1] However as this treatment entails many disadvantages, such as donor tissue availability and rejection, searches for alternative treatments are still going on. An alternative treatment of large bone defects may be found in the natural healing process of these defects, which heal by endochondral bone formation. At this moment, mesenchymal stem cells (MSCs) and growth factors, for example bone morphogenic protein 2 (BMP-2), are used to enhance fracture healing. However, the outcome of these treatments was often comparable to the outcome of treatment of the bone defect with bone grafts.[2] In these experiments, the MSCs were often induced towards the osteogenic lineage. Osteoblasts have a high oxygen demand and because the center of large bone defects is often poorly vascularized, necrosis of the osteoblasts in this area may occur, resulting in a poor outcome. MSCs can also produce bone by endochondral bone formation, a process involving differentiation of MSCs into chondrocytes. Chondrocytes produce cartilage that is subsequently substituted by bone (secondary bone healing). Chondrocytes demand less oxygen to proliferate and produce matrix and hence enhancing endochondral bone formation could give leads to new bone regenerative strategies.

Aim

The aim of this project was to study the local pathways that enhance endochondral bone formation in order to find new bone regenerative strategies. This project is embedded in the Tissue repair group of the Growth & Differentiation research focus area of Utrecht University and is being funded by the AO Foundation. The naturally occurring height variation in the canine species is an appropriate model to study the pathways influencing the pace of endochondral bone formation. In order to identify candidate targets for future regenerative strategies, the following questions were addressed:

Q1a: Which systemic and local pathways influence endochondral bone formation in a normal state (postnatal growth) and in a diseased state (fracture healing, bone defect) and how do they influence this process?

Q1b: Which pathways are differential regulated in small and large individuals?

Q1c: Is the height variation in the canine species an appropriate model to study pathways that enhance endochondral bone formation in order to translate new strategies in bone regenerative medicine?

These questions are being addressed by reviewing the literature regarding the different systemic and local pathways that influence endochondral bone formation in normal growth and fracture healing. Subsequently the phenomenon of variation in height was studied by reviewing GWAS and candidate-gene based approaches in order to investigate the pathways that are associated with height variation. Furthermore, a micro-array analysis was performed of the whole growth plate and adjacent bone of 5 great danes and miniature poodles in order to study the differential regulated genes in a large breed dog compared with a small breed dog. The results of this micro-array analysis were compared to the results of GWAS and candidate-gene based approaches and the current bone regenerative techniques to establish the suitability of employing canine height variation as a model in order to find new bone regenerative strategies.

In order to enable translation towards the clinics, the identified targets need to be evaluated in vitro followed by in vivo studies. Differentiation of MSCs towards osteoblast and chondrocytes is a suitable in vitro model to study the role of the identified targets. Since there are only limited reports on the characterization of canine MSCs, during the second part of the project the following question was addressed

Q2: How do MSCs differentiate towards the chondrogenic, osteogenic and adipogenic lineage following standard protocols?

For this purpose, canine bone marrow stem cells (BMSC's) and canine adipose-tissue derived stem cells (ASCs) were differentiated towards the three lineages; the adipogenic, osteogenic and chondrogenic lineage following standard protocols.

The results of these studies are discussed in the general discussion by addressing the different questions posed.

Chapter 2: Introduction into the systemic and local pathways regulating endochondral bone formation

Introduction

In the field of orthopedics, the restoration of large bone defects and treatment of complicated fracture healing, still represents a huge challenge. Large bone defects caused by extensive musculoskeletal trauma, resection of tumors or infected bone segments, are mostly treated with autografts, the state of the art treatment at this moment.[1] However, one major problem in large bone reconstructions is the generation of adequate blood supply, which is needed for the high oxygen demand of the osteoblasts. Due to the lag-time of vascularization of the large segments, hypoxia and nutrient deficiency occur within the cavity and result into decreased proliferation of the osteoblasts and into reduction of the quality and quantity of the matrix produced by the osteoblasts.[3] In addition, the quantity of available bone autograft tissue is limited in small patients.

Alternatives for autografts are allografts or xenografts.[1] The use of these therapies may solve the issues of limited graft tissue, but is hampered by graft rejection and does not address the problem of inadequate blood supply.

Naturally, bone defects heal secondary by endochondral bone formation, indicating that an alternative for bone grafts may be the use of mesenchymal stem cells (MSCs). MSCs can produce bone through the endochondral process by differentiating to chondrocytes. Because chondrocytes can withstand low oxygen tension, the use of MSC's provides an opportunity to overcome the obstacles of inadequate vascularization and the limited availability of graft tissue. [4] Bone regenerative strategies concentrate on the combination of MSC's, supportive scaffolds and growth factors to accelerate the process. Currently, members of the bone morphogenic proteins (BMPs) are already being used to enhance fracture healing in a clinical setting. [2] Although various animal and in vitro studies have demonstrated the positive effects of BMP, the results of clinical trials may not be as promising.[5] For example, the use of rBMP2 has been related to complications en BMP7 has been shown not to have an additive effect over autograft in achieving fusion of vertebrae (unpublished results).

Endochondral bone formation is also the process by which elongation of the long bone occurs. Developmental biology and fracture healing are being employed to identify new factors that have a significant biological role in the process of endochondral bone formation. A remarkable advantage of studying developmental biology is the variation in adult height, which in caused by diversity (a) in the pace of endochondral bone formation during postnatal growth between individuals and (b) in closure of the growth plate when skeletal maturation is

completed. Variation in height is a common phenomenon in many species, next to man. An immense intraspecies difference in adult height is observed within the canine species, which is an excellent opportunity to study the diversity in the pace of endochondral bone formation.

Fracture healing and endochondral bone formation

Normal fracture healing can occur by direct (primary) or indirect (secondary) bone healing. The first can only be achieved when the fracture edges are situated at a close distance from each other and the fracture is very stable. If this is not the case, the fracture will heal secondary by callus formation.
Secondary fracture healing is established by a combination of intramembranous and endochondral ossification and can be divided in four overlapping stages.

After bone fracture, a hematoma is formed due to rupture of the nearby vessels. This isolates the injury site from perfusion, leading to low oxygen tension and regional hypoxia.[6]Non-specific wound healing pathways are activated, initiating the inflammatory stage. [7] The hematoma is infiltrated by platelets, macrophages and other inflammatory cells that counter infection and secrete cytokines and growth factors. These cytokines (including IL-4 and -6 and TNF-α) and growth factors (including TGF-β and BMP) recruit additional inflammatory cells and facilitate the migration and invasion of MSCs. [78]

In the second phase, the soft callus is formed. The MSCs form condensations and differentiate to chondrocytes under the influence of SOX9, which is upregulated in the MSCs due to the low oxygen tension.[9] [10]. These chondrocytes, following the same path as chondrocytes in the growth plate, start proliferating and producing matrix. At a certain moment, proliferation ceases and the chondrocytes differentiate to a hypertrophic phenotype. At the end of the hypertrophic stage, the chondrocytes produce angiogenic factors, including VEGF, stimulating the invasion of blood vessels. The new vasculature ensures high oxygen tension and thereby supports differentiation of the MSCs towards osteoblasts. [7]

The replacement of cartilage by bone initiates the third phase. The hard callus, produced by the osteoblasts, consists of woven bone, which is irregular and inadequate remodeled. In the periosteum the hard callus is formed immediately after the fracture, without the preceding formation of a soft callus and provides the initial stabilization of the fracture. In addition, hard callus can also be formed in intramembranous bone formation during conditions of high mechanical stability. [7]

In the fourth and final stage of the fracture repair, the woven bone of the hard callus is remodeled by osteoclasts into the original cortical and/or trabecular bone configuration. When the remodeling is completed, the bone has regenerated itself without the formation of scar tissue and with a full restoration of function.

Systemic and local pathways in normal growth and fracture healing

During bone repair and regeneration, the recapitulated processes resemble largely those occurring during the process of endochondral bone formation during long bone growth. As opposed to fracture healing, endochondral bone formation during growth occurs in an orderly fashion. The growth plate is organized in a spatial manner and contains chondrocytes in four differentiation stages: the reserve, proliferative, hypertrophic and mineralization zone. The stem-like cells of the reserve zone replenish the pool of proliferative chondrocytes. Both bone repair and long bone growth are regulated by a network of endocrine and intracrine growth factors. Next to the classical and well known endocrine pathways, there is a complex network of other paracrine and autocrine growth factors and signaling molecules.

Systemic pathways

The Growth hormone (GH) and Insulin-like growth factor (IGF) axis

Both growth hormone (GH) and Insulin-like growth factor (IGF) are well known growth factors in normal (postnatal) growth. GH stimulates directly the resting chondrocytes to become active and begin proliferating. [11] This direct effect is supported by the presence of GH receptors on the chondrocytes and GH binding proteins in the matrix of the growth plate.[12] GH can also stimulate chondrocytes in an indirect manner by stimulating the production of IGF-I in both liver and locally in the proliferating chondrocytes.[13]

Besides IGF-I, the IGF family contains a second growth factor, IGF-II. This factor is important in the normal embryonic growth and although the role after birth is still unclear, a postnatal function is indicated by the finding of a high number of IGF-II receptors in the postnatal growth plate of Great Danes.[14]

The postnatal function of IGF-I is well established as IGF-I knockout mice have growth impairment and remain a smaller body size as their normal littermates.[15] [16] In the growth plate, IGF-I stimulates clonal expansion of proliferating chondrocytes and inhibits the expression of Parathyroid hormone-related peptide (PTHrP). [17]The expression of IGF-I in the growth plate, however, varies between animal species and ranges from all the zones to exclusively the resting zone or the hypertrophic zone. [12, 18]

Other important members of the IGF family is are the IGF binding proteins (IGFBPs). These proteins are produced in most mammalian cells and bind to IGF-I and IGF-II with an equal or

higher affinity than the IGF receptor does. [19] While IGFBP-4 and -6 have been consistently found to inhibit IGF actions, IGFBP-1,-2,-3, and -5 can both inhibit and potentiate IGF actions.[19]

Both GF and IGF seem to also influence fracture healing as GHR and IGF-I mRNA was present in the callus of an osteotomy model [20] and IGF-I and IGF-II mRNA expression was found in the MSCs of the fracture callus. [21]
In hypophysectomized animals, excluding the direct and indirect effects of GH, no differences in IGF-I gene expression in the fracture callus were found between the hypophysectomized animals and controls, indicating a local role for IGF-I, independent of GH, in the fracture callus. [22]

Studies investigating the effect of GH on fracture healing give inconsistent results, with variable effect of GH on fracture healing. The only clinical trial with human patients reported only enhancement of closed fracture healing after adminstration of GH. [23]

The effect of IGF-I on fracture healing seems to be more straight forward. Studies in knockout mice with an Insulin-receptor-substrate 1 null mutation, an essential essential molecule in the intracellular signaling of IGF-I, reveal impaired bone healing and support a crucial role for IGF-I in bone healing. In the mutant mice the chondrocytes in the fracture callus show less mitogenic ability and therefore less proliferation, which, combined with an increased hypertrophy and apoptosis, results in impaired callus formation. [24] Furthermore, the stimulatory effect of IGF-I on fracture healing is corroborated in all experiments that administer IGF-I continuously by pumps or by wires coated with IGF-I. [25, 26]

Thyroid hormone

The thyroid hormones, thyroxine (T_4) and triidothyronine (T_3), are crucial for normal growth. Juvenile hypothyroidism and hyperthyroidism result both in dwarfism. T4 and T3 stimulate the differentiation of chondrocytes in both a direct and indirect manner. The thyroid receptors TRα1, TRα2 and TRβ1 are expressed in the reserve and proliferating zone and are responsible for the direct inhibiting of proliferation. In addition, thyroid hormones stimulate the expression of GH and IGF-I and inhibit the expression of PTHrP. [27, 28]
The role of thyroid hormones in fracture healing is not widely studied, but there is evidence that delayed fracture repair is seen in patients with hypothyroidism. This delay is characterized by inhibition of endochondral bone formation, resulting in a smaller callus size with a significantly weaker peak force and stiffness. [29] -thyroxine replacement led to recovery of the impaired fracture repair process.[30]In contrast, hyperthyroidism enhanced bone repair

in rats with femoral defects.[31]
Thus far only two clinical studies focused on application of thyroid hormones during fracture healing report a positive effect on fracture healing.[32] [33]

Vitamin D3

Vitamin D3 is a steroid hormone which is converted in the liver to 25-hydroxyvitamin D_3 (25-$(OH_2)D_3$) by CYP27A1. This hormone is in turn activated by CYP27B1 to 1,25-dihydroxyvitamin D_3 (1,25-$(OH_2)D_3$) in the proximal kidney tubule. 25-$(OH_2)D_3$ is broken down by CYP24A1 to 24,25 dihydroxyvitamin D_3 (24,25-$(OH_2)D_3$). This enzyme also degrades 1,25-$(OH_2)D_3$.
It is well known that a deficiency in Vitamin D (or a lack of the vitamin D receptor) causes rickets. Due to a lack of vitamin D, the intestine is unable to actively absorb calcium and phosphate to ensure mineralisation of the growth plate. As a result, hypertrophic chondrocytes do not go into apoptosis, the matrix is not mineralized and chondroclasts fail to absorb the unmineralized cartilage , causing a widening of the hypertrophic zone. Altogether, based on mouse models it appears that vitamin D only plays an indirect role at the growth plate level, i.e. to maintain a correct systemic mineral balance.[34]
[35]

1,25-$(OH)_2D_3$ and 24,25$(OH)_2D_3$, have also a direct influence on the growth plate. Cyp27B1-deficient mice express a pseudo-vitamin D deficiency phenotype, supplementation of calcium and phosphate corrects all aspects of this phenotype except for the growth impairment of the long bones. Daily injections of 1,25-$(OH)_2D_3$ did restore the normal growth of the Cyp27B1 deficient mice. [36]In addition, in vitro experiments showed that 1,25-$(OH)_2D_3$ and 24,25$(OH)_2D_3$ directly influence chondrocytes. 1,25-$(OH)_2D_3$ appeared to inhibit proliferation in both resting and growth zone (proliferate and hypertrophic zone) chondrocytes and stimulate differentiation of the growth zone chondrocytes.[37] In contrast, 24,25$(OH)_2D_3$ inhibits proliferation in just the resting zone and stimulates differentiation of the resting zone chondrocytes.[37] {Furthermore, exposure of the resting zone chondrocytes to 24,25$(OH)_2D_3$ increased responsiveness to 1,25-$(OH)_2D_3$ and decreased responsiveness to 24,25$(OH)_2D_3$. In contrast, exposure of the resting zone chondrocytes to 1,25-$(OH)_2D_3$, did not had an effect on the responsiveness to 24,25$(OH)_2D_3$. [37]
These effects are obtained by two different receptors, a nuclear receptor and a membrane-mediated receptor. Both are expressed in the postnatal growth plate for 1,25-$(OH)_2D_3$ and a membrane-mediated receptor has been identified for 24,25$(OH)_2D_3$. [37, 38] Both receptors have a different distribution among the growth plate, matching their different effects.
Although it is likely that a nuclear vitamin D receptor is present in the fracture callus, no literature on this subject has been found. In the fracture callus of vitamin D depleted

chicks,however, evidence has been found for a membrane-mediated receptor for 1,25-$(OH)_2D_3$ as well as for 24,25$(OH)_2D_3$.[39, 40] Besides the presence of receptors, the expression of Cyp24A1 during fracture repair has also been studied. This expression was elevated compared to the undamaged contra-lateral bone.[41] In addition, fracture repair in Cyp24A1 knockout mice was found to be delayed and this effect could be reversed by treatment with 24,25$(OH)_2D_3$. [41]
In conclusion, vitamin D plays an essential role in fracture healing, based on the functional studies performed in mouse models and on the observed enhanced fracture healing after administration of a vitamin D metabolite in animals[4243], support the role of vitamin D3 in fracture healing.

Local pathways

In addition to endocrine pathways, many local pathways influence the process of endochondral bone formation during growth and fracture healing.

Indian Hedgehog (IHH) / Parathyroid hormone related peptide (PTHrP)

IHH belongs to the hedgehog proteins, a group of proteins which are very important in the embryonic development and postnatal growth. During postnatal growth, IHH is produced in the prehypertrophic and hyperthropic chondrocytes and binds to the Patched receptor (PTC), which is expressed in the same zones as IHH.[44]
IHH exerts several functions. The first is the well described negative feedback loop between IHH and PTHrP, regulating the transition of chondrocytes from the proliferative tot the hypertrophic zone. IHH diffuses towards the (pre) hypertrophic zone and stimulates the production of PTHrP. PTHrP then inhibits differentiation, which causes the chondrocyte to stay in the proliferative phase, unable to produce IHH anymore. [44]
In addition, IHH exerts a direct effect on the growth plate, inducing chondrocyte proliferation. [45] and seems to influence the differentiation of reserve zone chondrocytes into proliferating chondrocytes independent op PTHrP. [46]

Both *IHH* and *PTHrP* are expressed in the fracture callus in a similar pattern compared with the expression in the growth plate. The expression of *IHH* was visible within a few hours after fracture [47] or after one week in the prehypertrophic zone [48] and was found to be earlier downregulated in the callus of a stabilized fracture compared to a non-stabilized fracture. [49]The latter indicates that chondrocytes differentiate more rapidly towards terminal differentiation in a stabilized fracture.
Accordingly, in the fracture site PTHrP was expressed in MSC's and proliferating

chondrocytes and the PTH/PTHrP receptor was detected in proliferating and prehypertrophic chondrocytes. [50]

Despite of the clear presence of IHH and PTHrP in fracture healing, few studies investigated the effect of the administration of specifically PTHrP or PTHrP analogs on fracture healing. This PTHrP analogs have been shown to accelerate the process of fracture healing. [51] [52]
Even more so, endochondral bone formation in the fracture callus can also be influenced by parathyroid hormone (PTH), which binds to the same receptor as PTHrP. [53]
Various animal studies and clinical studies have shown a beneficial dose dependent effect of PTH in the enhancement of fracture repair. [54-56]

Transforming growth factor beta (TGF-β) super family

The TGF- β family consist of several families including TGF- ***β,*** bone morphogenic proteins (BMPs) and growth differentiation factors (GDFs).

Transforming growth factor beta (TGF-β)

The TGF- β family consists of three proteins, TGF- β1, -2 and -3. After the TGF- β ligands bind to TGF- β receptor type 2 (TGFBR2), the TGF- β receptor type 1 (TGFBR2) is phosphorylated by TGFBR2 and the signal is further mediated by SMAD2/3.
All members of the family are expressed in the growth plate. Although TGF- β1, 2 and 3 are expressed in the resting, proliferative and hypertrophic zone, the expression of TGF- β2, decreases during growth. [57] [58] In addition, both receptors are expressed in the proliferating and hypertrophic zone . [59] In the growth plate TGF- β stimulates proliferation of the chondrocytes and inhibits differentiation. [60]. The effect of TGF- β1 and -2 on the growth plate is demonstrated by TGF- β1 and -2 knock out mice which showed a reduction in bone length. [6162] SMAD 3 and TGFBR2 knock out mice showed premature terminal differentiation resulting in a disorganized growth plate and a decreased longitudinal growth. [6364]. The inhibiting effect of TGF- β on terminal differentiation of the chondrocytes could be PTHrP dependent as TGF- β 1 did not inhibit hypertrophic differentiation in PTHrP-null mice. [63]
In vitro, TGF- β stimulates chondrogenic differentiation of mesenchymal stem cells[65] and chondrocyte proliferation. [66]

Within 24 hours after fracture repair, TGF- β1 is released by platelets in the fracture callus and its expression increases during endochondral ossification.[67]. In patients with delayed fracture repair, TGF- β1 showed a stronger decrease during fracture repair compared with physiological fracture repair. [68] [69] TGF- β2 and -3 show stable expression during the process of fracture healing with a peak during chondrogenesis. [70] [71]

Continuous local application of TGF- β-1 by injection or by continuous local release increased callus formation and strength and enhances fracture healing in a dose dependent matter. [25, 72-74] This effect was not achieved by a single or double injection. [75, 76]

Bone morphogenic proteins (BMP)

The family of the BMPs is well known for its great osteoinductive activity and capability to induce ectopic bone formation. In the growth plate, BMP's stimulate proliferation and inhibit hypertrophy of the chondrocytes. This is validated by two examples. First, administration of the BMP antagonist noggin results in reduced chondrocyte proliferation and increased terminal hypertrophic differentiation. [77]

And secondly, the $Bmpr1a^{CKO}$ mice, knockout mice for the BMP 1a receptor, develop an expanded hypertrophic zone and a shortened proliferative zone. [78]

During fracture healing, several members of the BMP family are expressed and seem to be important regulators of the repair process. BMP-2, which is expressed within one day after fracture, is required to initiate the fracture repair process, as mesenchymal progenitor cells fail to differentiate in its absence. [79]

At this moment, two members of the BMP family, BMP-2 and BMP-7 are available in recombinant form and approved for clinical use. Although animal and preclinical studies seem to be very promising and the stimulating effect of BMP's on fracture healing and spinal fusion is evident, significant evidence of their benefit in clinical studies is missing. [52] Most of the clinical studies have shown that the use of BMP was comparable with an autologous bone graft. [80] Even more so, critical reviews debate the study design bias in the original trials and the adverse effects of BMP-2 . [8182] High dosage of BMP2 , is accompanied by a higher complication risk, the main concern being heterotrophic ossification. [283]

Growth differentiation factor (GDF)

The family of GDF contains ten members of which only a few are involved in bone formation. A well-known family member is GDF5. There are several natural occurring mutations of the GDF5 gene in humans and mice that are characterized by shortening of the long bones. In this GDF5 null mice, chondrogenesis is delayed but it is unclear whether this delay is caused by a decreased rate of proliferation or a prolonged hypertrophic phase. [84] Overexpression studies showed that GDF5 can increase the size of the early cartilage condensation, increasing cell proliferation or cell-adhesion or both, and can therefore initiate chondrogenesis. [85]

In the fracture callus, GDF5 expression is most pronounced during the chondrogenic phase.[71] { Its absence results in disorganized callus formation and finally in impaired bone

formation in GDF5 null mice caused by a delay in cellular recruitment and chondrocyte differentiation in the early stages of fracture repair. [86]

GDF6 null mice show defects in cartilage formation at distinct sites from those seen in GDF5 mutants suggesting a regulating function during chondrogenesis. [87] GDF7 null mutant mice exhibited a shorter hypertrophic phase and increased growth rate during postnatal growth. [88]

GDF8 normally regulates muscle development and does not seem to regulate normal growth. However, GDF8 deficient mice show a larger callus after osteotomy [89] and when GDF8 is inhibited in the fractured limb of wild type mice, fracture healing is improved. [90]

Fibroblast growth factor (FGF)

The family of FGFs contains at least 22 different FGF proteins which bind to four different receptors (FGFR1,-2,-3 and -4). FGF has an important function in the regulation of endochondral bone formation as activating mutations of FGFR3 result in several types of chondrodysplasia including achondroplasia, the most common form of human short-limbed skeletal dysplasia. [91]

Expression of FGFR3 is observed during chondrogenesis where it may enhance chondrocyte proliferation in the mesenchymal condensation. [92]This is contrary to the function of FGFR3 in the endochondral ossification of the growth plate in which it limits chondrocyte proliferation and differentiation. [92, 93] In the growth plate, FGFR3 is expressed in the proliferating zone and exerts its effects directly and indirectly by interaction with Ihh and BMP.[9294]

The other receptors are also expressed in the growth plate. Expression of FGFR1 is found in the (pre)hypertrophic zone [95] [92] FGFR2 is expressed in the resting zone and FGFR4 in the resting and proliferative zone. [95] FGFR2 and -4 are positive regulators of growth whereas FGFR1(together with FGFR3) is considered to be a negative regulator. [95]

Of the FGFR ligands, FGF2, and -18 seem to negatively regulate endochondral ossification in the growth plate. Overexpression of FGF2 in mice inhibits longitudinal growth, decreasing chondrocyte proliferation and hypertrophy and decreasing matrix production. [96] A deficiency of FGF18 causes increased chondrocyte proliferation and differentiation. [92, 93] However, FGF18 seems to positively regulate proliferation and differentiation in the osteogenesis. [97]

Overexpression of FGF2 in mice inhibits longitudinal growth, decreasing chondrocyte proliferation and hypertrophy and decreasing the production of cartilage matrix. [96]

In addition, a retrogene of FGF4, causing enhanced expression of *fgf4*, was recently found in chondrodysplastic dog breeds as the cause of chondrodysplasia in these dogs.[98]

Several members of the FGF family and their receptors are expressed during fracture healing. An excellent overview is provided by *Du et. Al. 2012* [93] FGFRs (especially FGFR3) and FGFs seem to be important in the process of fracture healing in different cell types, including chondrocytes, osteoblasts and mesenchymal cells[99, 100101]
FGF2 administration at the fracture site augments bone formation and healing rate. [92, 93]

Wnt pathway

The Wnt pathway consists of 19 proteins which are best known for their role in embryonic development. They mediate their effects through the canonical pathway, where Wnt proteins bind to receptors of the frizzled family, and through non-canonical pathways, which have the capacity to antagonize the canonical pathway.
The responses of (pre)chondrogenic cells on Wnt signalling depend on the stage of the cells at the moment of signal activation. A high Wnt/β-catenin signal in the condensation of mesenchymal stem cells inhibits chondrogenic differentiation but promotes osteogenic differentiation, resulting in intramembranous ossification. A low Wnt/β-catenin signal initiates endochondral ossification. [102]
In a later stage, when the MSC's are differentiated to chondrocytes, Wnt/ β-catenin signaling promotes terminal differentiation of the chondrocytes and the replacement of cartilage by bone. This Wnt/ β-catenin signal is provided by Wnt-4,(-2b and -10b) which are also expressed in the growth plate of postnatal mice. [103] Overexpression of Wnt-4 accelerates hypertrophic differentiation. [104] [105106] Whereas misexpression of Frzb-1, expressed in the prehypertrophic chondrocytes, delayes maturation. [107]
Other Wnt proteins expressed in the growth plate, Wnt-5a,-5b (and -11), belong to the non-canonical calcium dependent pathway and promote transition from the proliferative zone to the hypertrophic zone and inhibit differentiation of hypertrophic chondrocytes. [103108109]
Overexpression of these genes causes delayed hypertrophic differentiation. [105]
Notably, the expression of IHH in the growth plates resembles the expression pattern of the Wnt genes, however, there seems to be no correlation between the Wnt pathway and IHH. Both regulate the growth plate in a parallel but separate way. [103]

Several Wnt genes, including Wnt-4,-5a,-5b, and -11, and other members of the Wnt signaling pathway, such as Frizzled (Fz) and β-catenin, are upregulated during fracture repair. [110111112]During bone formation within the fracture, the Wnt/ β-catenin signal influences the fracture callus in a similar manner as the postnatal growth plate is influenced. In mice, in which the Wnt/β-catenin signaling pathway is inhibited, for example Lrp5 (a co-receptor with

Frizzled protein in the Wnt signaling) knockout mice or Col2a1-ICAT (an inhibitor of β-catenin) transgenic mice, retarded bone repair is observed. [113114]In the Col2a1-ICAT transgenic mice this retardation was caused by delayed hypertrophic differentiation of the chondrocytes. [114] Accordingly, absence of the Secreted frizzled-related protein 1 (SFRP1), an inhibitor of the Wnt signaling pathway, in knockout mice shows enhanced Wnt signaling in the fracture callus and stimulate intramembranous bone formation. [115]
In line with the role of the Wnt in fracture healing, upregulation of the Wnt/ β-catenin signal by Wnt-4 or lithium chloride, enhances fracture healing, mainly by the stimulation of intramembranous ossification. [111116]

Conclusion

The process of endochondral bone formation is regulated by many systemic and local growth factors. As can be seen from the small selection of contributing factors described in this chapter, the regulation of this process in fracture healing resembles the regulation in longitudinal growth; if a specific growth factor (for example BMP-2) stimulates growth, it will often enhance fracture repair. This provides the opportunity to learn something about fracture repair from studying longitudinal growth.

Chapter 3: The role of systemic and local pathways regulating variation in height at the growth plate level

Abstract

Studies on height variation can identify genes and pathways that regulate growth from a developmental point of view but also can give clues on possible candidate gene to be employed in bone regenerative strategies. Genes contributing to height variation have been identified with the aid of a candidate gene approach or genome wide association studies. In this respect, the dog has been an invaluable model in identifying genes determining size . *Within the canine species there is a large diversity in body size/height between different breeds and the canine growth plate resembles the human growth plate from a physiological perspective since they both fuse at skeletal maturity. Genetic association studies in dogs show that there are only a few genes (including, IGF-1, IGF-1R, HMGA2.) that explain a large part of the height variation in specific breeds. However, polymorphisms in these genes explain only a part of the human height variation and GH treatment of children with idiopathic short stature and growing miniature poodles only had a small effect on the final adult height. Whole genome expression profiling of the growth plate and adjacent bone of Great Danes (a large, fast-growing breed dog) with Miniature Poodles (a small, slowly growing breed dog). identified 3010 genes that were significantly differential regulated between the two breeds. Subsequent* SPIA analysis showed an up regulation of pathways that are logically associated with enhanced growth and matrix production such as an activated cell cycle pathway, an activated ECM-receptor interaction and an activated tight-junction pathway. Even more so, 83 of these differentially regulated genes overlapped with list of 207 loci that have been previously been associated with human adult height variation studies. Altogether, these findings point out the additive value of the canine model as species to identify pathways regulating endochondral bone formation. Even more so, from a translation point of view, the canine model seems to have potential in identifying targets to be employed in bone regenerative strategies.

Introduction

The natural variation in adult height is caused by differences in skeletal growth orchestrated by endocrine and local signalling pathways coordinating endochondral bone formation at the growth plate level. Height is a highly heritable trait and therefore, many studies have searched for the cause of this natural variation. Genes contributing to height variation have been identified with the aid of a candidate gene approach or genome wide association study (GWAS). Recent meta-analysis of >50 GWAS concerning >183.000 individuals [117] identified more than 180 loci to be associated with adult height. Most of these loci were enriched for genes that were connected to each other in biological pathways that under lied skeletal growth defects. [117] Nevertheless, all this data combined only explained 10% of the heritability of height.

Specifically in studies evaluating the role of genes in natural height variation, GWAS candidate genes are selected based on their known function or presence in pathways related to postnatal growth. However, using SNPs in a GWAS frequently results in larger genomic regions correlated with the phenotype. This correlation can easily be caused by variations in neighboring genes as well as transcription regulating regions.
In order to overcome this, *Lui e.a. (2012)* performed micro-arrays and compared the expression between the murine whole growth plate and three different soft tissues (lung, kidney and heart) during growth and identified spatially or temporally regulated genes in the different zones of the rat growth plate.[118] Genes were selected based on the possession of two out of three criteria; 1) genes that had higher expression in growth plate cartilage than in other tissues; 2) genes that were spatially regulated across different zones and 3) genes that are temporally regulated.[118] Of the 420 genes that met the criteria, 38 corresponded with the 180 loci of the GIANT GWAS , and 22 of these represented the gene closest to the SNP identified by GWAS. [118] This overlap shows a strong enrichment of the growth plate genes in the GWAS list. In addition, 38 genes that have a growth plate phenotype in knockout mice and 27 genes that cause human skeletal dysplasia's were found in the GWAS list. [118] Such integrative approaches help unravel the signalling pathways related to height variation; rodent models facilitate identifying the role of the gene with transgenic mice However, mice and rats do not share similar growth plate physiology with humans; they do not close their growth plates at skeletal maturity. [119]

In this respect, the dog has been an invaluable model in identifying genes determining size within the “Dog Genome Project” at the National Human Genome Research Institute.[120] Within the canine species there is not only a large diversity in body size/height between different breeds; the canine growth plate resembles the human growth plate from a physiological perspective since they both fuse at skeletal maturity. [121] Notably, the difference in growth rate between small and large breed dogs is accompanied by distinct morphological differences at the growth plate level (Figure 1). The growth plate of Great Danes, a large breed, is twice as thick compared to Miniature Poodles, a small breed, at the same age. [122] Even more so, the thicker growth plate is constituted of an absolutely larger proliferative and an absolutely and relatively larger hypertrophic zone compared to Miniature Poodles. [122] This is in agreement with the important contribution of hypertrophic chondrocyte differentiation to the lengthening of the long bones.[123]

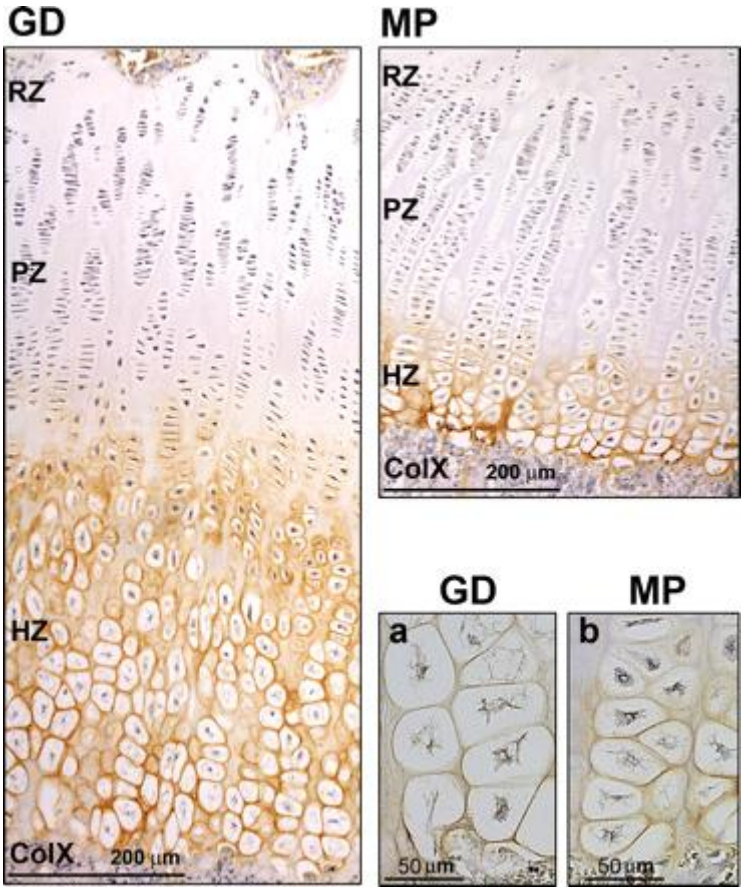

Figure 1: Growth plate of a Great Dane (GD) compared with a Miniature Poodle (MP) at the same age. The GD growth plate is larger and contains a relative and absolute larger hypertrophic zone compared to the MP growth plate {{144 Tryfonidou,M.A. 2010}}

The limited role of the GF/IGF axis in explaining variation in height

A genome wide scan performed by *Chase e.a. 2002* identified a QTL on chromosome 15, influencing size variation within the Portuguese Water Dog (PWD) breed. {{461 Chase, Kevin 2002}} Subsequent analysis of the genetic variation in relation to body size surrounding this QTL identified SNPs related to the IGF-I gene; dogs homozygous for haplotype B had a smaller median skeletal size and lower IGF-I plasma levels than dogs homozygous for haplotype I. {{170 Sutter,N.B. 2007}} This specific haplotype B is shared by 14 small breed dogs and explained 15% of the variation in height in the PWD. {{170 Sutter,N.B. 2007}} GWAS of 915 small and large breed dogs confirmed this association between the IGF-I gene and variation in adult height. {{392 Boyko,A.R. 2010; 391 Vaysse,A. 2011}} In line with the possible role of the IGF-I in height variation, a nonsynonymous SNP within the second protein-coding exon of IGF1R was associated with tiny size; the SNP was

found in a diverse set of small dog breeds, but almost no large breeds carried it. {{386 Hoopes,B.C. 2012}}

In addition, polymorphisms in the GH/IGF-I pathways were found in humans by a candidate gene based approach and GWAS. Common found SNPs associated with variation in height include SNPs in the GH promoter region, a SNP in intron 4 of the GH promoter, which seems to have an effect on GH secretion {{147 Millar,D.S. 2003; 145 Hasegawa,Y. 2000; 388 Van Heemst,Diana 2005}}, and polymorphisms in the IGF-I gene. {{148 Vaessen,N. 2001}}{{108 Schneid,H. 1990}} But, these studies employed a relatively small sample sizes and a larger study identified no polymorphisms in the GH and IGF-1 gene and in six other genes of the GH-IGF pathway. {{125 Lettre,G. 2007}}

As the GH/IGF axis is a critical regulator of skeletal growth plays and association between this axis and variation in adult height were found, variances in plasma levels of the respective hormones were thought to explain the height diversity both in humans and dogs. Clinical studies in constitutional tall and short children revealed a correlation between IGF-I levels and body height {{109 Binoux,M. 1987; 108 Schneid,H. 1990}} and between growth velocity and GH secretion {{107 Rochiccioli,P. 1989}}. In line with this, Great Dane dogs undergo a period of high basal GH concentrations during growth as compared to Beagles and Miniature Poodles.{{123 Nap, RC 1992}} {{143 Favier,R.P. 2001}} {{385 Tryfonidou,M.A. 2003}} Furthermore, circulating IGF-I plasma levels were positively correlated with size and body weight. {{121 Eigenmann,J.E. 1988; 122 Eigenmann,J.E. 1984}} However, in both human and canine species there are clues pointing towards a limited effect of GH in height variation. More explicably, 24hour -GH secretion did not correlate with body weight and height in humans with normal stature. {{106 Costin,Gertrude 1989}} Administration of clonidine, stimulating GH secretion, did not appear to affect the circulating IGF-I levels in a cohort of dogs.{{122 Eigenmann,J.E. 1984}}

Even more so, GH treatment of children with idiopathic short stature had a small effect (0,4 SD) on the final adult height. {{381 Cohen,P. 2008}} In parallel to humans, GH treatment of growing miniature poodles resulted in a modest 10% gain in height compared to controls, while there were no differences in other endocrine systems, including the thyroid pathway and PTH. {{384 Tryfonidou,M.A. 2003}}

Despite the endocrine differences in GH and IGF-I plasma concentrations between small and large breed dogs, there were no differences in the gene expression of the IGF-I, IGF-II and their receptor at the growth plate level. However, in large breed dogs gene expression of IGFBP-2,4,-6 , known to bind and inactivate IGF-I, was significantly decreased at the growth plate level compared to small breed dogs {{144 Tryfonidou,M.A. 2010}} indicating that during

rapid growth rates, less IGF-I is bound to binding proteins resulting into the higher local IGF-I levels to facilitate rapid growth rates. Altogether, these findings indicate that although the GH/IGF-I axis is important in growth, it may have a limited role in defining the pace of growth and hence height variation.

The discovery of HMGA2, SMAD2 and ADAMTS17 by GWAS as potential contributors to variation in height

Besides the IGF-I gene, the high motility group AT-hook 2 (HMGA2) gene was one of the first genes that was associated with variation in height in human GWAS {{99 Weedon,M.N. 2007}} and was later found in canine GWAS {{391 Vaysse,A. 2011; 392 Boyko,A.R. 2010}}and a SNP scan of specific regions of the canine genome {{462 Jones, Paul 2008}}. HMGA2 seemed an excellent candidate gene for height because deletions of (parts of) the HMGA2 gene caused significant short stature in children{{172 Lynch,S.A. 2011}} and HMGA2 deficient mice developed a pygmy phenotype. {{101 Brants,J.R. 2004}} However, only 0,3% of the human variation in height could be explained by this gene{{443 Weedon,M.N. 2007}}. Other targets identified by canine GWAS were SMAD2{{392 Boyko,A.R. 2010}}, which mediates the TGF-β signalling and ADAMTS17 {{386 Hoopes,B.C. 2012}}. Although SMAD2 has not been associated with size determination in humans, a homozygous mutation of ADAMTS17 was found to cause short stature in humans{{463 Khan, Arif O 2012}}. Very recently, a study by *Rimbault e.a.* showed that a combination of the variance in the HMGA2, SMAD2, IGF1,IGF1R, GHR and STC2 genes explain 46-52.5% of the variance in body size of dogs.{{468 Rimbault, Maud 2013}} However, these genotypes only account for variance in breeds with small and medium weights and not for the gigantism of large dog breeds. {{468 Rimbault, Maud 2013}}

Candidate-gene approaches of the Vitamin D pathway and IHH/PTHrP feedback loop explain only a small part of height variation

There are limited reports investigating the role of other endocrine regulators and height variation. Vitamin D is essential hormone in maintaining calcium homeostasis and skeletal growth. A positive correlation was found between 25-$(OH_2)D_3$ plasma levels and height in young women[148] and the plasma levels of its active metabolite 1,25-$(OH)_2D_3$ have been reported to differ in canine individuals with distinct height differences and concomitant differences in the GH/IGF-I plasma levels.[142, 147] In the vitamin D pathway polymorphisms in the human VDR receptor are found, the bsml polymorphism is most often identified and explains 0,3 – 8 % of the height variation. [149-151]

Even less researched was done on the influence of the IHH/PTHrP feedbackloop on adult height variation. A polymorphism in the P3 promoter region of the PTHRP1 gene has been

found consisting of a repetition of a sequence (AAAG) which changes the transcription activity of the gene.[152] [153]. Taller individuals had one or two repeats of the sequence compared with the control group which had none. [152]. However, this polymorphism also explains only 0,8% of the variation in height. [152]

It appears that studying the canine species with its vast variation in skeletal height would give clues in determining the local pathways that define the pace of endochondral bone formation at the growth plate.

In order to show the proof of principle we conducted a two-colour microarray with a reference design experiment on 44k Canine Gene Expression Microarrays V1 (G2519F, Agilent Technologies) with the total RNA of the growth plates of five great danes and miniature poodles. The common RNA reference pool consisted of a multitude of canine organs, including liver, spleen, kidney, lung, hart, intestine and bone.

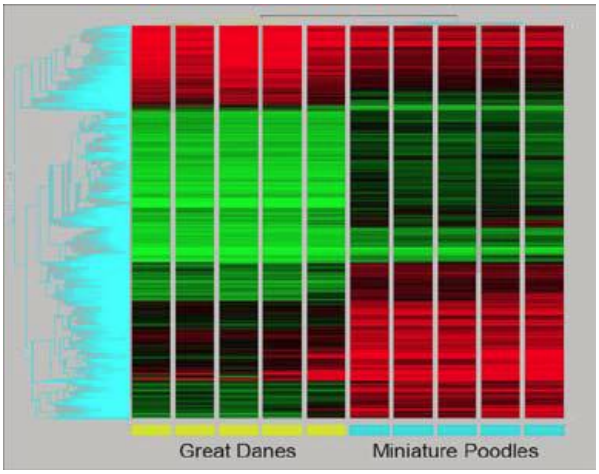

Figure 2: Micro-array of 5 Great Danes (GD) and Miniature Poodles (MP). 1193 DE-genes were upregulated (red) and 1817 DE-genes were downregulated (green) in the GD compared with MP.

Differential expression was investigated using the R (2.15.2) package limma, yielding 3522 significant (FDR<0.05) differentially (-1.3< fold change >1.3) expressed CanFam3.1 annotated probes (DE-genes), representing 3010 unique, annotated genes; 1193 DE-genes were upregulated and 1817 DE-genes were down regulated.

Among the top-10 upregulated DE-genes were genes that regulate chondrocyte differentiation (Adseverin[154] and upper zone of growth plate and cartilage matrix associated gene (*UCMA)* [155]), associated with mesenchymal stem cells (six transmembrane epithelial antigen of the prostate family member 2 (*STEAP2)* [156]), influence pathways that are associated with skeletal development (tissue factor pathway inhibitor 2 (*TFPI2)* [157], procollagen C-endopeptidase enhancer 2 (*PCOLCE2)* [158]) or are involved in pathologies of the skeletal system (3'-phosphoadenosine 5'-phosphosulfate synthase 2 (*PAPSS2)* [159], solute carrier family 1 (*SLC1A1)* [160]). (Table 1, Annex I) Among the DE-down regulated genes were many calcium binding proteins (*S100A8*, *S100A9* and *S100A12*) which are associated with osteoblast differentiation and calcification of the cartilage matrix. [161] (Table 2, Annex I)

Number	Fold Change	Gene	ReporterId	CfEnsId	Description
1	5,6	SCIN	CFAB035019		Adseverin (Scinderin)
2	4,9	UCMA	CFAB014719	ENSCAFG00000004749	upper zone of growth plate and cartilage matrix associated
3	4,7	CHRNB3	CFAB019142	ENSCAFG00000005460	cholinergic receptor, nicotinic, beta 3
4	4,6	TFPI2	CFAB012171	ENSCAFG00000002040	tissue factor pathway inhibitor 2
5	4,5	STEAP2	CFAB033585	ENSCAFG00000001870	STEAP family member 2, metalloreductase
6	4,5	SQLE	CFAB006899	ENSCAFG00000001056	squalene epoxidase
7	4,1	PAPSS2	CFAB007288	ENSCAFG00000015654	3'-phosphoadenosine 5'-phosphosulfate synthase 2
8	4,1	SLC1A1	CFAB010956	ENSCAFG00000002067	excitatory amino acid transporter 3
9	4,0	PCOLCE2	CFAB013887	ENSCAFG00000007915	procollagen C-endopeptidase enhancer 2
10	3,9		CFAB010131		

Table 1: Top 10 upregulated DE-genes in the Great Dane compared with the Miniature Poodle

Nr.	Fold Change	Gene	ReporterId	CfEnsId	Description
1	-74,1	S100A8	CFAB026148	ENSCAFG00000017557	protein S100-A8
2	-51,8	S100A12	CFAB026149	ENSCAFG00000023324	S100 calcium binding protein A12
3	-49,4	Q1ERY9	CFAB013656	ENSCAFG00000030286	Uncharacterized protein
4	-35,8	Q2LC20	CFAB020932	ENSCAFG00000013763	Uncharacterized protein
5	-25,8	Q1ERY9	CFAB017317	ENSCAFG00000030286	Uncharacterized protein
6	-24,4	S100A9	CFAB008767	ENSCAFG00000029470	S100 calcium binding protein A9
7	-22,5		CFAB023697		
8	-22,4	MYH1	CFAB016099	ENSCAFG00000030337	Myosin-1
9	-20,3		CFAB032244	ENSCAFG00000005427	**Novel protein**
10	-19,8	HBA	CFAB016483	ENSCAFG00000029904	Hemoglobin subunit alpha

Table 2: Top 10 downregulated DE-genes in the Great Dane compared with the miniature poodle

The differential expression lists from the array comparisons were converted to their human homologues and a signaling pathway impact analysis (SPIA) was performed (Table 3, Annex II). The SPIA calculates which pathways are significant up regulated by combining the over-representation of DE-genes in a certain pathway with the effect of the expression changes of these DE-genes on the perturbation of the pathway, thereby incorporating the pathway topology.[162]

The SPIA analysis of the micro-array showed an up regulation of pathways that are logically

associated with enhanced growth and matrix production such as an activated cell cycle pathway, an activated ECM-receptor interaction and an activated tight-junction pathway (Annex II). Taking into account the semi-quantitative nature of the micro-array, resulting in a lower sensitivity, pathways related to skeletal development such as the mineral absorption pathway, TGF-beta signalling pathway and VEGF signalling pathway were also regulated (Annex II), although not significantly regulated after correcting for multiple testing . The upregulation of TGF-beta signalling facilitates the increased pace of endochondral bone formation large breed dogs compared to small breed dogs. The mineral absorption pathway was inhibited while the VEGF pathway was activated, the latter at least facilitating angiogenesis during the final phase of endochondral bone formation in the growth plate. This counterintuitive finding may find its explanation in the nature of the samples in the micro-array; samples consist of all the zones of the growth plate combined. While the mineral absorption pathway may be activated in the hypertrophic zone, this may not be the case in the reserve and proliferative zone. Subsequently, the inhibited gene expression of the other zones may outweigh the stimulating gene expression in the hypertrophic zone, resulting in an overall inhibited mineral absorption pathway.

ID		Name	ID	pSize	NDE	pNDE	tA	pPERT	pG	pGFdr	pGFWER	Status	KEGGLINK
5150	1	Staphylococcus aureus infection	5150	31	18	6,42E-06	-19,384	0,006	6,96E-07	9,39E-05	9,39E-05	Inhibited	KEGG-link
4110	2	Cell cycle	4110	105	44	7,65E-07	8,582281	0,339	4,19E-06	0,000283	0,000566	Activated	KEGG-link
5322	3	Systemic lupus erythematosus	5322	54	22	0,000690665	-8,32175	0,015	0,000129	0,005049	0,017451	Inhibited	KEGG-link
4512	4	ECM-receptor interaction	4512	64	27	8,80E-05	4,922075	0,138	0,00015	0,005049	0,020197	Activated	KEGG-link
4530	5	Tight junction	4530	101	38	7,71E-05	0,06558	0,991	0,000801	0,02162	0,108102	Activated	KEGG-link
4670	6	Leukocyte transendothelial migration	4670	89	32	0,000698053	-11,2205	0,279	0,001859	0,036695	0,250926	Inhibited	KEGG-link
4115	7	p53 signaling pathway	4115	51	22	0,000264496	0,660446	0,828	0,002064	0,036695	0,278695	Activated	KEGG-link
5162	8	Measles	5162	98	35	0,000464237	-3,85262	0,5	0,002175	0,036695	0,293564	Inhibited	KEGG-link
4610	9	Complement and coagulation cascades	4610	54	19	0,010360511	-23,3443	0,033	0,003071	0,046059	0,414528	Inhibited	KEGG-link
5145	10	Toxoplasmosis	5145	101	34	0,001810032	5,996937	0,279	0,004338	0,052846	0,585687	Activated	KEGG-link
5166	11	HTLV-I infection	5166	213	61	0,004009031	11,50113	0,132	0,004522	0,052846	0,610403	Activated	KEGG-link
5164	12	Influenza A	5164	118	38	0,002500349	-7,44072	0,221	0,004697	0,052846	0,634151	Inhibited	KEGG-link
4612	13	Antigen processing and presentation	4612	39	17	0,001122335	-1,04864	0,54	0,005096	0,052921	0,687971	Inhibited	KEGG-link
4510	14	Focal adhesion	4510	158	50	0,00090233	0,837395	0,944	0,006872	0,06627	0,927782	Activated	KEGG-link
5144	15	Malaria	5144	37	16	0,001727033	-0,56956	0,589	0,008027	0,072239	1	Inhibited	KEGG-link
4978	16	Mineral absorption	4978	32	14	0,002902651	0	1	0,01986	0,167571	1	Inhibited	KEGG-link
4810	17	Regulation of actin cytoskeleton	4810	173	47	0,027231724	12,01607	0,219	0,03651	0,281129	1	Activated	KEGG-link
5412	18	Arrhythmogenic right ventricular cardiomyopathy (ARVC)	5412	60	20	0,016411675	0,386339	0,375	0,037484	0,281129	1	Activated	KEGG-link
4350	19	TGF-beta signaling pathway	4350	62	15	0,302772891	11,47411	0,024	0,04305	0,303441	1	Activated	KEGG-link
4370	20	VEGF signaling pathway	4370	57	19	0,019042821	4,153969	0,402	0,044954	0,303441	1	Activated	KEGG-link

Table 3 : SPIA analysis of the DE-genes. Further elaboration of the different significant upregulated pathways can be found in annex II

To examine the value of the canine model in identifying major genes of height variation, the outcome of the micro-array was compared with the GIANT GWAS results. Of the 207 loci that were associated with adult height variation by the GWAS, 83 contained genes that were significantly differential regulated in the micro-array comparing great danes with miniature poodles. Of these genes, 47 represented the gene closest to the SNP identified by the GWAS and in 17 of these genes the SNP was intragenic. By combining the list of corresponding genes with GO terms, several functional categories were distinguished including skeletal system development, regulation of cell cycle and apoptosis, cell differentiation and extracellular matrix. (Annex III)

Functional Category	Gene	SNP	Proximity	Fold Change
Skeletal system development	SOX9	rs2158917	Intragenic	3,1
(GO:0001501)	IHH	rs12470505	2nd	2,5
	BMP6	rs3812163	Intragenic	2,5
	HHIP	rs7689420	Intragenic	1,9
	MEF2C	rs10037512	Intragenic	1,7
	ACAN	rs16942341	Intragenic	1,7
	BMP2	rs2145272	Intragenic	1,7
	COL11A	rs12047268	Intragenic	1,5

Table 4: Genes assigned to the Skeletal system development category by GO terms that were identified in both the GIANT GWAS as well as the micro-array.

In the functional category skeletal system development, genes well known for their role in longitudinal growth appear such as the transcription factor *SOX9,* indian hedgehog (*IHH),* growth factors *BMP-2* and *-6* and extracellular matrix components as collagen type XIa and aggrecan (Table 4). All were upregulated in the GD compared with MP. In addition *HHIP*, a gene often found in GWAS studying variation in height, appears also in this category. Overexpression of hedgehog interacting protein (*HHIP)* diminishes *ihh* signaling in mice resulting in severe skeletal defects including shortlimbed dwarfism.[163] Surprisingly, *HHIP* is upregulated in the GD compared with the MP, indicating downregulation of the IHH signalling in the GD compared with the MP. Contrary, gene and protein *IHH* expression have been reported to be upregulated in the growth plate of GD compared to MPs [122], whereas other members of the *IHH* pathway are downregulated, such as *GLI3*, *PTCH2*. Based on these findings, it has been suggested that the *PTHrP/IHH* feedback loop has a different equilibrium, supporting higher proliferation rates and hypertrophy, which in turn can explain the growth plate phenotype and rapid growth rate as seen in Great Danes. However, one of the major limitations of the current study is the fact that the DE-genes have been identified on mixture of all growth plate zones, including primary spongiosum. The current study design addressed the endochondral bone formation as a total. However, future studies, should concentrate on determining the DE-genes within the different growth plate zone of large and small breed dogs. The use of high-throughput mRNA sequencing (RNA-seq) allows the discovery of new genes and transcripts and measure transcript expression at the same time. RNAseq will, in contrast to microarray analysis, allow an unbiased examination of the transcriptome and the detection of novel and alternative spliced transcripts while measuring the expression of these transcripts and will do so with an enhanced sensitivity and at least an equal accuracy.

Conclusion

Integration of the identified pathways related to a differential pace of endochondral bone formation at the growth plate level, with the GIANT GWAS analysis resulted in a tremendous overlap of genes being related to height variation/pace of endochondral bone formation. Altogether, these findings point out the additive value of the canine model as species to enlighten the pathways regulating endochondral bone formation. Even more so, from a translation point of view, the canine model seems to have potential in identifying targets to be employed in bone regenerative strategies. One representative example is the fact that *BMP-2* is significantly upregulated in the micro array, identified as a candidate gene in the GIANT GWAS and used currently on a clinical basis to enhance fracture healing. Longitudinal growth and the restoration of bone after bone loss or fracture healing are being achieved by the process of endochondral bone formation. In the former, endochondral bone formation occurs in a spatial and organized manner and hence is a valuable model for studying the different pathways that contribute to natural growth and to the pace of endochondral bone formation. Instead of focusing on mutations that cause dysregulation of growth, the more natural phenomenon of variation in height can be studied in order to gain more knowledge about the different endocrine and local pathways that influence bone formation and deduct promising candidates for strategies augmenting bone formation. The canine species is an excellent model to study variation in height due to the extreme intraspecies differences and the resembling growth plate physiology to that of humans. Local differences related to a differential pace of endochondral bone formation in the growth plate of the canine species, can identify new targets that could be translated towards regenerative medicine.

Chapter 4: Characterization of canine bone marrow- and adipose-tissue derived mesenchymal stem cells

Abstract

Mesenchymal stem cells (MSCs) possess the ability of self-renewal and differentiating toward different lineages and can be easily obtained from donor tissue. Because of these characteristics, MSCs are an excellent therapy candidate in the regenerative medicines. Although the dog is an excellent experimental model and the employment of MSCs is clinically relevant in the veterinary practise, limited research have been performed on canine MSCs (cMSCs). The aim of this study was therefore to characterise cMSCs and compare the differentiation potential of MSCs derived from bone marrow and from adipose tissue. For this purpose, cMSCs derived from bone marrow (BMSCs) and adipose tissue (ASCs) were differentiated towards the three lineages; osteogenic, adipogenic, and chondrogenic. Osteogenic differentiation was demonstrated in 6 out of 18 donors by staining of the mineral deposits with alizarin red and upregulation of the SPP1 and Osteocalcin gene compared with the control group. Adipogenic differentiation was achieved in all donors and was visualized by staining of the lipid droplets with Oil-red-O and corroborated by upregulation of the ADIPOQ and PPARG genes. Unfortunately, all attempts at differentiation the MSCs toward the chondrogenic lineage did not succeed.

Canine MSCs showed osteogenic and adipogenic lineage differentiation potential and adherence to the culture plastic and could therefore be characterized as being MSCs. However, a difference in potential was noticed between BMSCs and ASCs; BMSCs were able to differentiate more easily towards the osteogenic lineage whereas ASCs seemed to have a better potential to differentiate towards the adipogenic lineage, given the fact that they stained more intense for Oil-red-O and the upregulation of the adipogenic genes.

Introduction

Mesenchymal stem cells (MSCs) are adult stem cells that possess the ability of self-renewal while maintaining themselves in an undifferentiated stage and can differentiate to multiple lineages.[164] Although the differentiation of MSCs was thought to be limited to the tissue it resides in, in vitro studies demonstrated that MSCs can differentiate also towards derivatives of germ layers other than the mesoderm.[165] However, MSCs, being adult stem cells, do not equalize the high potency of embryonic stem cells, which are capable of easily differentiating into all three germ layers (endoderm, ectoderm and mesoderm).

Due to a lack of specific markers, MSCs are defined based on three characteristics: 1) their adherence to cell culture plastic 2) positive expression of the CD105, CD73 and CD90 surface antigen markers and lack of the CD45, CD34, CD14 or CD11b, CD79α or CD19 markers and 3) the ability to differentiate into the adipogenic, osteogenic, and chondrogenic lineages in vitro. [166]

MSCs have been conventionally isolated from bone marrow but more recently from many other tissues such as adipose tissue, liver, muscle and brain. Although the MSC populations presented similar morphology and cell surface markers, there was a variation in the differentiation potential depending on the source of the MSC itself. [167]

At this moment, local applications for MSCs are tested in for example human clinical trials concerning the use of MSC to treat peripheral arterial diseases[168] and acute myocardial infarction[169] but also to treat orthopedic defects, for example large bone defects[170171] and cartilage defects .[172] All clinical trials show promising results for the use of MSCs in field of regenerative medicine.

MSCs have a high potential to be used in regenerative medicine because the cells are easily obtained and cultured in vitro. After expansion of the MSCs *in vitro* (and if necessary differentiation), the patient could receive autologous cells, which decreases the risk of rejection. However, the tissue of origin of the MSC may be an important factor in the use of MSC in regenerative medicine. For example, adipose derived stem cells (A(D)SC) have several advantages compared to bone marrow derived MSCs (BMSCs), including an easy accessibility and higher stem cells concentration. Although the morphology of ASCs resembles the morphology of BMSCs and both differentiate to the adipogenic and osteogenic lineage, the CD marker expression and the osteogenic differentiation potential differs between the two MSC populations. [173174] Even more so, the bone regenerative potential of ASCs compared with BMSCs was studied *in vivo* in a critical sized defect of a sheep tibial in which ASCs showed inferior osteogenic potential compared with BMSCs.[175]

Although the dog is an excellent experimental model as well as a clinically important patient, limited research have been performed in the field of regenerative medicine on canine MSCs (cMSCs). cMSCs have been successfully differentiated to the osteogenic, adipogenic and chondrogenic lineage. [176][177-180]These cells positively expressed the CD29, CD44 and CD90 cell surface markers, which are markers used to identify human MSC, and lacked the expression of CD34 and CD45, which are hematopoietic markers.[176, 179, 180] In addition, positive expression of the pluripotency-associated transcription factors SOX2, OCT4 and NANOG has been shown. [176, 179].

The main aim of this study was to characterise cMSCs and compare the differentiation potential of MSCs derived from bone marrow and from adipose tissue. For this purpose, cMSCs derived from bone marrow and adipose tissue were differentiated towards the three lineages; osteogenic, adipogenic and chondrogenic to characterise cMSCs as being true MSCs. To complete the characterization of these cMSCs, another master student, working parallel to this project with FACS, studied the expression of surface markers of the cMSCs (data not shown here).

Methods and Materials

Isolation of MSCs

Donors

All materials used in this study were collected from animals euthanized in other, unrelated experiments approved by the Ethics Committee on Animal Experimentation (DEC) of Utrecht University.

Bone marrow derived stem cells

After euthanasia of the dog, the limbs were removed and were washed twice with Chlorexidine for disinfection. Thereafter, via an incision in the skin, the femur or humerus was exposed. Subsequently the diaphysis of the femur or humerus was removed with an ossilating saw and collected in a 50 ml tube containing α-MEM (Invitrogen, 22561-021), 10% FCS (PAA Cell Culture Company), 1% penicillin/streptomycin (PAA, P11-010) and 15-20 IU/ml heparin (Leo Pharmaceutical Products BV, DG7794). To prevent aggregation of the red blood cells (RBC), and hence entrapment of the mononucleas cells within the aggregates resulting into lower yields of BMSCs, this medium was kept at room temperature and heparin was added to the medium.

The bone marrow was flushed out and collected in a sterile petridish. After an automatic cell count (Biorad TC10 automated cell counter) the cells were plated on a T175 flask at a density of 1,3-2*10^6 live cells/cm^2 in expansion medium (10% FC, α-MEM, 1%

penicillin/streptomycin , 0.1 mM ascorbic acid (Sigma A8960) and 10^{-9}M dexamethasone (Sigma D1756)). After 24 hours incubation at 37°C in 5% CO_2 and 20% O_2 , the unattached, dead cells and debris were removed by washing the cells twice with Hanks solution (PAA) containing 2% FCS, added to prevent the loss of loosely attached MSCs.

Adipose tissue derived stem cells

After shaving and disinfecting of the skin, an incision in the back of the dog was made to remove subcutaneous fat. Fat was collected in 50 ml tubes with α-MEM with 1% penicillin/streptomycin without FCS.

The blood vessels and fibrous tissue-connections were dissected with a knife blade no 10 in a sterile petri dish. 0,04% Collagenase type 1 (C9891, Sigma) was added at a ratio of 1:1 of the weight of the fat and the tissue was agitated for approximately 60 minutes at 37°C on an orbital shaker at 250 rpm till the fat was viscous. After centrifuging the mixture at 1500 rpm for 15 minutes at RT, the supernatant was removed and the cell pellets were resuspended in 10% FCS α-MEM medium. Thereafter, the suspension was filtered with a 70um cell strainer (BD falcon) and centrifuged at 1500 rpm for 5 minutes at RT. The cell pellets were resuspended in expansion medium (10% FCS, α-MEM, 1% penicillin/streptomycin, 0.1 mM ascorbic acid and 10^{-9}M dexamethasone) and plated in a T175 flask at a density of 7* 10^6 live cells/cm^2. After 12-24 hours erythrocytes and unattached cells were removed by washing with Hanks 2% FCS.

Differentiation of the MSCs towards the three lineages

Pilot experiment in Rotterdam performed by F. Verseijden

Before the start of this Honours Programma, a pilot differentiation experiment was performed by F. Verseijden (which will be mentioned further on as the Rotterdam experiment). The techniques used in this pilot experiment were the same as described in this paper and performed during this Honours Programma year. The analysis of this Rotterdam experiment (qPCR and GAG/DNA analysis) was performed during this Honours Programma by M.Teunissen in Utrecht.

Expansion

Media changes were performed twice a week during the expansion phase. Cells were passaged two times at 80-90% confluence.

Osteogenic differentiation

For osteogenic differentiation, cells were plated at a density of 3000 cells/cm^2 in six-well plates (Greiner bio-one Cellstar, 657160) and supplemented with an osteogenic medium consisting of DMEM high glucose (Invitrogen, 31966-021), 10% FCS, 1% penicillin/streptomycin, 0.1 mM acorbic acid, 10^{-7} M dexamethasone and 10 mM β-Glycerol-

Phosphate (Sigma G6376) for 21 days. For each donor, four wells were used for osteogenic differentiation and two wells were used as a control which were given expansion medium for 21 days.
After 21 days cells of two osteogenic differentiated wells and one control well were collected in 350 µl RLT for qPCR and two osteogenic differentiated wells and the other control well were stained with Alizarin Red for a histological and morphological evaluation.

Adipogenic differentiation

For adipogenic differentiation, cells were plated at the seeding density of 150.000 cells/cm_2 in six-well plates and supplemented at a confluency of 90-100% with an adipogenic medium consisting of DMEM high glucose , 10% FCS, 1% penicillin/streptomycin, 0.1 mM acorbic acid, 10^{-6} M dexamethasone, 0.2 mM indomethacin (Sigma i7378), 0.5 mM 1 methyl-3-isobutyl xanthine (IBMX)(Sigma i5879) and two different concentrations of insulin; 0,1 mg/ml and 0,01 mg/ml (Sigma i9278) for 21 days. For each donor, duplicate samples were used for adipogenic differentiation and one sample was used as a control for each concentration of insulin. Cells in the control wells were seeded at the same density and received expansion medium for 21 days.
For each donor, after 21 days, cells of two adipogenic differentiated wells and one control well were collected in 350 µl RLT for qPCR and two adipogenic differentiated wells and the other control well were stained with Oil red O for a histological and morphological evaluation.

Chondrogenic differentiation

For chondrogenic differentiation a pellet culture was used in which $0.2*10^6$ cells/well were suspended in 0.2 ml and placed in a 96-well plate (Corning Costar 7007), a plate with a round bottom and made of polystyrene resulting in an ultra-low attachment of the cells . The plate was centrifuged for 5 minutes at 1500 rpm at room temperature. After 24 hours (37°C, 5% CO_2), pellets were formed and chondrogenic medium was supplemented. This medium consisted of DMEM high glucose, 1% penicillin/streptomycin, 1% ITS (BD-354350), 0.04 mg/ml proline (Sigma P5607),0.1 mM acorbic acid, 10^{-7} M dexamethasone and 10 ng/ml TGF-β1 (R&D systems 240-B-010). The pellets were cultured for 35 days and for each donor, three conditions were tested; a control condition with chondrogenic medium but without TGF-β1, a condition with TGF-β1 and a condition with TGF-β1 and 10 ng/ml BMP-6 (Peprotech Cat#: 120-06). BMP-6 was added to study the positive effect of BMP-6 on the chondrogenic differentiation potential of the ASCs.[181] Medium was changed two times a week. After 35 days from each condition 3 pellets were collected in 350 µl Trizol (Invitrogen, 15596018) for qPCR, 3 pellets were collected for GAG/DNA content determination and 3 pellets were collected for histology and stained with safranin-O/Fast Green.

In Annex V are different variants of the chondrogenic experiment described because the design of the experiment mentioned above did not resulted in chondrogenic differentiation.

Staining

Alizarin Red staining

To visualize osteogenic differentiation, Alizarin Red staining was used. After discarding the medium, the cells were washed with hanks and 2 ml of neutral buffered formalin (10%) (NBF) was added and the cells were incubated for 30 minutes. Next the cells were washed with distilled water and 1 ml of Alizarin Red(Sigma A5533-256, pH 4.1-4.3, final concentration 2%) was added. The cells were incubated with alizarin red for 30 minutes at room temperature. Calcium deposits were detected by their red color with light microscopy.

Oil red O staining

The cells of the adipogenic differentiation were washed with hanks after discarding of the old medium and fixed with 2 ml of neutral buffered formalin (10%) for 30 minutes at room temperature. Subsequently the cells were washed two times with hanks and 1 ml of Oil red O (Sigma, O0625) was added for 20 minutes after which the staining was carefully removed and the cells were washed again with hanks. Droplets of fat stained red and were visible with light microscopy.

Safranin-O/Fast green staining

Pellets treated with chondrogenic medium were fixed in 200 µl NBF for 2 -24 hours at 4°C. Hereafter 2 µl of 10% eosine was added to the NBF (Final concentration; 0,1% eosine in NBF), fixing the pellet overnight. Eosine (Boom BV Memmel, K886235) was added to pre-stain the pellets, increasing the visibility of the pellet during the processing of the pellet. After fixing and dehydration, pellets were embedded in paraffin, cut into 5 µm thick sections and stained with Safranin O/Fast green staining.

Slides were deparaffinised, hydrated and stained paced in Hematoxylin (Vector, H3404) for 10 seconds. After washing in tap water the slides were stained with 0.4% Fast Green (Sigma, F7252) for 4 minutes. Next the slides were rinsed in two changes of 1% Acetic Acid and stained with 0.125% Safranin O (Sigma, S8884). Safranin O stained the proteoglycans in cartilage red while the background stained blue/green by the Fast green staining.

Gene expression analysis using quantitative PCR

RNA isolation

Samples were stored with RLT or Trizol in -70°C. Total RNA of the osteogenic and adipogenic differentiation samples was isolated using the RNeasy minikit (Qiagen 74134), according to the manufacturers protocol, including an on column DNAse step. Before RNA extraction, the pellets were crushed with a pellet pestle (Argos technologies Inc, 9951-901)

in Trizol until the pellet was homogenized after which total RNA was isolated using the RNeasy microkit (74004), consistent with the protocol. The amount of RNA was quantified using NanoDrop ND-1000 spectophotometer (Isogen Life Science, De Meern, the Netherlands) and the RNA integrity was determined using the Bioanalyzer 2100 (Agilent Technologies, Amstelveen, the Netherlands).

cDNA

cDNA was synthesized from approximately 350 ng RNA using iScript™ cDNA Synthesis Kit (Biorad) according to the manufacturers protocol.

qPCR

qPCR was performed using a BioRad CFX-384 cycler and IQ SYBRGreen SuperMix (BioRad, Veenendaal, the Netherlands). Each sample had at least two biological replicates and two technical replicates. And included No template controls (NTC) and positive controls (adipose tissue, bone and cartilage).

The primers that were used were dog-specific and the primers of the genes of interest were all validated in silico using BLAST (specificity analysis) and M-fold (secondary structure) And the formed PCR-products were checked using gel electrophoresis and sequencing analysis. (Annex V)

Selection of Osteogenic, Adipogenic and Chondrogenic Genes

The primers that were designed for the determination of the adipogenic differentiation were adiponectin (*ADIPOQ*) and perixome proliferator-activated receptor gamma *(PPARG*). Adiponectin is expressed in and excreted by exclusively adipose tissue [182] and *PPARG* promotes adipogenic differentiation.[183]

Primers selected for osteogenic differentiation were Osteonectin *(SPARC),* Osteopontin *(SPP1) and* Osteocalcin *(BGLAP).* Osteonectin is an early bone specific osteogenic differentiation marker [184] while osteocalcin is considered to be a late differentiation marker. [185] Osteopontin regulates the formation and remodeling of the mineralized tissue en is expressed during the osteoblast and osteocyte stages. [185186]

Collagen type X *(COLX), SOX9,* Collagen type II *(COLII) and* Aggrecan *(ACAN)* were chosen for chondrogenic differentiation. Sox9 is the earliest chondrocyte marker and is a necessary transcription factor for chondrocyte proliferation.[187] Activation of Sox9 leads to activation of other early chondrocyte differentiation markers as collagen type II and aggrecan, both cartilage matrix components. [187] Collagen type X is a late chondrocyte differentiation marker as collagen X is mainly found in the hypertrophic phase of chondrogenic differentiation.

15 referenece genes were chosen to estimate the relative expression of the differentiation genes; *Glyceraldehyde-3-phosphate dehydrogenase* (*GAPDH*), *hypoxanthine guanine phosphoribosyl transferase (HPRT), beta-actin (L), Ribosomal protein S19 (RPS19), heterogeneous nuclear ribonucleoprotein H (HNRPH), Ribosomal protein L8 (RPL8), glucoronidase beta (GUSB), Ribosomal protein S5 (RPS5), Signal recognition particle receptor (SRPR), Beta 2 Microglobulin (B2MG), hydroxymethylbilane synthase (HMBS), Ribosomal protein L13 (RPL13), succinate dehydrogenase complex, subunit A (sDHA), tyrosine 3-monooxygenase/tryptophan 5-monooxygenase activation protein (YWHAZ), TATA box binding protein (TBP)* (Annex V) The amplication efficiency of all genes was between 95% and 105 % with the exception of β-actin (89%), TBP (92%) and PPARG (110%).

Relative expression of the genes of interests was estimated using the efficiency-corrected delta-delta Ct (ΔΔCt) method (Pfaffl) and $2^{\wedge- \Delta\Delta CT}$ method (the Litvak method) using a set of six reference genes. (see: choosing the optimal reference gene)

GAG/DNA analysis of the pellets during chondrogenic differentiation

To evaluate the formation of cartilage matrix by the differentiated MSCs, the amount of glycosaminoglycans (GAGs), a cartilage matrix component, is measured. The amount of GAGs are corrected for the size of the tissue by measuring the amount of GAGs per DNA.

Pellets were washed with PBS and frozen in -70°C without any liquid until further analysis. Subsequently the pellets were digested with 300 µl proteinase K in Tris EDTA buffer (pH 7.6) containing 185 µg iodoacetamide (I6125 Sigma Aldrich) and 1 µg/ml pepstatin A (P4265 Sigma Aldrich) overnight (>16 hours) at 56°C. After digestion, the tubes were centrifuged and the supernatant was used to determine DNA and GAG content.

Determination of DNA content

First a standard DNA curve was prepared in a 96-wells plate ranging from 0 µg DNA to 1,25 µg DNA in six steps. Technical duplicates were placed in the 96-wells plate, using 50 µl of sample per well. Subsequently, 100 µl heparin (8,3 IU/ml; Leo Pharmaceutical Products BV) and 50 µl RNAse (0,05 mg/ml; Sigma R5125) were added to the samples and standards and the plate was incubated at 37°C for 30 minutes. After incubation, 50 µl ethidium bromide (25 µg/ml; GibcoBR1, 15585-011) was added to the standards and the samples and the plate were read on a Wallac 1420 Victor microplate reader at an excitation of 340 nm and a emission of 590 nm. A standard curve was calculated based on the extinction of a sample of the standard line with a specified amount of DNA. Subsequently the amount of DNA in the sample was calculated by the formula; (extinction - y-intercept of the standard curve) / slope of the standard curve.

Determination of GAG content

Before the experiment, 0.016 g DMB (Polysciences 03610) was solved in 5 ml 100% ethanol and placed overnight on a stirrer at room temperature. 2.37 g NaCl and 3.04 g Glycine were solved in 500 ml of demi water and mixed with the DMB solution. After the pH was adjusted to 3.0, water was added up to 1 liter and the solution was placed on a stirrer overnight at room temperature.

Three different amounts of sample(5 µl, 10 µl and 50 µl) were pipetted in a 96-wells plate after which PBS-EDTA was added to a total volume of 100 µl. A standard was diluted in 11 steps ranging from 0 to 20 µl of Chondroitin Sulfate C (0.5 mg/ml Sigma C4348) and PBS-EDTA was added till 100 µl. Next, 200 µl of DMB solution was added to standards and samples and the plate was read as fast as possible at an extinction of 590 nm and 530 nm. A standard curve was calculated based on the 530/590 ratio of the standard line. The y-intercept and slope of this curve are used to calculate the amount of GAGs in a sample with the formula; (($530_s/590_s$-blanco) - y intercept of the standard curve) / slope of the standard curve.

This GAG content was corrected for the amount of DNA to calculate the relative GAG content per pellet.

Data analysis

Statistical analysis was performed using R statistical software. For analysis of the qPCR data, the ΔCT values were used and the GAG/DNA value was used for the analysis of the GAG production during chondrogenic differentiation. A linear model with random effects was used to analyze these data. The random effects took the correlation of the observations within a donor into account while the fixed effects consisted of the cell lineage and cell type and the interaction between cell lineage and cell type. In the analysis of the GAG/DNA content the age of the donors was also a fixed effect that should be taken into account. The models were chosen based on the Akaike Information Criterion (AIC). Conditions for the use of the linear mixed model, including normal distribution of the data, were assessed by analyzing the residuals with a QQ plot and a shapiro test; no violations were observed. P-values were estimated to analyze differences between differentiation group (Control, adipogenic, osteogenic and within the chondrogenic group between no growth factor, TGFβ1 and TGF β1 + BMP6) and between cell type (ASC and BMSC). A p-value of < 0.05 was considered to be significant.

Results and Discussion

MSC isolation and expansion

After 24-48 hours, adherent cells were observed and non-adherent cells were removed by changing the medium. Morphologically, these adherent cells had a spindle-shaped, fibroblast-like appearance and were stretched out on the bottom of the flask. (Figure 3) After two days the cells of the young donors started to form colony forming units (CFUs). These young donors reached 80-90% confluence after 4 days after which the cells were passed. Older donors formed CFUs after 4 days and reached confluence after 6-7 days. CFUs were observed in BMSC populations as well as ASC populations.

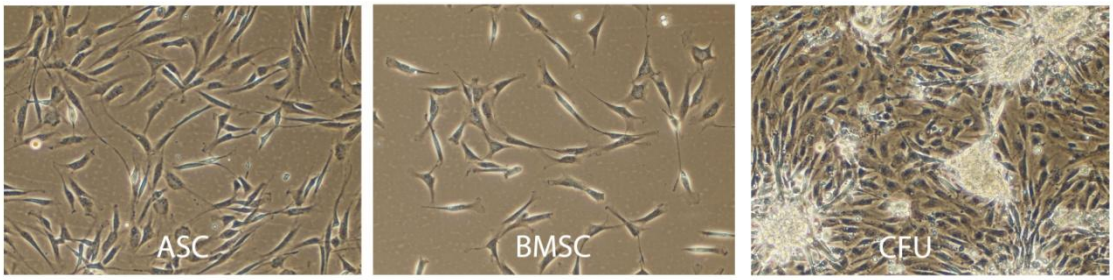

Figure 3: Adipose derived (ASC) and bone marrow derived (BMSC) MSCs with the typical spindle-shaped, fibroblast-like appearance during expansion. After 2-4 days at P0, Colony forming units (CFUs) could be observed.

Staining

Osteogenic differentiation

Cells were cultured in osteogenic medium for 21 days. These cells gradually adapted a more round, polygonal appearance and small nodules started appearing after two weeks. After 21 days the cells were stained with alizarin red to demonstrate mineral deposits characteristic for osteogenic differentiation. At this time point, five out of nine BMSC donors and one out of nine ASC donors showed alizarin red positive noduli (Figure 4). The other donors did stain red without the characteristic nodulus formation. Notably, wells that were less confluent showed relatively more noduli.

Control wells cultured on expansion medium became over-confluent after 21 days and cells detached massively. However, control wells in which the cell layer stayed attached, no positive staining for alizarin red was apparent and no noduli were present.

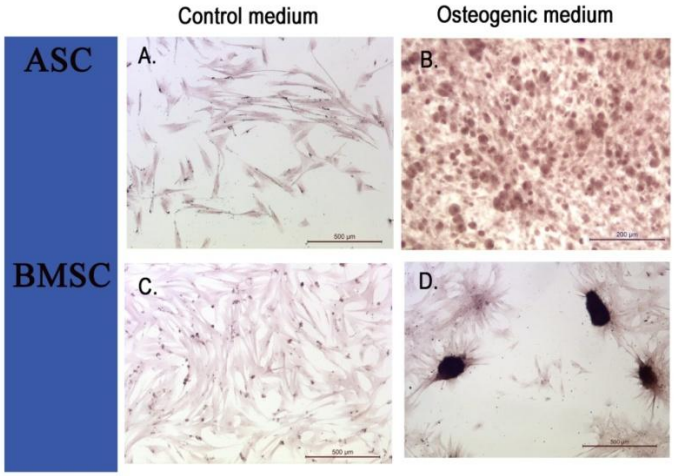

Figure 4: Osteogenic differentiation of adipose-derived stem cells (ASCs; A,B) and bone-marrow derived stem cells (BMSCs; C,D) in control medium (A,C) and osteogenic medium (B,D) stained with Alizarin red after 21 days of culture. The mineralized osteogenic noduli stain red. Scale bar = 500 µm.

Adipogenic differentiation

The cells cultured in adipogenic medium for 21 days were stained with Oil-red-O to show intracellular lipid droplets (Figure 5). All donors were successfully differentiated to the adipogenic lineage. However, the intensity of the staining differed between BMSC and ASC; in the ASC cytoplasmic lipid droplets were larger and more abundant compared with the BMSCs and the colour of the staining was a brighter red. Furthermore, there were no distinct macroscopic differences between the two different concentrations of insulin.

The control wells did not show oil-red-o positive droplets in the BMSC populations but in the ASCs cultured in expansion medium, spontaneous differentiation was sporadically seen.

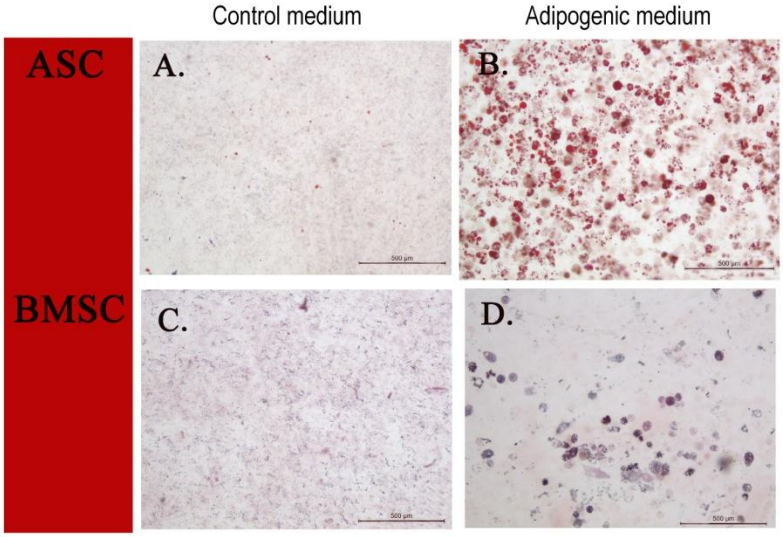

Figure 5: Adipogenic differentiation of adipose-derived stem cells (ASCs; A,B) and bone-marrow derived stem cells (BMSCs; C,D) in control medium (A,C) and adipogenic medium (B,D) stained with Oil-red-O. Cytoplasmatic deposits of vet stain red. Scale bar = 500 µm.

Chondrogenic differentiation

Small white pellets were formed at the bottom of the plate 24 hours after seeding and centrifugation of the cells (Figure 6).

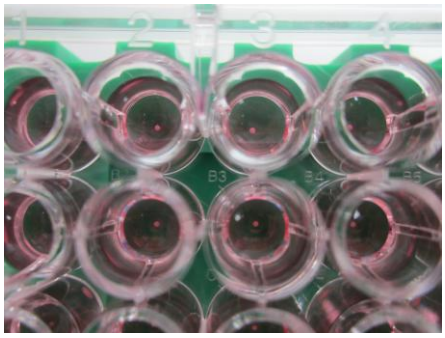

Figure 6: Pellet culture of MSCs in 96-wells plate

Pellets which did not receive growth factor seemed to remain smaller compared with the other two conditions. None of the pellets cultured under chondrogenic conditions stained positive for Safranin-O at 35 days of culture. Together with the absence of chondrocytes and lacunae, there were no indications for a successful chondrogenic differentiation. Some pellets contained an outer layer which did not contain any nuclei and consisted of amorphous material, the thickness of this layer differed between pellets and was not consisted with a specific condition. The central zone consisted of many polymorphic cells with small sometimes pyknotic or karyorrhectic nuclei.

Notably, pellets of canine BMSCs and ASCs cultured in a similar chondrogenic medium for 35 days before in the orthopaedics laboratory of Rotterdam provided a positive staining for Safranin-O in three out of six donors, of which two were BMSC donors and one was an ASC donor. Histology showed a red cartilage like centre surrounded with a green layer of fibroblast-like cells without nuclei (Figure 7).

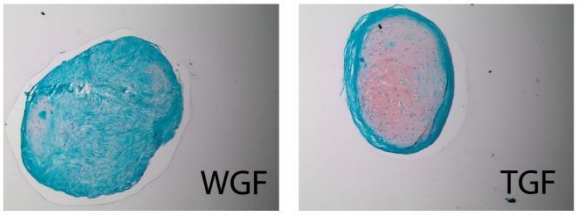

Figure 7: Representative example of chondrogenic differentiation of MSCs performed in a previous study in collaboration with the group of Orthopedics in Rotterdam. Without growth factor (WGF) and with TGF-β1 (TGF). In the pellet conditioned in medium with TGF-β1, a positive staining for safranin-O (red) is seen.

After these unsuccessful attempts of chondrogenic differentiation with the described protocol, the expansion medium composition was adapted on the basis that the expansion period may also affect chondrogenic differentiation.
FGF is known to enhance the chondrogenic differentiation potential of human BMSCs in vitro[188] , and was therefore added during expansion of the MSCs. Unfortunately, no chondrogenic differentiation was demonstrated. We repeated the experiment adjusting the approach (Annex V); FCS and bovine serum albumin (BSA) was added but had no effect. Then, the TGF-β1 was replaced by TGF-β2, but again no effect was observed. In the end none of the experiments contained pellets stained positive for the safranin-O staining.

Currently, an experiment is ongoing and chondrogenic culture will be terminated in the second half of September 2013. The expectation is that with the addition of bFGF to the expansion medium and ITS+ and TGF- β1 from R&D to the chondrogenic medium, the chondrogenic differentiation will succeed. In the literature ITS+ is used most of the time to induce chondrogenic differentiation instead of ITS. In addition the activity of TGF- β1 from R&D is suspected to be higher than the activity of TGF- β1 from Peprotech.

mRNA analysis by qPCR

Optimisation of the reference genes

It is generally accepted to normalize gene expression with an internal reference or housekeeping gene because several variables (such as the amount of starting material and enzymatic efficiencies) have to be controlled. The expression of this gene should not differ

between the samples (tissues or cells) that are investigated. Unfortunately this perfect reference gene does not exist. However, in most of the literature describing the differentiation of MSCs, only one gene (GADPH, B-actin or B2MG) is chosen to normalize the gene expression of the qPCR results. The relative expression of this gene may however differ in different samples and differs most likely at least between ASCs and BMSCs as both cells show a different gene expression pattern. A more reliable option is to normalize the gene expression with a set of reference genes that are chosen based on analysis of the stability of these genes in the samples.

In this project the optimal set of reference genes for BMSCs and ASCs was investigated using two methods; Normfinder[191] and Genorm[192] (Table 1).

	All		BMSCs		ASCs	
Rank	**Genorm**	**Normfinder**	**Genorm**	**Normfinder**	**Genorm**	**Normfinder**
1.	RPL8 | RPS5	sDHA	RPS19 | sDHA	sDHA	RPL8 | RPS5	SRPR
2.		GADPH		RPS19		HPRT
3.	RPS19	HMBS	GUSB	GADPH	RPS19	GADPH
4.	sDHA	TBP	B2MG	TBP	HNRPH	sDHA
5.	GUSB	RPS19	RPS5	HMBS	SRPR	HMBS
6.	B2MG	RPS5	RPL8	B2MG	sDHA	HNRPH
7.	GADPH	RPL8	GADPH	GUSB	GADPH	RPS19
8.	HMBS	GUSB	HMBS	YWHAZ	GUSB	RPS5
9.	TBP	YWHAZ	TBP	RPL8	B2MG	TBP
10.	YWHAZ	B2MG	YWHAZ	RPS5	HPRT	RPL8

Table 1: Ranking of the reference genes based on Genorm and Normfinder.

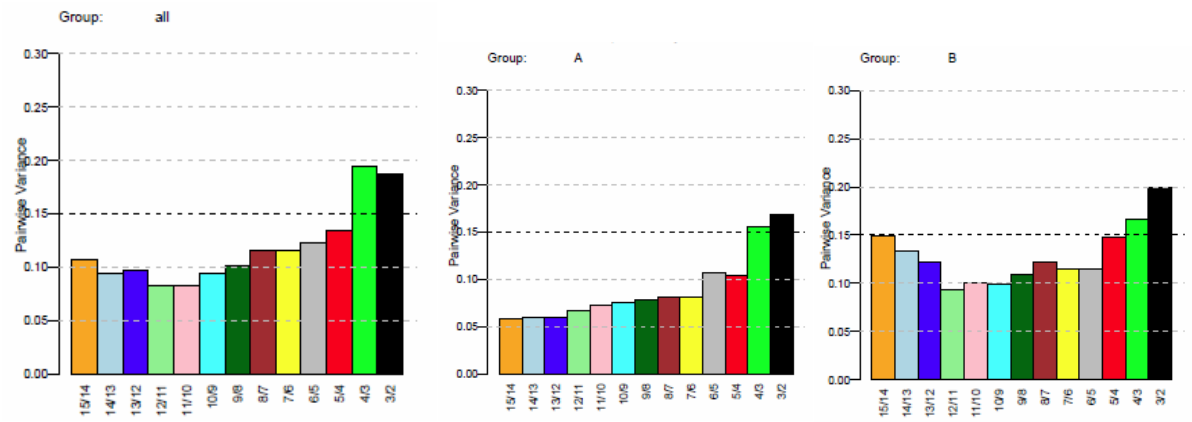

Figure 7: Pairwise variation of reference genes in different groups. All = ASCs and BMSCs combined, A = ASC, B = BMSC, indicating that the 5 reference genes would be sufficient for reliable normalization of the data with all samples, 5 reference genes for the ASC data and 6 reference genes for the BMSC data.

For all (ASCs (A) and BMSCs (B) combined), Genorm analysis (Figure 7) revealed that 5 reference genes would be sufficient for reliable normalization with the three ribosomal reference genes; *RPL8*, *RPS5* and *RPS19*, and *sDHA* and *GUSB*. This set of reference genes is similar to the set of reference genes that Genorm analysis revealed for the BMSC group, with the addition of B2MG due to the need for a sixth reference gene for a reliable normalization of the gene expression of BMSC group. However, the Genorm analysis showed a different optimal set of reference genes for the ASC group in which 5 genes were needed for a reliable normalization. In the ASC group *HNRPH* and *SRPR* were added to the three ribosomal genes which were also the most stable in the BMSC and the combined group.

When using the Normfinder analysis, a different set of reference genes was found. The most outstanding difference is the disappearance of the ribosomal reference genes in the top of the list of stable genes. Normfinder analysis revealed that *sDHA*, *GADPH*, *HMBS*, *TBP* and RPS19 were the most stable reference genes for the combined group and *sDHA, RPS19, GADPH, TBP, HMBS* and *B2MG* were most stable for the BMSC group. But again these two groups are very much alike. For the ASC group the Normfinder analysis revealed that *SRPR*, *HPRT*, *GADPH*, *sDHA*, *HMBS* were the most stable reference genes.

The difference between the two methods could be caused by the co-regulation of the ribosomal reference genes (*RPS5*, *RPL8* and *RPS19*). Because these reference genes are co-regulated, their expression patterns are very much alike, resulting in a low average pairwise variation with the Genorm analysis and a high place in the stability ranking of this analysis. Taking this co-regulation into account, the first six reference genes for each group (ASC and BMSC) were chosen from the Genorm ranking to normalize the gene expression of the genes of interest of the qPCR data.

Relative gene expression

qPCR analysis was performed to compare the osteogenic and adipogenic differentiation with undifferentiated MSCs of both BMSCs and ASCs.

When the relative expression (N-fold change) was calculated for all the samples together no significant regulation of the osteogenic markers *osteopontin* (*SPP1)* and *osteocalcin* (*BGLAP)* was seen while *osteonectin (SPARC)* was significantly downregulated in the osteogenic group with respectively 3.2 and 4.6-fold compared with the control group in both the ASC as well as the BMSC.

The unexpected down-regulation of SPARC can be attributed to the fact that only 6/18 donors revealed osteogenic differentiation based on the alizarin red staining. However, none of the donors showed individually an upregulation of *SPARC* in the osteogenic group compared with the control group even if *SPP1* and *BGLAP* were upregulated(figure 8). In

these cases, *SPARC* could be down regulated because *SPARC* is an early marker for osteogenic differentiation and *SPP1* and *BGLAP* are late markers of osteogenic differentiation.

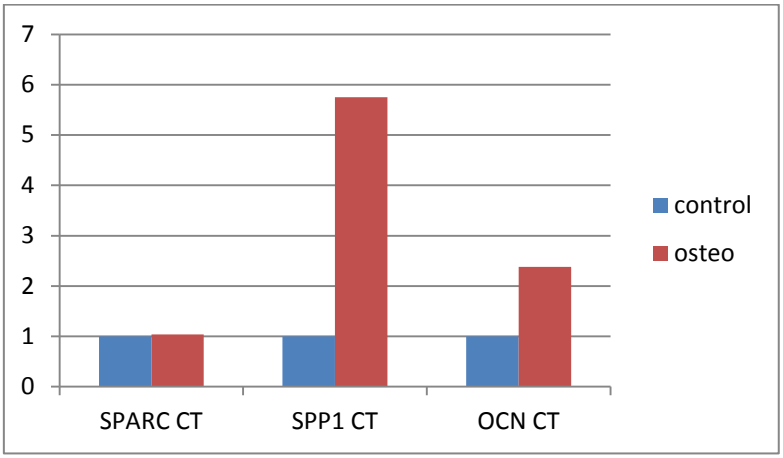

Figure 8: Relative gene expression of *SPARC, SPP1, Osteocalcin (OCN)* in one donor (ASC). Upregulation of *SPP1* and *OCN* is seen in osteogenic group compared with their own control, but no upregulation of *SPARC* is seen.

In order to investigate this hypothesis, samples should be taken at different time points of osteogenic differentiation in order to identify if *SPARC* is upregulated at the onset of osteogenic differentiation of the MSCs. For the samples in which *SPP1* and *BGLAP* are also downregulated or not differential regulated, it is likely that no osteogenic differentiation was present in the sample and therefore no upregulation of associated genes.

In order to be able to identify the value of the chosen gene markers in identifying ostegenesis, a subset of data was made of samples that stained positively for the Alizarin red staining (N=6) and samples that showed an individual upregulation of both *SPP1* and *BGLAP* (N = 2). First, it is worth mentioning that the gene expression of both *SPP1* and *BGLAP* differed in the control groups of the ASC and BMSC and therefore the relative gene expression of the genes was calculated for the ASCs and BMSCs separately, using their own control group as the calibrator.

Statistical analysis of this subset of data revealed that *SPP1* was upregulated in both ASC and BMSC in the osteogenic group compared with the control group with a N-fold change of respectively 233 ± 31 and 12 ± 2.6 (Figure 9) . *BGLAP* was significantly upregulated in the osteogenic group compared with the control group in both ASC (3.4 ± 0.4) and BMSC (2.2 ± 0.4) (Figure 10).

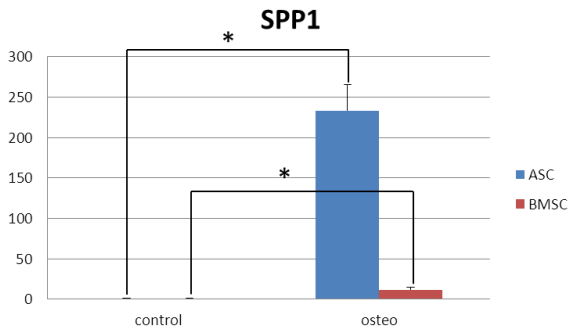

Figure 9: Relative gene expression of *SPP1* in a subset of donors with macroscopi noduli formation staining red with Alizarin red. Upregulation of *SPP1* is seen in both the ASC and the BMSC group cultured under osteogenic conditions compared with their own control cultured in expansion medium, * indicates differences (P < 0.05) between groups, Error bars are the sd of the N-fold .

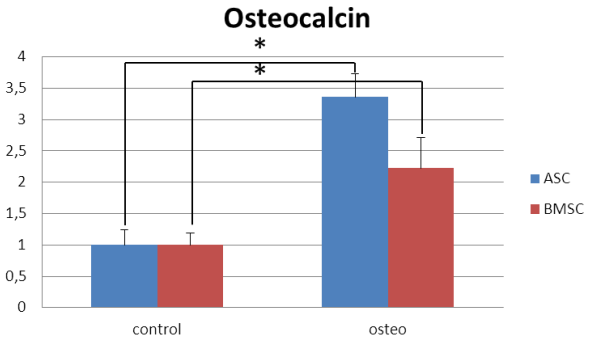

Figure 10: Relative gene expression of *Osteocalcin* in a subset of donors with macroscopi noduli formation staining red with Alizarin red.. Upregulation of *Osteocalcin* is seen in both the ASC and the BMSC group cultured under osteogenic conditions compared with their own control cultured in expansion medium, * indicates differences (P < 0.05) between groups, Error bars are the sd of the N-fold

For the verification of adipogenic differentiation the relative expression of *PPARG* and *ADIPOQ* was calculated. *PPARG* was significantly upregulated in the adipogenic group compared with the control group in ASCs as well as in the BMSCs for both concentrations of insulin. BMSCs revealed a significantly higher PPAR gene expression with a fold change of 36 ± 1 compared to the fold change of 12 ± 0.7 in the ASCs cultured under the same adipogenic conditions (Figure 11). A ten-fold higher insulin concentration resulted in significant increase of gene expression in the ASCs but not in the BMSCs, resulting in an upregulation of *PPARG* that did not differ between BMSCs and ASCs cultured under the same conditions.

The relative gene expression of *ADIPOQ* was significantly higher in the adipogenic group compared with the control group in ASCs and BMSCs in both insulin concentration groups (Figure 12). A ten-fold higher insulin concentration resulted in an increased gene expression in both groups, but this was not significant. The relative gene expression of ADIPOQ was significantly different between the ASCs and BMSCs cultured under the same conditions.

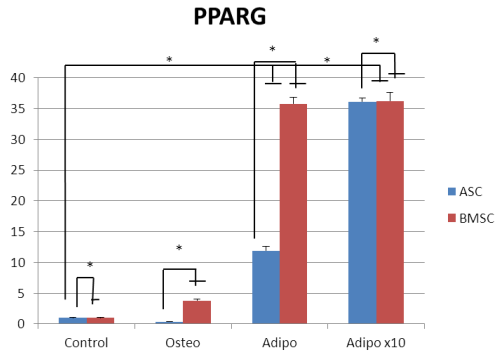

Figure 11: Relative gene expression of *PPARG* in a subset of donors with clear fat deposition in the cytoplasm staining red with Oil red O. Upregulation of *PPARG* is seen in both the ASC and the BMSC groups for both concentrations of insulin (0,1 mg/ml and 0,01 mg/ml) compared with their own control cultured in expansion medium, * indicates differences (P < 0.05) between groups, Error bars are the sd of the N-fold

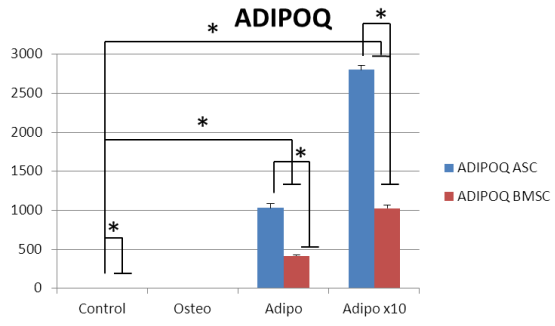

Figure 12: Relative gene expression of *ADIPOQ* in a subset of donors with clear vat deposition in the cytoplasm staining red with Oil red O. Upregulation of *ADIPOQ* is seen in both the ASC and the BMSC groups for both insulin concentrations (0,1 mg/ml and 0,01 mg/ml) compared with their own control cultured in expansion medium, * indicates differences (P < 0.05) between groups, Error bars are the sd of the N-fold

For chondrogenic differentiation Collagen type X *(COLX), SOX9,* Collagen type II *(COLII) and* Aggrecan *(ACAN)* were chosen to be measured but no significant upregulation, indicating chondrogenic differentiation, was found in the combined data. Only two donors showed upregulation of the chosen markers; these donors were cultured at the orthopaedics laboratory of Rotterdam (Figure 13).

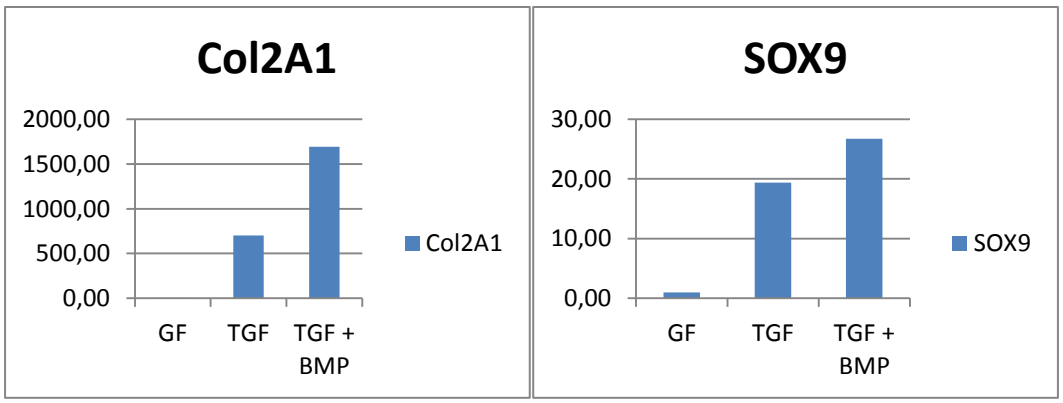

Figure 13: Chondrogenic differentiation of canine BMSC pellets indicated by an increase in Collagen type 2α1 and SOX9 in pellets cultured in chondrogenic medium with growth factors (TGF-β1 or TGF-β1 and BMP-6) compared to pellets cultured in basal medium. Note that the addition of BMP6 seems to have an additive effect on the chondrogenic potential of TGf-β1, which is in line with previous reports.[181193]

GAG/DNA content

Statistical analysis of the GAG/DNA data revealed a significant difference in GAG/DNA content of the TGF-β1 group compared with the control group for the BMSCs, this is in line with the hypothesis of TGF-β1 stimulating chondrogenic differentiation resulting in more GAG production. In addition the amount of GAG/DNA significantly differed between young and old donors within the TGF- β1 group, which is also in line with the expectations: MSCs of young animals have a higher differentiation potential. No other significant differences were discovered.

Most of the samples cultured in control medium resulted in very poor DNA content, indicating that growth factors are essential for the survival of MSCs in pellet formation. This poor DNA content was probably caused by a lower amount of living cells in the pellet and could also be seen macroscopically as the pellets cultured in control medium were much smaller in size than the pellets cultured in chondrogenic medium.

Notably, not all the pellets used in the statistical analysis of the GAGs/DNA data were confirmed to undergo chondrogenic differentiation by qPCR and staining. Therefore the GAGs/DNA analysis should be repeated with more samples that are confirmed to be differentiated towards the chondrogenic lineage by qPCR and staining. In figure 14 the amount of GAGs/DNA is shown for two donors which are confirmed to be differentiated towards the chondrogenic lineage by qPCR and staining.

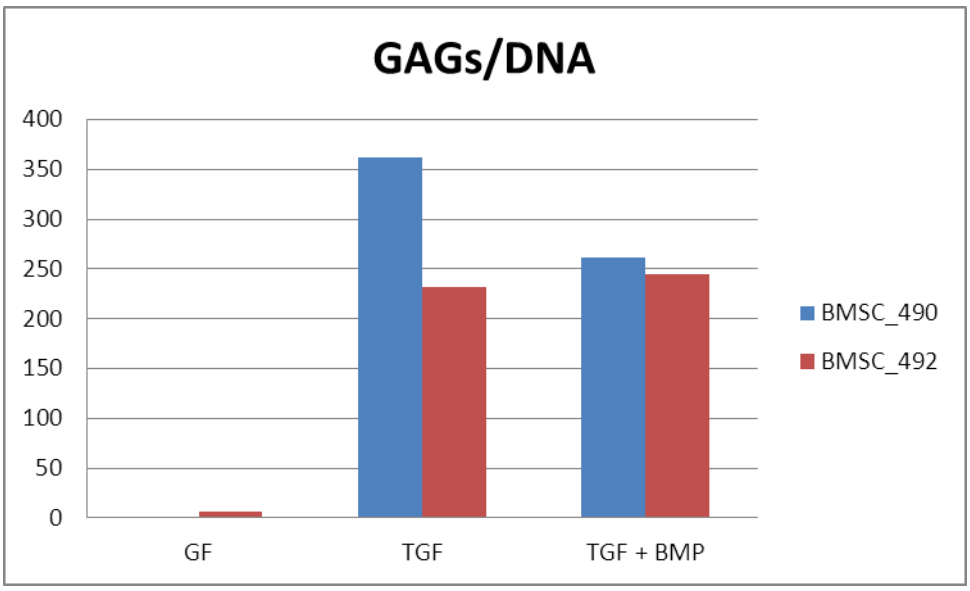

Figure 14: The GAG/DNA content of BMSC donors which showed differentiation towards the chondrogenic lineage by qPCR and safranin-O staining. The amount of GAG is upregulated in both the TGF-β1 (TGF) as well as the TGF-β1 + BMP-6 (TGF+BMP) group compared with the control group (GF).

Conclusion and discussion

MSCs are defined based on three characteristics: 1) their adherence to cell culture plastic 2) positive expression of certain surface antigen markers and lack of hematopoeitic markers and 3) the ability to differentiate into the adipogenic, osteogenic, and chondrogenic lineages in vitro. [166]

In this study, two out of three characteristics were tested in canine adipose derived stem cells (ASCs) and canine bone marrow stem cells (BMSCs). Both cell populations met the first condition; both cell populations adhered to the cell culture plastic.

The third condition was more difficult to meet. Cells of both ASC and BMSC origin differentiated easily to the adipogenic lineage, based on both the presence of intra-cellular lipid depositions as shown by the Oil red o staining and by the significant upregulation of the relative gene expression in the adipogenic differentiated groups of both ASCs and BMSCs compared to controls. The osteogenic differentiation was more difficult to obtain and not all donors succeed to differentiate to the osteogenic lineage (33% success). A great difference was found here between ASC and BMSC as only one ASC donor showed differentiation towards the osteogenic lineage while 5 BMSC donors differentiated. This could be explained by the nature of the BMSCs which are supposed to differentiate towards bone and may need less stimulation to differentiate. However, even in the BMSCs donor variation is present. This donor variation is in line with the variation described for human MSCs in which the human BMSCs showed differences in growth rate and bone-specific gene expression.[194]. In addition, 60% variation in staining intensity with the Von Kossa staining is described in human MSCs. [195] Furthermore, ambiguities arised about the use of the *SPARC* gene as a marker for osteogenic differentiation as no donor showed an upregulation of this gene at 21 days of culture even when distinct mineral depositis were stained positive. However, this could be explained by the nature of this marker, being an early marker of osteogenic differentiation. The inability of the other donors to establish osteogenic differentiation is difficult to explain. There may be a different potential of the donor to differentiate into this specific lineage and in that case the donor may need an extra stimulation, such as BMP-2 of bFGF which are used in other studies to enhance the osteogenic differentiation. [196]This could be further investigated in follow-up studies in which the gene expression of the *SPARC*, *SPP1* and *BGLAP* also should be measured at different time points to study the usefulness of *SPARC* as a marker for osteogenic differentiation in cASCs and cBMSCs. Unfortunately, although we documented that cBMSCs and cASCs have a chondrogenic potential in collaboration with the Orthopedics groups at the Erasmus University, Rotterdam

we did not achieve chondrogenic differentiation of the cMSCs. It is most likely that further optimization of the protocol by employing bFGF in the expansion medium and TGF-β1 from R&D and ITS+ in the chondrogenic medium will lead to a successful chondrogenic differentiation.

Although there are still some problems with the differentiation towards the chondrogenic lineage, it seems that our population of adipose derived and bone marrow derived cells can be characterised as being mesenchymal stem cells. The cells showed adherence to the culture plastics and differentiated towards the adipogenic and osteogenic lineage.

Chapter 5: General Discussion and Future perspectives

In **Chapter 2** the systemic and local pathways that influence endochondral bone formation in both postnatal growth and fracture healing are being described. Investigation of the different factors showed that the regulation of the pace of endochondral bone formation is very much alike in both situations; most of the factors that stimulated bone formation in postnatal growth also stimulate fracture healing. However, it is debatable whether endochondral bone formation during normal growth resembles the process in fracture healing enough in order to be able to state that a factor should be important in fracture healing because it is important in normal growth. For example, BMP-2 is considered to be necessary for the initiation of bone formation in fracture repair and is currently being used to enhance this process in the clinic. In normal growth, on the other hand, it does not seem to have the same importance as a deficiency of BMP2 does not have detrimental effects on skeletal growth. Furthermore, this situation is reversed for the GH/IGF-I pathway which is considered to be the most important contributor to postnatal growth at this moment, whereas in fracture healing administration of GH did not have major effects on the enhancement of the fracture repair.
Despite these differences in the effect of the regulation in the two different processes, it is still possible to identify new targets by studying, not the process as a whole, but the pathways that cause a difference in the pace of endochondral bone formation. The latter is expected to be comparable between endochondral bone formation during skeletal growth and facture healing. One of the methods to study the factors that define the pace of endochondral bone formation is to study the natural variation in growth that contributes to the variation in adult height.

Extensive analysis of all the genes identified to be related to height variation with the aid of genetic studies (**Chapter 3**) revealed that many of the systemic and local factors that are considered to be important in endochondral bone formation were found to be differential regulated between individuals of different height. Most of these differences were found by GWAS and candidate-gene based approaches. However, only a small part of the variation in height could be explained with the results of these studies. Another way of studying variation in height, without the need for an enormous amount of individuals (note that the last GWAS consisted of data collected from more than 183.000 individuals), may be found in the use of a model in which height variation is more extreme. The canine species may be an excellent candidate because in addition to the huge variation in height between the different dog breeds, the canine growth plate also resembles the human growth plate in closure at skeletal maturity.
Therefore a micro-array analysis was performed **(Chapter 3)** to study the differences in gene

expression at the growth plate level between Great Danes (a large breed dog) and Miniature Poodles (a small breed dog). Many differences were found, consisting of differences resembling those found by the GWAS studies as well as many genes that were not previously associated with variation in height. Thus, the canine model seems to have potential as a way to study known and unknown pathways that enhance endochondral bone formation.
However, one limitation of the micro-array was the fact that it studied the whole growth plate including the primary spongiosa. The pace of endochondral bone formation is determined by the proliferative and hypertrophic zone (both contributing to longitudinal growth). In order to define which pathways specifically affect these two differentiation phase of the chondrocytes, the different zones of the growth plate should be compared individually between the two dog breeds. Thus far, there are only reports on the gene expression profiles of specific growth plate zones of mice and rats. [118]

In addition to a comparison of the micro-array data with the reviewed literature, the effect of the identified pathways on endochondral bone formation should be tested in vitro and in vivo. Hereby, the role of the specific pathway on endochondral bone formation can be investigated and further translated to new strategies in the bone regenerative field.

For this purpose, the use of MSCs seem to be a valid option for multiple reasons:

(a) MSCs can be differentiated towards the chondrogenic lineage and when that has succeed via hypertrophic differentiation towards the formation of bone, resembling the process of endochondral bone formation. It is even described that MSCs that are differentiating towards the chondrogenic lineage gradually obtain a gene expression profile resembling a profile similar to that of the cartilage in the epiphyseal growth plate, which shows the potential of MSCs as a model to study the process of endochondral bone formation in the growth plate.[197]
    If the genes that are differential regulated between large and small breed dogs raise the pace of endochondral bone formation, those genes should also stimulate this differentiation of MSCs.
(b) MSCs are currently used in the bone regenerative medicine field. MSCs embedded in a scaffold were used to treat critical size bone defects in sheep[198] and in rats[199]. In both animals, the scaffolds with MSCs resulted in a higher percentage of union of the bone tissue compared with the scaffold alone.[198, 199] And at this moment human clinical trials are on-going for the use of MSCs in bone regenerative medicine.

Altogether, using MSCs provides both the opportunity to study the effect of the differential regulated pathways of the micro-array on endochondral bone formation as well as a strategy for the use of this pathways in the bone regenerative medicine field.

Therefore, canine cells derived from bone marrow and adipose tissue were characterized in **Chapter 4** in order to estimate their true nature as being mesenchymal stem cells (MSCs) and to study the differentiation of these cells towards the osteogenic, adipogenic and chondrogenic lineage. While the adipogenic differentiation was achieved easily, more problems were encountered in the differentiation towards the osteogenic and chondrogenic lineage. Although in human MSCs variation in osteogenic potential is described [194], variation is not reported for the canine MSCs. Only one study mentions that osteogenic differentiation was detected in all MSCs derived from three dogs after 8 weeks of induction with osteogenic medium.[179] Other studies only mention that osteogenic differentiation was successful[180178] or have not shown osteogenic differentiation at all[177].
Our attempts at differentiating MSCs to the chondrogenic lineage were unsuccessful as no positive staining with safranin-O was detected and the morphological appearance of the pellet did not resembled the cartilage-like structure of the pellets as shown in our pilot study in collaboration with Rotterdam. Other studies report also difficulties in obtaining cartilage tissue from cMSCs.[179] And again, many other studies report succeeding in chondrogenic differentiation without any further elaboration. Even more so, in some papers, the only proof for chondrogenic differentiation provided is one image of chondrogenic differentiation without control pellet to compare with, which is in addition often stained with alcian blue.[178] The pellets in this project were also stained with alcian blue, resulting in a blue staining resembling those showed in the literature. However, these pellets did not form any cartilage. This raises the question of the reliability of the reports on the chondrogenic differentiation of canine MSCs and the use of the alcian blue staining to show chondrogenic differentiation of MSCs.

The variation in chondrogenic differentiation between the studies could be explained by technique differences. Although it has been proven that a 3-D culture system is more efficient for chondrogenesis of human BMSCs than a monolayer culture system [200], variation in the protocols of chondrogenic differentiation remains. For example, in the often used protocol for chondrogenic differentiation described by Pittenger[190], no bFGF was used during expansion of MSCs. However, recently it was reported that expansion of human MSCs in the presence of bFGF is needed in order to preserve the chondrogenic potential of the cells.[201] The protocol for chondrogenic differentiation of cMSCs is further being optimized.

Altogether, cells derived from bone marrow and adipose tissue adhered to plastic, differentiated towards the adipogenic and osteogenic lineage and were positive for the cell surface markers CD73, CD90 and CD150 (data not shown), which indicates that the canine cells that were isolated can be characterized as being MSCs.

Future perpectives

In addition to the micro-array, parallel to this HP project, a high-throughput mRNA sequencing (RNA-seq) has been performed and is analysed at this moment. An advantage of the RNA-seq compared to the micro-array analysis is that the RNA-seq allows an unbiased examination of the transcriptome and detection of novel and alternative spliced transcripts while quantitatively measuring the expression of these transcripts with an enhanced sensitivity and at least an equal accuracy. Even more, for the RNA-seq the different zones of the growth plate were separated in order to investigate the specific regulation of the pathways in a particular zone.

Targets identified from this RNA-seq analysis will be studied for their potential to enhance the chondrogenic differentiation of MSCs. But in order to do so, the chondrogenic differentiation protocol has to be successful. This will be our main priority in the upcoming period. As mentioned in chapter 3, a new experiment is being performed combining three probable important factors in chondrogenic differentiation: bFGF in the expansion medium, and ITS+ and TGF-β1 from R&D in the differentiation medium.

When the protocol for 'normal' chondrogenic differentiation is optimized, the effect of the pathways that are differential regulated between GD and MP on the chondrogenic differentiation is tested. In addition, the presence of the identified targets in the growth plate will be investigated immuno-histochemically.
The final goal of this project would be to investigate the effect of the combination of MSCs with this new growth factor on fracture repair.

Chapter 6: Summary

In the orthopaedics regenerative medicine field, large bone defects still represent a huge challenge. The use of autografts is the current state-of-the-art treatment. However, due to disadvantages, such as the need for a large amount of donor tissue and the chance of rejection, new bone regenerative strategies concentrate on alternatives employing scaffold in combination with cells and/or modulating factors. Candidate modulating factors can be identified by studying the natural healing process of bone defects, which heal by endochondral bone formation. Even more so, studying endochondral bone formation at the growth plate level may also simplify the approach, since at the growth plate level chondrocyte proliferation and differentiation occur at an orderly manner.

The overall aim of this project was to study the local pathways that enhance endochondral bone formation in order to identify new bone regenerative strategies. In this respect, this project investigated whether the naturally occurring height variation in the canine species is an appropriate model to study these pathways and set up the in vitro platform in which selected candidates can be evaluated for their efficacy to augment endochondral bone formation.

In **Chapter 2** the influence of systemic pathways (GH/IGF-I pathway, thyroid pathway and vitamin D pathway) and local pathways (IHH/PTHrP feedback loop, TGF-β family, FGF pathway and Wnt signaling pathway) on normal postnatal growth and fracture healing was investigated by means of a review study. Most of these pathways regulated growth in the same way as they regulated the process of endochondral bone formation in fracture repair. In order to extrapolate the role of these systemic and local pathways in regulating variation in height an additional literature study was performed concentrating on genetic studies. GWAS and candidate-gene based approaches in human and canine populations discovered many genes that were differential regulated in individuals with different heights. However, these differences explained only 10% of human height variation. Within the canine species height variation is much more pronounced. Furthermore, the canine growth plate resembles the human growth plate in that they both close after maturity, which makes the canine species a suitable model to study the local pathways that enhance endochondral bone formation at the growth plate level.

A micro-analysis was performed in **Chapter 3**, comparing the growth plates of Great Danes (a large, fast-growing breed dog) with Miniature Poodles (a small, slowly growing breed dog). The micro-array detected 3010 genes that were significantly differential regulated between the two breeds of which 1193 genes were upregulated and 1817 genes were down

regulated. Many of the genes that were associated by the GWAS with height variation, were also differential regulated between the GD and MP.

A characterization of canine mesenchymal stem cells (MSCs) was performed in the studies of **Chapter 4** in which presumable canine MSCs were differentiated towards the osteogenic, adipogenic and chondrogenic lineage. Adipogenic differentiation was confirmed by Oil-red-O staining, showing red lipid droplets, and qPCR, showing an upregulation of *PPARG* and *ADIPOQ*. Osteogenic differentiation was achieved in 5 out of 9 BMSC donors and 1 out of 9 ASC donors and was confirmed by Alizarin red staining, showing red mineral deposits, and qPCR, showing an upregulation of *SPP1* and *Osteocalcin* in the sub group of samples that stained positive with Alizarin red. Chondrogenic differentiation of the MSCs was not successful; safranin-O/fast green was negative and the qPCR did not show an upregulation of the chondrogenic markers. This may be caused by the absence of bFGF in the expansion medium and the replacement of ITS+ by ITS in the earlier experiments in combination with a less active TGF-β1 from another distributor.

Altogether, the naturally occurring height variation of the canine species seems to be an appropriate model to study the local pathways that enhance the pace of endochondral bone formation in order to find new bone regenerative strategies. However, in order to fully verify this model, chondrogenic differentiation should be obtained to test the effect of the differential regulated genes of the micro-array on the chondrogenic differentiation of MSCs.

Chapter 6: List of attended courses during the project

Courses

Sept 2012:	Basis molecular techniques
Nov-Dec 2012:	Writing in English for Publication (Babel)
Jan-Feb 2013:	Statistics course 2013
Sept 2013:	ECTS PhD trainings course (Presentation included)

Congresses/Symposia

13th Oktober 2012	Symposium 'Feline geneeskunde'
1st February 2013	Symposium 'Molecules and Medicine'
4th March 2013	Symposium 'Extracellular Vesicles in Health & Disease'
18th-20th April 2013	European Veterinary Conference "Voorjaarsdagen" (Presentation for the Research Award)
6th June 2013	Symposium 'Cartilage Regeneration: Genes, Cells and Technology'
18th June 2013	BMM/TeRM/DCTI Annual Meeting 2013
Monthly:	RM lunch seminars in UMCU

Chapter 7: Annexes

Annex I: Top 50 Up- and Downregulated DE-genes

Top 50 upregulated DE-genes

Number	Fold Change	Gene	ReporterId	CfEnsId	Description
1	5,6	SCIN	CFAB035019		Adseverin (Scinderin)
2	4,9	UCMA	CFAB014719	ENSCAFG00000004749	upper zone of growth plate and cartilage matrix associated
3	4,7	CHRNB3	CFAB019142	ENSCAFG00000005460	cholinergic receptor, nicotinic, beta 3 (neuronal)
4	4,6	TFPI2	CFAB012171	ENSCAFG00000002040	tissue factor pathway inhibitor 2
5	4,5	STEAP2	CFAB033585	ENSCAFG00000001870	STEAP family member 2, metalloreductase
6	4,5	SQLE	CFAB006899	ENSCAFG00000001056	squalene epoxidase
7	4,1	PAPSS2	CFAB007288	ENSCAFG00000015654	3'-phosphoadenosine 5'-phosphosulfate synthase 2
8	4,1	SLC1A1	CFAB010956	ENSCAFG00000002067	excitatory amino acid transporter 3
9	4,0	PCOLCE2	CFAB013887	ENSCAFG00000007915	procollagen C-endopeptidase enhancer 2
10	3,9		CFAB010131		
11	3,9	TSPAN13	CFAB034246	ENSCAFG00000002432	tetraspanin 13
12	3,8		CFAB028251		
13	3,8		CFAB008829		
14	3,8	LEPREL1	CFAB015339	ENSCAFG00000013985	leprecan-like 1
15	3,7	PCOLCE2	CFAB005631	ENSCAFG00000007915	procollagen C-endopeptidase enhancer 2
16	3,7		CFAB009145		
17	3,7	NGEF	CFAB007607	ENSCAFG00000011587	neuronal guanine nucleotide exchange factor
18	3,6	PRELP	CFAB032009	ENSCAFG00000009462	proline/arginine-rich end leucine-rich repeat protein
19	3,6	IL17B	CFAB024930	ENSCAFG00000032384	interleukin 17B
20	3,5	Q005W6	CFAB033834	ENSCAFG00000024645	BCL2/adenovirus E1B 19kDa interacting protein 3
21	3,5	NKX3-2	CFAB005311	ENSCAFG00000015412	NK3 homeobox 2
22	3,5		CFAB012405		
23	3,4	SAMD4A	CFAB028838	ENSCAFG00000014940	sterile alpha motif domain containing 4A
24	3,3	SLC17A8	CFAB018952	ENSCAFG00000006786	solute carrier family 17 (sodium-dependent inorganic phosphate cotransporter), member 8
25	3,3		CFAB039413		

Number	Fold Change	Gene	ReporterId	CfEnsId	Description
26	3,3	CAPS	CFAB011108	ENSCAFG00000018746	calcyphosin
27	3,3	GMEB1	CFAB023276	ENSCAFG00000011711	glucocorticoid modulatory element binding protein 1
28	3,2		CFAB040176		
29	3,2		CFAB010056		
30	3,2	SERINC5	CFAB007361	ENSCAFG00000008891	serine incorporator 5
31	3,2	TFPI2	CFAB008074	ENSCAFG00000002040	tissue factor pathway inhibitor 2
32	3,2	PLD3	CFAB039947	ENSCAFG00000005362	phospholipase D family, member 3
33	3,1	COMP	CFAB013509	ENSCAFG00000014616	cartilage oligomeric matrix protein
34	3,1	HAPLN3	CFAB024499	ENSCAFG00000011542	hyaluronan and proteoglycan link protein 3
35	3,1	SOX9	CFAB008152	ENSCAFG00000004374	transcription factor SOX-9
36	3,1	ADML	CFAB011004	ENSCAFG00000007539	ADM Adrenomedullin Proadrenomedullin N-20 terminal peptide
37	3,1	PPIF	CFAB006554	ENSCAFG00000032043	peptidylprolyl isomerase F
38	3,1		CFAB000566		
39	3,1	EFCAB1	CFAB014617	ENSCAFG00000006629	EF-hand calcium binding domain 1
40	3,0		CFAB035723		
41	3,0	SCRG1	CFAB014138	ENSCAFG00000007857	stimulator of chondrogenesis 1
42	3,0	DRP2	CFAB033523	ENSCAFG00000017618	dystrophin related protein 2
43	3,0		CFAB018273	ENSCAFG00000002495	
44	3,0	A2SXS6	CFAB023871	ENSCAFG00000011790	extracellular calcium-sensing receptor precursor
45	3,0		CFAB040994		
46	3,0	PPT2	CFAB006837	ENSCAFG00000000766	palmitoyl-protein thioesterase 2
47	3,0	PGAM4	CFAB029921	ENSCAFG00000009062	phosphoglycerate mutase family member 4
48	3,0		CFAB004382		
49	3,0		CFAB029726		
50	2,9	HAS2	CFAB018409	ENSCAFG00000029394	hyaluronan synthase 2

Top 50 downregulated DE-genes

Nr.	Fold Change	Gene	ReporterId	CfEnsId	Description
1	-74,1	S100A8	CFAB026148	ENSCAFG00000017557	protein S100-A8
2	-51,8	S100A12	CFAB026149	ENSCAFG00000023324	S100 calcium binding protein A12
3	-49,4	Q1ERY9	CFAB013656	ENSCAFG00000030286	Uncharacterized protein
4	-35,8	Q2LC20	CFAB020932	ENSCAFG00000013763	Uncharacterized protein
5	-25,8	Q1ERY9	CFAB017317	ENSCAFG00000030286	Uncharacterized protein
6	-24,4	S100A9	CFAB008767	ENSCAFG00000029470	S100 calcium binding protein A9
7	-22,5		CFAB023697		
8	-22,4	MYH1	CFAB016099	ENSCAFG00000030337	Myosin-1
9	-20,3		CFAB032244	ENSCAFG00000005427	**Novel protein**
10	-19,8	HBA	CFAB016483	ENSCAFG00000029904	Hemoglobin subunit alpha
11	-19,5	PLEKHG6	CFAB014464	ENSCAFG00000015203	pleckstrin homology domain containing, family G, member 6
12	-18,7		CFAB008248		
13	-18,6	Q1ERY9	CFAB021375	ENSCAFG00000030286	Uncharacterized protein
14	-18,1	LYSC2	CFAB011450	ENSCAFG00000000426	Lysozyme C, spleen isozyme
15	-17,6	KLHL41	CFAB015434	ENSCAFG00000012305	kelch-like 41 (Drosophila)
16	-16,8	MYL1	CFAB015545	ENSCAFG00000013875	myosin, light chain 1, alkali
17	-16,4	TTN	CFAB017014	ENSCAFG00000014025	titin
18	-16,4	PAX5	CFAB018026	ENSCAFG00000002357	paired box 5
19	-16,3	Q6TN20	CFAB011187	ENSCAFG00000012896	cathelicidin antimicrobial peptide precursor
20	-16,2	S100A9	CFAB026150	ENSCAFG00000029470	S100 calcium binding protein A9
21	-16,0	BACH2	CFAB018322	ENSCAFG00000003116	BTB and CNC homology 1, basic leucine zipper transcription factor 2
22	-13,8	CSRP3	CFAB013707	ENSCAFG00000009424	cysteine and glycine-rich protein 3 (cardiac LIM protein)
23	-13,5	PDLIM3	CFAB006248	ENSCAFG00000029034	PDZ and LIM domain 3
24	-13,4	PPP1CA	CFAB012893	ENSCAFG00000011565	serine/threonine-protein phosphatase PP1-alpha catalytic subunit
25	-13,2		CFAB025948		

Nr.	Fold Change	Gene	ReporterId	CfEnsId	Description
26	-13,2		CFAB016043		
27	-12,8		CFAB034473		
28	-12,6		CFAB005666	ENSCAFG00000025410	Uncharacterized protein
29	-11,9	ASPN	CFAB032586	ENSCAFG00000002307	asporin
30	-11,5		CFAB011823	ENSCAFG00000000686	Uncharacterized protein
31	-11,4		CFAB033849		
32	-11,4	DESM	CFAB033798	ENSCAFG00000015475	Desmin
33	-11,3	MYBPC1	CFAB030335	ENSCAFG00000007134	myosin binding protein C, slow type
34	-11,0	PDIA2	CFAB006544	ENSCAFG00000015429	protein disulfide isomerase family A, member 2
35	-10,8		CFAB034291		
36	-10,6	HEMGN	CFAB011752	ENSCAFG00000002461	hemogen
37	-10,3	CCDC33	CFAB007695	ENSCAFG00000017833	coiled-coil domain containing 33
38	-10,1	A8QWU1	CFAB036482	ENSCAFG00000028626	secretory leukocyte peptidase inhibitor precursor
39	-10,0	MYBPC1	CFAB012361	ENSCAFG00000007134	myosin binding protein C, slow type
40	-9,9	SRGN	CFAB007416	ENSCAFG00000013817	serglycin
41	-9,9	NISCH	CFAB013437	ENSCAFG00000009389	nischarin
42	-9,8	FAM63A	CFAB007871	ENSCAFG00000012326	family with sequence similarity 63, member A
43	-9,7	SPSB1	CFAB016196	ENSCAFG00000019732	splA/ryanodine receptor domain and SOCS box containing 1
44	-9,7	Q8WN71	CFAB010883	ENSCAFG00000008524	myosin regulatory light chain 2, ventricular/cardiac muscle isoform
45	-9,6		CFAB040049		
46	-9,6		CFAB001391		
47	-9,5	DNTT	CFAB022810	ENSCAFG00000008507	deoxynucleotidyltransferase, terminal
48	-9,4		CFAB027276	ENSCAFG00000011192	
49	-9,3	KCRM	CFAB013285	ENSCAFG00000004507	Creatine kinase M-type
50	-9,2	NKX6-3	CFAB033000	ENSCAFG00000005710	NK6 homeobox 3

Annex II: SPIA analysis

Total analysis

ID		Name	ID	pSize	NDE	pNDE	tA	pPERT	pG	pGFdr	pGFWER	Status	KEGGLINK
5150	1	Staphylococcus aureus infection	5150	31	18	6,42E-06	-19,384	0,006	6,96E-07	9,39E-05	9,39E-05	Inhibited	KEGG-link
4110	2	Cell cycle	4110	105	44	7,65E-07	8,582281	0,339	4,19E-06	0,000283	0,000566	Activated	KEGG-link
5322	3	Systemic lupus erythematosus	5322	54	22	0,000690665	-8,32175	0,015	0,000129	0,005049	0,017451	Inhibited	KEGG-link
4512	4	ECM-receptor interaction	4512	64	27	8,80E-05	4,922075	0,138	0,00015	0,005049	0,020197	Activated	KEGG-link
4530	5	Tight junction	4530	101	38	7,71E-05	0,06558	0,991	0,000801	0,02162	0,108102	Activated	KEGG-link
4670	6	Leukocyte transendothelial migration	4670	89	32	0,000698053	-11,2205	0,279	0,001859	0,036695	0,250926	Inhibited	KEGG-link
4115	7	p53 signaling pathway	4115	51	22	0,000264496	0,660446	0,828	0,002064	0,036695	0,278695	Activated	KEGG-link
5162	8	Measles	5162	98	35	0,000464237	-3,85262	0,5	0,002175	0,036695	0,293564	Inhibited	KEGG-link
4610	9	Complement and coagulation cascades	4610	54	19	0,010360511	-23,3443	0,033	0,003071	0,046059	0,414528	Inhibited	KEGG-link
5145	10	Toxoplasmosis	5145	101	34	0,001810032	5,996937	0,279	0,004338	0,052846	0,585687	Activated	KEGG-link
5166	11	HTLV-I infection	5166	213	61	0,004009031	11,50113	0,132	0,004522	0,052846	0,610403	Activated	KEGG-link
5164	12	Influenza A	5164	118	38	0,002500349	-7,44072	0,221	0,004697	0,052846	0,634151	Inhibited	KEGG-link
4612	13	Antigen processing and presentation	4612	39	17	0,001122335	-1,04864	0,54	0,005096	0,052921	0,687971	Inhibited	KEGG-link
4510	14	Focal adhesion	4510	158	50	0,00090233	0,837395	0,944	0,006872	0,06627	0,927782	Activated	KEGG-link
5144	15	Malaria	5144	37	16	0,001727033	-0,56956	0,589	0,008027	0,072239	1	Inhibited	KEGG-link
4978	16	Mineral absorption	4978	32	14	0,002902651	0	1	0,01986	0,167571	1	Inhibited	KEGG-link
4810	17	Regulation of actin cytoskeleton	4810	173	47	0,027231724	12,01607	0,219	0,03651	0,281129	1	Activated	KEGG-link
5412	18	Arrhythmogenic right ventricular cardiomyopathy (ARVC)	5412	60	20	0,016411675	0,386339	0,375	0,037484	0,281129	1	Activated	KEGG-link
4350	19	TGF-beta signaling pathway	4350	62	15	0,302772891	11,47411	0,024	0,04305	0,303441	1	Activated	KEGG-link
4370	20	VEGF signaling pathway	4370	57	19	0,019042821	4,153969	0,402	0,044954	0,303441	1	Activated	KEGG-link

Cell cycle pathway elaborated

4110	2	Cell cycle	4110	105	44	7,65E-07	8,582281	0,339	4,19E-06	0,000283	0,000566	Activated
	ENTREZid	Name	EnsemblId	logFC	logFC	logFC	Description					
	4173	MCM4	ENSCAFG00000006598	-0,41			minichromosome maintenance complex component 4					
	4174	MCM5	ENSCAFG00000001709	-0,38			minichromosome maintenance complex component 5					
	4175	MCM6	ENSCAFG00000005143	-0,84			minichromosome maintenance complex component 6					
	4176	MCM7	ENSCAFG00000014748	-0,39			minichromosome maintenance complex component 7					
	23594	ORC6	ENSCAFG00000003683	-0,75	-0,60		origin recognition complex, subunit 6					
	4998	ORC1	ENSCAFG00000003744	-1,77			origin recognition complex, subunit 1					
	8697	CDC23	ENSCAFG00000001209	0,41			cell division cycle 23 homolog (S. cerevisiae)					
	8454	CUL1	ENSCAFG00000003440	-0,49			cullin 1					
	983	CDK1	ENSCAFG00000012904	-0,43			cyclin-dependent kinase 1					
	5111	PCNA	ENSCAFG00000006030	-0,93			proliferating cell nuclear antigen					
	10926	DBF4	ENSCAFG00000001845	-0,60			DBF4 homolog (S. cerevisiae)					
	4085	ENSCAFG00000025619	ENSCAFG00000025619	-1,03								
	699	BUB1	ENSCAFG00000007062	-0,59			budding uninhibited by benzimidazoles 1 homolog (yeast)					
	9184	BUB3	ENSCAFG00000012700	-0,50			budding uninhibited by benzimidazoles 3 homolog (yeast)					
	11200	CHEK2	ENSCAFG00000011919	-0,49			CHK2 checkpoint homolog (S. pombe)					
	4193	MDM2_CANFA	ENSCAFG00000000418	0,40			E3 ubiquitin-protein ligase Mdm2					
	7465	WEE1	ENSCAFG00000007416	-0,56			WEE1 homolog (S. pombe)					
	9232	XM_536445.2	ENSCAFG00000017264	-0,85								
	1647	GADD45A	ENSCAFG00000029474	-1,81			growth arrest and DNA-damage-inducible, alpha					
	4616	GADD45B	ENSCAFG00000019386	0,58			growth arrest and DNA-damage-inducible, beta					
	1027	CDN1B_CANFA	ENSCAFG00000013244	-1,00			Cyclin-dependent kinase inhibitor 1B					
	1030	Q9GMF2_CANFA	ENSCAFG00000001680	0,80	-0,59		Cyclin-dependent kinase 4/6 inhibitor-a Fragment					
	7042	Q19KA8_CANFA	ENSCAFG00000010815	0,65			Transforming growth factor beta 2 Fragment					
	8317	CDC7	ENSCAFG00000020182	0,42			cell division cycle 7 homolog (S. cerevisiae)					
	994	CDC25B	ENSCAFG00000006175	-0,48			cell division cycle 25 homolog B (S. pombe)					
	990	CDC6	ENSCAFG00000016106	-0,85			cell division cycle 6 homolog (S. cerevisiae)					
	85417	CCNB3_CANFA	ENSCAFG00000015996	-0,40			G2/mitotic-specific cyclin-B3					
	891	ENSCAFG00000006595	ENSCAFG00000006595	-0,50			Uncharacterized protein					
	9133	CCNB2	ENSCAFG00000016600	-0,63			cyclin B2					
	890	CCNA2	ENSCAFG00000004133	-0,41			cyclin A2					
	1021	CDK6	ENSCAFG00000001998	-0,42			cyclin-dependent kinase 6					
	898	CCNE1	ENSCAFG00000007614	-0,74			cyclin E1					
	9134	CCNE2	ENSCAFG00000009408	-1,61	-1,61		cyclin E2					
	894	CCND2	ENSCAFG00000015381	0,84			cyclin D2					
	896	CCND3	ENSCAFG00000001618	-1,12			cyclin D3					
	7272	TTK	ENSCAFG00000002842	-0,67			TTK protein kinase					
	1031	CDKN2C	ENSCAFG00000028905	-0,45			cyclin-dependent kinase inhibitor 2C (p18, inhibits CDK4)					
	9126	SMC3	ENSCAFG00000010762	-0,51			structural maintenance of chromosomes 3					
	10274	STAG1	ENSCAFG00000007380	-0,57			stromal antigen 1					
	10735	STAG2	ENSCAFG00000018587	-0,65	-0,48		stromal antigen 2					
	5885	RAD21	ENSCAFG00000000822	-0,85	-0,82	-0,79	RAD21 homolog (S. pombe)					
	7709	ZBTB17	ENSCAFG00000016122	-0,77			zinc finger and BTB domain containing 17					
	7027	XM_844504.1	ENSCAFG00000006384	0,50								
	7029	TFDP2	ENSCAFG00000007742	-0,81			transcription factor Dp-2 (E2F dimerization partner 2)					

ECM-receptor interaction elaborated

4512	4	ECM-receptor interaction	4512	64	27	8,80E-05	4,922075	0,138	0,00015	0,005049	0,020197	Activated
	ENTREZid	Name	EnsemblId	logFC	logFC	logFC	Description					
	3910	LAMA4	ENSCAFG00000004043	0,58			laminin, alpha 4					
	3918	NP_001003351.1	ENSCAFG00000013243	-0,39			laminin-5 gamma 2					
	1277	CO1A1_CANFA	ENSCAFG00000017018	-0,89	-1,21		Collagen alpha-1(I) chain Precursor (Alpha-1 type I collagen)					
	1278	CO1A2_CANFA	ENSCAFG00000002069	-0,57	-0,50	-0,47	Collagen alpha-2(I) chain Precursor (Alpha-2 type I collagen)					
	1280	NP_001006952.1	ENSCAFG00000009059	1,15			collagen, type II, alpha 1					
	1281	COL3A1	ENSCAFG00000014812	-1,12	-0,48		collagen, type III, alpha 1					
	1290	COL5A2	ENSCAFG00000014837	-0,54			collagen, type V, alpha 2					
	1302	Q5TJG2_CANFA	ENSCAFG00000000903	1,55			Collagen type XI alpha 2 Fragment					
	50509	COL5A3	ENSCAFG00000017958	0,52			collagen, type V, alpha 3					
	3371	TNC	ENSCAFG00000003426	-0,88			tenascin C					
	7143	TNR	ENSCAFG00000014301	-0,82			tenascin R (restrictin, janusin)					
	2815	GP9	ENSCAFG00000004342	-0,42			glycoprotein IX (platelet)					
	7059	THBS3	ENSCAFG00000017017	1,29			thrombospondin 3					
	3655	ITGA6	ENSCAFG00000013006	0,72			integrin, alpha 6					
	3685	ITGAV	ENSCAFG00000014597	0,41			integrin, alpha V (vitronectin receptor, alpha polypeptide, antigen CD51)					
	3676	ITGA4	ENSCAFG00000014175	-1,16	-1,71		integrin, alpha 4 (antigen CD49D, alpha 4 subunit of VLA-4 receptor)					
	961	A1Z2X6_CANFA	ENSCAFG00000009887	-0,71			CD47					
	948	CD36	ENSCAFG00000006401	-1,16	-0,54		CD36 molecule (thrombospondin receptor)					
	9900	SV2A	ENSCAFG00000011588	-0,51			synaptic vesicle glycoprotein 2A					
	6385	SDC4	ENSCAFG00000030211	0,62			syndecan 4					
	9672	SDC3	ENSCAFG00000011234	1,29			syndecan 3					
	3339	Q6TYZ5_CANFA	ENSCAFG00000014773	1,36	1,25		Perlecan Fragment					
	3693	ITGB5	ENSCAFG00000012477	-0,46	-0,55		integrin, beta 5					
	3680	ITGA9	ENSCAFG00000004820	0,61			integrin, alpha 9					
	3678	ITGA5	ENSCAFG00000006491	0,67			integrin, alpha 5 (fibronectin receptor, alpha polypeptide)					
	960	Q28285_CANFA	ENSCAFG00000006889	0,63			CD44 variant					
	3673	ITGA2	ENSCAFG00000018423	0,83			integrin, alpha 2 (CD49B, alpha 2 subunit of VLA-2 receptor)					

Tight Junction elaborated

4530	5	Tight junction	4530	101	38	7,71E-05	0,06558	0,991	0,000801	0,02162	0,108102	Activated
	ENTREZid	Name	EnsemblId	logFC	logFC	logFC	Description					
	58494	JAM2	ENSCAFG00000008482	-0,51	-0,78		junctional adhesion molecule 2					
	5579	PRKCB	ENSCAFG00000017622	-1,03			protein kinase C, beta					
	5580	KPCD_CANFA	ENSCAFG00000008689	-0,57			Protein kinase C delta type (EC 2.7.11.13)(nPKC-delta)					
	5588	PRKCQ	ENSCAFG00000005169	-0,93	-0,77		protein kinase C, theta					
	1,01E+08	OCLN_CANFA	ENSCAFG00000007805	-0,40			Occludin					
	1364	CLDN4	ENSCAFG00000012523	0,58			claudin 4					
	5010	CLDN11	ENSCAFG00000014851	-0,91	1,03		claudin 11					
	9071	CLDN10	ENSCAFG00000005458	0,40			claudin 10					
	9074	CLDN6	ENSCAFG00000019337	-1,00			claudin 6					
	50855	PARD6A	ENSCAFG00000031576	-1,26			par-6 partitioning defective 6 homolog alpha (C. elegans)					
	56288	PARD3	ENSCAFG00000003737	0,55			par-3 partitioning defective 3 homolog (C. elegans)					
	2035	EPB41	ENSCAFG00000011677	-1,17			erythrocyte membrane protein band 4.1 (elliptocytosis 1, RH-linked)					
	2036	EPB41L1	ENSCAFG00000008413	1,06			erythrocyte membrane protein band 4.1-like 1					
	8777	MPDZ	ENSCAFG00000001498	-0,49	0,41		multiple PDZ domain protein					
	3059	HCLS1	ENSCAFG00000011559	-0,43			hematopoietic cell-specific Lyn substrate 1					
	9218	VAPA	ENSCAFG00000018733	0,42			VAMP (vesicle-associated membrane protein)-associated protein A, 33kDa					
	1457	CSNK2A1	ENSCAFG00000006946	-0,48			casein kinase 2, alpha 1 polypeptide					
	29895	MYLPF	ENSCAFG00000016543	-3,06			myosin light chain, phosphorylatable, fast skeletal muscle					
	4619	MYH1_CANFA	ENSCAFG00000030337	-4,49			Myosin-1					
	4626	MYH8_CANFA	ENSCAFG00000017522	-1,15			Myosin-8 (Myosin heavy chain 8)					
	4628	MYH10	ENSCAFG00000017262	-0,90			myosin, heavy chain 10, non-muscle					
	4633	NP_001003069.1	ENSCAFG00000008524	-3,28			ventricular myosin light chain 2					
	93408	MYL10	ENSCAFG00000013765	-0,97			myosin, light chain 10, regulatory					
	8531	Q9N1Q2_CANFA	ENSCAFG00000013401	-1,28			Y-box protein ZONAB-B					
	5584	PRKCI	ENSCAFG00000014823	0,39	1,02		protein kinase C, iota					
	22800	RRAS2	ENSCAFG00000008396	0,44			related RAS viral (r-ras) oncogene homolog 2					
	22808	MRAS	ENSCAFG00000007541	0,69			muscle RAS oncogene homolog					
	10000	Q6PVW1_CANFA	ENSCAFG00000015806	0,42			Protein kinase B gamma-like protein Fragment					
	207	AKT1	ENSCAFG00000018354	0,90	0,42		v-akt murine thymoma viral oncogene homolog 1					
	2770	GNAI1	ENSCAFG00000016413	-0,61			guanine nucleotide binding protein (G protein), alpha inhibiting activity polypeptide 1					
	2771	GNAI2_CANFA	ENSCAFG00000010740	0,39			Guanine nucleotide-binding protein G					
	57530	CING_CANFA	ENSCAFG00000012729	0,50			Cingulin					
	51776	ENSCAFG00000013140	ENSCAFG00000013140	-0,53	-0,58	-0,51	Uncharacterized protein					
	11336	EXOC3	ENSCAFG00000010918	0,39			exocyst complex component 3					
	10207	INADL	ENSCAFG00000018822	0,56			InaD-like (Drosophila)					
	87	ACTN1	ENSCAFG00000016534	-0,42			actinin, alpha 1					
	88	ACTN2	ENSCAFG00000010822	-2,02			actinin, alpha 2					
	7525	YES_CANFA	ENSCAFG00000018362	0,42			Proto-oncogene tyrosine-protein kinase Yes					

Mineral absorption elaborated

Mineral absorption	4978	32	14	0,003	0	1	0,01986	0,167571	1	Inhibited
Name	EnsemblId	logFC	logFC	logFC	Description					
ATP2B1	ENSCAFG00000006121	0,53			ATPase, Ca++ transporting, plasma membrane 1					
NRAM1_CANFA	ENSCAFG00000014645	-0,77			Natural resistance-associated macrophage protein 1 (NRAMP 1)					
SLC40A1	ENSCAFG00000009343	-1,01			solute carrier family 40 (iron-regulated transporter), member 1					
FRIL_CANFA	ENSCAFG00000003861	-0,73			Ferritin light chain (Ferritin L subunit)					
FRIH_CANFA	ENSCAFG00000030465	-0,42			Ferritin heavy chain					
HMOX2	ENSCAFG00000019207	-1,54			heme oxygenase (decycling) 2					
HEPH	ENSCAFG00000016633	0,49			hephaestin					
TF	ENSCAFG00000006540	0,43	0,57	0,68	transferrin					
SLC31A1	ENSCAFG00000003215	0,39			solute carrier family 31 (copper transporters), member 1					
MT2_CANFA	ENSCAFG00000023759	0,49			Metallothionein-2 (MT-2)(Metallothionein-II)(MT-II)					
STEAP2	ENSCAFG00000001870	2,18			STEAP family member 2, metalloreductase					
XM_532454.2	ENSCAFG00000001866	0,75								
ATOX1_CANFA	ENSCAFG00000017846	0,93			Copper transport protein ATOX1 (Metal transport protein ATX1)					
ATP1B4	ENSCAFG00000018484	-0,50			ATPase, Na+/K+ transporting, beta 4 polypeptide					

TGF-beta signaling elaborated

TGF-beta signaling	4350	62	15	0,303	11,47	0,024	0,04305	0,303441	1	Activated
Name	EnsemblId	logFC	logFC	logFC	Description					
Q2PPL3_CANFA	ENSCAFG00000005843	0,60			Latent transforming growth factor binding protein-1 Fragment					
THBS3	ENSCAFG00000017017	1,29			thrombospondin 3					
CUL1	ENSCAFG00000003440	-0,49			cullin 1					
ACVR1C	ENSCAFG00000009269	-0,42			activin A receptor, type IC					
SP1	ENSCAFG00000006950	-0,51			Sp1 transcription factor					
Q9GMF2_CANFA	ENSCAFG00000001680	0,80	-0,59		Cyclin-dependent kinase 4/6 inhibitor-a Fragment					
XM_844504.1	ENSCAFG00000006384	0,50								
ID4	ENSCAFG00000010205	1,25			inhibitor of DNA binding 4, dominant negative helix-loop-helix protein					
INHBA	ENSCAFG00000003550	0,48			inhibin, beta A					
RPS6KB1	ENSCAFG00000017679	0,56			ribosomal protein S6 kinase, 70kDa, polypeptide 1					
SMAD5	ENSCAFG00000001094	-0,45			SMAD family member 5					
Q19KA8_CANFA	ENSCAFG00000010815	0,65			Transforming growth factor beta 2 Fragment					
PGS2_CANFA	ENSCAFG00000006142	-2,63			Decorin Precursor (Bone proteoglycan II)(PG-S2)					
BMPR1B	ENSCAFG00000010107	0,41			bone morphogenetic protein receptor, type IB					
BMP2	ENSCAFG00000031497	0,73			bone morphogenetic protein 2					

VEGF-pathway elaborated

VEGF signaling pathway	4370	57	19	0,019	4,154	0,402	0,044954	0,303441	1	Activated
Name	EnsemblId	logFC	logFC	logFC	Description					
PLA2G4E	ENSCAFG00000024908	0,74			phospholipase A2, group IVE					
PLA2G2E	ENSCAFG00000023233	-1,31			phospholipase A2, group IIE					
PLA2G4A	ENSCAFG00000013778	0,57			phospholipase A2, group IVA (cytosolic, calcium-dependent)					
PLA2G6	ENSCAFG00000001424	0,70			phospholipase A2, group VI (cytosolic, calcium-independent)					
PLA2G10	ENSCAFG00000018788	1,50			phospholipase A2, group X					
HSPB1_CANFA	ENSCAFG00000013544	-1,12			Heat shock protein beta-1 (HspB1)(Heat shock 27 kDa protein)(HSP 27)					
CHP1	ENSCAFG00000009525	0,56			calcineurin-like EF-hand protein 1					
PPP3CB	ENSCAFG00000014818	0,63	0,71	-0,64	protein phosphatase 3, catalytic subunit, beta isozyme					
WDR92	ENSCAFG00000003248	0,66	-0,42		WD repeat domain 92					
Q6PVW1_CANFA	ENSCAFG00000015806	0,42			Protein kinase B gamma-like protein Fragment					
AKT1	ENSCAFG00000018354	0,90	0,42		v-akt murine thymoma viral oncogene homolog 1					
PIK3CD	ENSCAFG00000019735	-0,54			phosphoinositide-3-kinase, catalytic, delta polypeptide					
B9A1S4_CANFA	ENSCAFG00000007626	-0,45			Phosphatidylinositol 3-kinase regulatory subunit alpha Fragment					
PIK3R2	ENSCAFG00000014978	0,42			phosphoinositide-3-kinase, regulatory subunit 2 (beta)					
NFAT5	ENSCAFG00000020254	0,39			nuclear factor of activated T-cells 5, tonicity-responsive					
PRKCB	ENSCAFG00000017622	-1,03			protein kinase C, beta					
PTK2	ENSCAFG00000001217	0,42	0,65		PTK2 protein tyrosine kinase 2					
MK14_CANFA	ENSCAFG00000001378	-0,75	-0,41		Mitogen-activated protein kinase 14					
VEGFA_CANFA	ENSCAFG00000001938	1,01	0,41		Vascular endothelial growth factor A Precursor					

Annex III: GWAS compared with micro-array

Functional Category	Gene	SNP	Proximity	Fold Change
Skeletal system development	SOX9	rs2158917	Intragenic	3,1
(GO:0001501)	IHH	rs12470505	2nd	2,5
	BMP6	rs3812163	Intragenic	2,5
	HHIP	rs7689420	Intragenic	1,9
	MEF2C	rs10037512	Intragenic	1,7
	ACAN	rs16942341	Intragenic	1,7
	BMP2	rs2145272	Intragenic	1,7
	COL11A	rs12047268	Intragenic	1,5
Regulation of cell cycle	SOX9	rs2158917	Intragenic	3,1
(GO:0051726)	BMP2	rs2145272	Intragenic	1,7
	CCNA2	rs6824258	2nd	-1,3
	CDK6	rs42235	Intragenic	-1,3
	CRLF3	rs17780086	20th	-1,4
	DTL	rs10863936	Intragenic	-1,4
	EZH2	rs822552	2nd	-1,5
	NUSAP1	rs316618	5th	-1,7
	SLBP	rs2247341	Intragenic	-1,8
Regulation of apoptotic process	SOX9	rs2158917	Intragenic	3,1
(GO:0042981)	PPIF	rs2145998	Intragenic	2,6
	MEF2C	rs10037512	Intragenic	1,7
	BMP2	rs2145272	Intragenic	1,7
	TNFSF10	rs572169	3rd	-1,4
	CAMK1D	rs7909670	3rd	-1,6
	TOP2A	rs528045	Intragenic	-1,9
	NTRK2	rs7853377	10th	-2,3
Extracellular matrix	IHH	rs12470505	2nd	2,5
(GO:0031012)	ACAN	rs16942341	Intragenic	1,7
	SERPINE2	rs2629046	Intragenic	1,5
	COL11A1	rs12047268	Intragenic	1,5
	LAMC2	rs9425569	3rd	-1,3
	LTBP2	rs862034	Intragenic	-1,5
	EFEMP1	rs3791675	Intragenic	-1,5
	ADAMTSL3	rs11259936	Intragenic	-2,0
	ECM2	rs9969804	5th	-2,1
	OGN	rs9969804	8th	-5,2
	ASPN	rs9969804	6th	-10,1

Cell differentiation (GO:0030154)	SOX9	rs2158917	Intragenic	3,1
	BMP6	rs3812163	Intragenic	2,5
	ID4	rs1047014	Intragenic	2,4
	HHIP	rs7689420	Intragenic	1,9
	MEF2C	rs10037512	Intragenic	1,7
	ACAN	rs16942341	Intragenic	1,7
	BMP2	rs2145272	Intragenic	1,7
	SERPINE2	rs2629046	Intragenic	1,5
	COL11A1	rs12047268	Intragenic	1,5
	GNA12	rs798489	Intragenic	1,4
	MYO6	rs9360921	3rd	1,4
	FARP2	rs12694997	3rd	1,4
	CLIC4	rs4601530	Intragenic	1,4
	FRS2	rs10748128	Intragenic	1,3
	SYNE1	rs543650	3rd	-1,3
	CDK6	rs42235	Intragenic	-1,3
	CBFA2T2	rs7274811	7th	-1,3
	PPP2R3A	rs9844666	4th	-1,4
	EZH2	rs822552	2nd	-1,5
	FLI1	rs654723	Intragenic	-1,6
	AGTPBP1	rs7853377	11th	-1,6
	CAMK1D	rs7909670	3rd	-1,6
	HLA-DQB1	rs6457620	Intragenic	-2,3
	STK25	rs12694997	5th	-2,3
	NTRK2	rs7853377	10th	-2,3
RNA binding (GO:0003723)	MEF2C	rs10037512	Intragenic	1,7
	HDLBP	rs12694997	2nd	1,5
	GTF2B	rs6699417	2nd	-1,3
	EZH2	rs822552	2nd	-1,5
	IGF2BP2	rs720390	Intragenic	-1,5
	SLBP	rs2247341	Intragenic	-1,8
Receptor binding (GO:0005102)	BMP6	rs3812163	Intragenic	2,5
	BMP2	rs2145272	Intragenic	1,7
	SERPINE2	rs2629046	Intragenic	1,5
	SOCS2	rs11107116	Intragenic	1,4
	RSPO3	rs1490384	4th	1,4
	NSD1	rs422421	2nd	1,4
	SOCS5	rs12474201	Intragenic	1,4
	FRS2	rs10748128	Intragenic	1,3
	GTF2B	rs6699417	2nd	-1,3
	TNFSF10	rs572169	3rd	-1,4
	EFEMP1	rs3791675	Intragenic	-1,5

Oxidoreductase activity (GO:0016491)	SMOX	rs1741344	Intragenic	-1,4
	FAR2	rs2638953	3rd	-1,4
Zinc ion binding (GO:0008270)	HHIP	rs7689420	Intragenic	1,9
	ZNF341	rs7274811	Intragenic	1,9
	ENPP2	rs16892729	Intragenic	1,6
	NSD1	rs422421	2nd	1,4
	TRIM27	rs3129109	8th	1,3
	GTF2B	rs6699417	2nd	-1,3
	TAX1BP1	rs1708299	3rd	-1,3
	ZCCHC6	rs8181166	Intragenic	-1,4
	JAZF1	rs1708299	Intragenic	-1,4
	SUZ12	rs17780086	2nd	-1,4
	LIMD2	rs2665838	14th	-1,7
	ADAMTSL3	rs11259936	Intragenic	-2,0
Focal adhesion (GO:0005925)	TNS1	rs1351164	2nd	1,5
Identical protein binding (GO:0042802)	RAB11FIP4	rs17780086	10th	1,8
	SSSCA1	rs3782089	Intragenic	1,4
	SH3GL3	rs11259936	3rd	1,3
	TOP2A	rs528045	Intragenic	-1,9
	STK25	rs12694997	5th	-2,3
Transmembrane transport (GO:0055085)	SLC16A7	rs17122670	Intragenic	-2,8

Annex IV: Primers

Marker	Gene	Primer sequence	Exon	Amplicon Size (bp)	Annealing temperature (°C)	Accession no.
Osteoblasts	OSTEONECTIN (SPARC)	Forward TCTGTATGAAAGGGATGAGGAC	6	82	64	XM_849889
		Reverse GCTTCTCGTTCTCGTGGA	7			
	OSTEOPONTIN (SPP1)	Forward GAATGCTGTGCTGACTGAGG	4	113	66-67	XM_003434024
		Reverse TGGCTATCCACATCGTCTCC	5			
	OSTEOCALCIN (BGLAP)	Forward CTGATGGTCCTTGCCCT	1	116	60-63	XM_547536
		Reverse CTTGGACACGAAGGTTGC	2 and 3			
Adipocytes	ADIPOQ	Forward AGAGAAAGGAGATGCAGGT	1 and 2	141	62	NM_001006644
		Reverse CGAACGGTGTACATAGGC	2			
	PPARg	Forward ACTGGAATTAGATGACAGCGAC	6	84	60-61	NM_001024632
		Reverse CTTCACATTCAGCAAACCTGG	7			
Chondrocytes	Col2a1	Forward GCAGCAAGAGCAAGGAC	52	150	60.5-65	NM_001006951
		Reverse TTCTGAGAGCCCTCGGT	53			
	ACAN	Forward GGACACTCCTTGCAATTTGAG	14	110	61-62	NM_001113455
		Reverse GTCATTCCACTCTCCCTTCTC	15			
	ColX	Forward CCAACACCAAGACACAG	1	80	61	XM_849417
		Reverse CAGGAATACCTTGCTCTC	2			
	SOX9	Forward CGCTCGCAGTACGACTACAC	3	105	62-63	NM_001002978
		Reverse GGGGTTCATGTAGGTGAAGG	3			
Housekeeping	GAPDH	Forward TGTCCCCACCCCCAATGTATC	2	100	58	NM_001003142
		Reverse CTCCGATGCCTGCTTCACTACCTT	2			
	HPRT	Forward AGCTTGCTGGTGAAAAGGAC	5/6	104	56+58	NM_001003357
		Reverse TTATAGTCAAGGGCATATCC	7			
	beta-actin (L)	Forward GATATCGCTGCGCTTGTGGTC	1	384	58	NM_001195845
		Reverse GGCTGGGGTGTTGAAAGTCTC	3			
	RPS19	Forward CCTTCCTCAAAAAGTCTGGG	2 and 3	95	61+63	XM_533657
		Reverse GTTCTCATCGTAGGGAGCAAG	3			
	HNRPH	Forward CTCACTATGATCCACCACG	5	151	61,2	XM_538576
		Reverse TAGCCTCCATAACCTCCAC	5 and 6			
	RPL8	Forward CCATGAATCCTGTGGAGC	4 and5	64	55	XM_532360
		Reverse GTAGAGGGTTTGCCGATG	5			
	GUSB	Forward AGACGCTTCCAAGTACCCC	4	103	62	NM_001003191
		Reverse AGGTGTGGTGTAGAGGAGCAC	5			
	RPS5	Forward TCACTGGTGAGAACCCCCT	2 and 3	141	62,5	XM_533568
		Reverse CCTGATTCACACGGCGTAG	3			
	SRPR	Forward GCTTCAGGATCTGGACTGC	7	81	61,2	XM_546411
		Reverse GTTCCCTTGGTAGCACTGG	7 and 8			
	B2MG	Forward TCCTCATCCTCCTCGCT	1	85	61,2+63	AB745507
		Reverse TTCTCTGCTGGGTGTCG	2			
	HMBS	Forward TCACCATCGGAGCCATCT	6	112	61	XM_546491
		Reverse GTTCCCACCACGCTCTTCT	6/7			
	RPL13	Forward GCCGGAAGGTTGTAGTCGT	3	87	61	AJ388525

	Reverse GGAGGAAGGCCAGGTAATTC	4			XM_003432726
SDHA	Forward GCCTTGGATCTCTTGATGGA	6	92	61	DQ402985
	Reverse TTCTTGGCTCTTATGCGATG	6			
YWHAZ	ForwardCGAAGTTGCTGCTGGTGA	2	94	58	XM_843951
	ReverseTTGCATTTCCTTTTTGCTGA	2/3			XM_849432
TBP	Forward CTATTTCTTGGTGTGCATGAGG	5'	96	57	
	Reverse CCTCGGCATTCAGTCTTTTC	5'			

Annex V: Different designs for chondrogenic differentiation

FGF is known to enhance the chondrogenic differentiation potential of human BMSCs in vitro.[188] For this purpose, MSCs were expanded (α-MEM, 10% FCS, 1% penicillin/streptomycin , 0.1 mM ascorbic acid and 10^{-9}M dexamethasone) in the presence of 1 ng/ml basic fibroblast growth factor (bFGF; AbDSerotec PHP105) and compared to the previous expansion conditions (no FGF). After expansion, cells were seeded and cultured as described before and 7 conditions were tested per expansion group

a. Basic medium without growth factors: DMEM high glucose with pyruvate (Invitrogen), 1% penicillin/streptomycin, 1% ITS (BD-354350) with 2% Bovine Serum Albumine (BSA (Sigma, A3059), 0.04 mg/ml proline (Sigma P5607),0.1 mM acorbic acid, 10^{-7} M dexamethasone. BSA was added to the medium in order to bind the TGF-β1 within the medium, preventing the TGF-β1 from binding to the side of the plate.
b. Chondrogenic medium consisting of basic medium supplemented with:

    1. 5 ng/ml TGF-β1 (Peprotech 100-21C)
    2. 10 ng/ml TGF-β1 (Peprotech 100-21C)
    3. 20 ng/ml TGF-β1 (Peprotech 100-21C)
    4. 10 ng/ml TGF-β2 (R&D 240-B-002) and
    5. 10 ng/ml TGF-β1 (Peprotech 100-21C) and 10% FCS. The latter was added because a positive effect of FCS on chondrogenic differentiation is described.[189]

c. Basic medium without growth factors: DMEM high glucose with pyruvate (Invitrogen), 1% penicillin/streptomycin, 1% ITS (BD-354350), 0.04 mg/ml proline (Sigma P5607),0.1 mM acorbic acid, 10^{-7} M dexamethasone. Note that the latter condition is similar to the conditions employed during the first experiment.

Pellets were cultured for 21 days in the described chondrogenic media and were harvested at 14 and 21 days based on the fact that during chondrogenic differentiation of human MSCs Pittinger et al reported GAG production detected by Safranin O as early as 14 days of culture.[190] After fixation as described before, pellets were stained with Safranin O/Fast Green staining. Unfortunately, no differences in pellet size were observed and no pellets were positively stained for cartilage proteoglycans.

Subsequently, in order to rule out the possible effect of the FCS during the expansion of the MSCs and to study the additive effect of ITS+ compared to ITS for the ability to stimulate

chondrogenic medium additional experiments were performed. Cells were expanded in α-MEM (Invitrogen), 1% penicillin/streptomycin () , 0.1 mM ascorbic acid (Sigma A8960), 1 ng/ml basic fibroblast growth factor (bFGF; AbDSerotec PHP105) supplemented with two different FCS (Invitrogen 16000-044) and (). After expansion, cells were seeded and cultured as described before. The chondrogenic differentiation medium consisted of DMEM high glucose with pyruvate (Invitrogen), 1% penicillin/streptomycin, 1% ITS+ (Insulin, Tranferrin, Selenious acid, Bovine serum albumin and Linoleic acid, BD-354352), 0.04 mg/ml proline (Sigma P5607),0.1 mM acorbic acid, 10^{-7} M dexamethasone and 10 ng/ml TGF-β1 (R&D systems 240-B-010). Please note, that TGF-b1 was purchased from R&D instead from peprotec on the basis of personal communication with the laboratory of orthopedics at the Erasmus Rotterdam and the UMCU. They both reported that they had experience trouble with chondrogenic differentiation of human MSCs when the employed TGf-b originating from Peprotec.

This experiment is ongoing and chondrogenic culture will be terminated in the second half of September 2013. The expectation is that with the addition of bFGF to the expansion medium and ITS+ and TGF- β1 from R&D to the chondrogenic medium, the chondrogenic differentiation will succeed. In the literature ITS+ is used most of the time to induce chondrogenic differentiation instead of ITS. In addition the activity of TGF- β1 from R&D is suspected to be higher than the activity of TGF- β1 from Peprotech.

Chapter 8: References

References

1. Dimitriou, R., Jones, E., McGonagle, D. & Giannoudis, P. Bone regeneration: current concepts and future directions. *BMC Medicine* 9, 66 (2011).

2. Lissenberg-Thunnissen, S. N., de Gorter, D. J., Sier, C. F. & Schipper, I. B. Use and efficacy of bone morphogenetic proteins in fracture healing. *Int. Orthop.* 35, 1271-1280 (2011).

3. Utting, J. C. *et al*. Hypoxia inhibits the growth, differentiation and bone-forming capacity of rat osteoblasts. *Exp. Cell Res.* 312, 1693-1702 (2006).

4. Gawlitta, D. *et al*. Modulating endochondral ossification of multipotent stromal cells for bone regeneration. *Tissue Eng. Part B. Rev.* 16, 385-395 (2010).

5. Garrison, K. R. *et al*. Bone morphogenetic protein (BMP) for fracture healing in adults. *Cochrane Database Syst. Rev.* (6):CD006950. doi, CD006950 (2010).

6. Komatsu, D. E. & Warden, S. J. The control of fracture healing and its therapeutic targeting: Improving upon nature. *J. Cell. Biochem.* 109, 302-311 (2010).

7. Schindeler, A., McDonald, M. M., Bokko, P. & Little, D. G. Bone remodeling during fracture repair: The cellular picture. *Semin. Cell Dev. Biol.* 19, 459-466 (2008).

8. Dimitriou, R., Tsiridis, E. & Giannoudis, P. V. Current concepts of molecular aspects of bone healing. *Injury* 36, 1392-1404 (2005).

9. Akiyama, H., Chaboissier, M., Martin, J. F., Schedl, A. & de Crombrugghe, B. The transcription factor Sox9 has essential roles in successive steps of the chondrocyte differentiation pathway and is required for expression of Sox5 and Sox6. *Genes & Development* 16, 2813-2828 (2002).

10. Robins, J. C. *et al*. Hypoxia induces chondrocyte-specific gene expression in mesenchymal cells in association with transcriptional activation of Sox9. *Bone* 37, 313-322 (2005).

11. Wang, J., Zhou, J., Cheng, C., Kopchick, J. & Bondy, C. Evidence supporting dual, IGF-I-independent and IGF-I-dependent, roles for GH in promoting longitudinal bone growth. *Journal of Endocrinology* 180, 247-255 (2004).

12. Parker, E. A. *et al*. Spatial and temporal regulation of GH–IGF-related gene expression in growth plate cartilage. *Journal of Endocrinology* 194, 31-40 (2007).

13. Nilsson, A. *et al*. Regulation by growth hormone of number of chondrocytes containing IGF-I in rat growth plate. *Science* 233, 571-574 (1986).

14. Nap, R. C., Mol, J. A. & Hazewinkel, H. A. Age-related plasma concentrations of growth hormone (GH) and insulin-like growth factor I(IGF-I) in Great Dane pups fed different dietary levels of protein. *Domest. Anim. Endocrinol.* 10, 237-247 (1993).

15. Wang, J., Zhou, J., Powell-Braxton, L. & Bondy, C. Effects of Igf1 Gene Deletion on Postnatal Growth Patterns. *Endocrinology* 140, 3391-3394 (1999).

16. Liu, J., Baker, J., Perkins, A. S., Robertson, E. J. & Efstratiadis, A. Mice carrying null mutations of the genes encoding insulin-like growth factor I (Igf-1) and type 1 IGF receptor (Igf1r). *Cell* 75, 59-72 (1993).

17. Wang, Y. *et al*. IGF-1R signaling in chondrocytes modulates growth plate development by interacting with the PTHrP/Ihh pathway. *Journal of Bone and Mineral Research* 26, 1437-1446 (2011).

18. Schlegel, W. *et al*. IGF expression patterns and regulation in growth plate chondrocytes. *Mol. Cell. Endocrinol.* 327, 65-71 (2010).

19. Duan, C. & Xu, Q. Roles of insulin-like growth factor (IGF) binding proteins in regulating IGF actions. *Gen. Comp. Endocrinol.* 142, 44-52 (2005).

20. Theyse, L. F. *et al*. Expression of osteotropic growth factors and growth hormone receptor in a canine distraction osteogenesis model. *J. Bone Miner. Metab.* 24, 266-273 (2006).

21. Andrew, J. G., Hoyland, J., Freemont, A. J. & Marsh, D. Insulinlike growth factor gene expression in human fracture callus. *Calcif. Tissue Int.* 53, 97-102 (1993).

22. Edwall, D., Prisell, P. T., Levinovitz, A., Jennische, E. & Norstedt, G. Expression of insulin-like growth factor I messenger ribonucleic acid in regenerating bone after fracture: influence of indomethacin. *J. Bone Miner. Res.* 7, 207-213 (1992).

23. Raschke, M. *et al*. Effects of growth hormone in patients with tibial fracture: a randomised, double-blind, placebo-controlled clinical trial. *European Journal of Endocrinology* 156, 341-351 (2007).

24. Shimoaka, T. *et al*. Impairment of Bone Healing by Insulin Receptor Substrate-1 Deficiency. *Journal of Biological Chemistry* 279, 15314-15322 (2004).

25. Schmidmaier, G. *et al*. Synergistic effect of IGF-I and TGF-ß1 on fracture healing in rats Single

versus combined application of IGF-I and TGF-ß1. *Acta Orthop* 74, 604-610 (2003).

26. Myers, T. J. *et al*. Systemically delivered insulin-like growth factor-I enhances mesenchymal stem cell-dependent fracture healing. *Growth Factors* 30, 230-241 (2012).

27. Bauer, D. C., Ettinger, B., Nevitt, M. C., Stone, K. L. & Study of Osteoporotic Fractures Research Group. Risk for fracture in women with low serum levels of thyroid-stimulating hormone. *Ann. Intern. Med.* 134, 561-568 (2001).

28. Stevens, D. A. *et al*. Thyroid Hormones Regulate Hypertrophic Chondrocyte Differentiation and Expression of Parathyroid Hormone-Related Peptide and Its Receptor During Endochondral Bone Formation. *Journal of Bone and Mineral Research* 15, 2431-2442 (2000).

29. Loftus, M. J. & Peterson, L. J. Delayed healing of mandibular fracture in idiopathic myxedema. *Oral Surgery, Oral Medicine, Oral Pathology* 47, 233-237 (1979).

30. Urabe, K. *et al*. Inhibition of endochondral ossification during fracture repair in experimental hypothyroid rats. *J. Orthop. Res.* 17, 920-925 (1999).

31. Barth, R., Zimmerman, P. & McDonnell, J. Early transient hyperthyroidism enhances bone repair in a rat femoral defect model. *Orthop Trans* 12, 491 (1988).

32. Ashton, I. K. & Dekel, S. Fracture repair in the Snell dwarf mouse. *Br. J. Exp. Pathol.* 64, 479-486 (1983).

33. Koskinen, E. *The repair of experimental fractures under the action of growth hormone, thyrotropin and cortisone. A tissue analytic, roentgenologic and autoradiographic study.* (Annales chirurgiae et gynaecologiae Fenniae. Supplementum Ser. 48, 1959).

34. Amling, M. *et al*. Rescue of the skeletal phenotype of vitamin D receptor-ablated mice in the setting of normal mineral ion homeostasis: formal histomorphometric and biomechanical analyses. *Endocrinology* 140, 4982-4987 (1999).

35. Anderson, P. H. & Atkins, G. J. The skeleton as an intracrine organ for vitamin D metabolism. *Mol. Aspects Med.* 29, 397-406 (2008).

36. Dardenne, O., Prud'Homme, J., Hacking, S. A., Glorieux, F. H. & St-Arnaud, R. Rescue of the Pseudo-Vitamin D Deficiency Rickets Phenotype of CYP27B1-Deficient Mice by Treatment With 1,25-Dihydroxyvitamin D3: Biochemical, Histomorphometric, and Biomechanical Analyses. *Journal of Bone and Mineral Research* 18, 637-643 (2003).

37. Boyan, B. D., Sylvia, V. L., Dean, D. D., Del Toro, F. & Schwartz, Z. Differential regulation of growth plate chondrocytes by 1alpha,25-(OH)2D3 and 24R,25-(OH)2D3 involves cell-maturation-specific membrane-receptor-activated phospholipid metabolism. *Crit. Rev. Oral Biol. Med.* 13, 143-154 (2002).

38. Pedrozo, H. A. *et al*. Physiological importance of the 1,25(OH)2D3 membrane receptor and evidence for a membrane receptor specific for 24,25(OH)2D3. *J. Bone Miner. Res.* 14, 856-867 (1999).

39. Kato, A., Seo, E. -., Einhorn, T. A., Bishop, J. E. & Norman, A. W. Studies on 24R,25-dihydroxyvitamin D3: evidence for a nonnuclear membrane receptor in the chick tibial fracture-healing callus. *Bone* 23, 141-146 (1998).

40. Kato, A., Bishop, J. E. & Norman, A. W. Evidence for a 1α,25-Dihydroxyvitamin D3Receptor/Binding Protein in a Membrane Fraction Isolated from a Chick Tibial Fracture-Healing Callus. *Biochem. Biophys. Res. Commun.* 244, 724-727 (1998).

41. St-Arnaud, R. & Naja, R. P. Vitamin D metabolism, cartilage and bone fracture repair. *Mol. Cell. Endocrinol.* 347, 48-54 (2011).

42. Fu, L., Tang, T., Miao, Y., Hao, Y. & Dai, K. Effect of 1,25-dihydroxy vitamin D3 on fracture healing and bone remodeling in ovariectomized rat femora. *Bone* 44, 893-898 (2009).

43. Lindgren, J. U., Narechania, R. G., McBeath, A. A., Lange, T. A. & DeLuca, H. F. Effects of 1,24 dihydroxyvitamin D3 and calcitonin on fracture healing in adult rats. *Clin. Orthop. Relat. Res.* (160), 304-308 (1981).

44. van der Eerden, B. C., Karperien, M., Gevers, E. F., Lowik, C. W. & Wit, J. M. Expression of Indian hedgehog, parathyroid hormone-related protein, and their receptors in the postnatal growth plate of the rat: evidence for a locally acting growth restraining feedback loop after birth. *J. Bone Miner. Res.* 15, 1045-1055 (2000).

45. St-Jacques, B., Hammerschmidt, M. & McMahon, A. P. Indian hedgehog signaling regulates proliferation and differentiation of chondrocytes and is essential for bone formation. *Genes Dev.* 13, 2072-2086 (1999).

46. Kobayashi, T. *et al*. Indian hedgehog stimulates periarticular chondrocyte differentiation to regulate growth plate length independently of PTHrP. *J. Clin. Invest.* 115, 1734-1742 (2005).

47. Ito, H. *et al*. Hedgehog Signaling Molecules in Bone Marrow Cells at the Initial Stage of Fracture Repair. *Biochem. Biophys. Res. Commun.* 262, 443-451 (1999).

48. Murakami, S. & Noda, M. Expression of Indian hedgehog during fracture healing in adult rat femora. *Calcif. Tissue Int.* 66, 272-276 (2000).

49. Le, A. X., Miclau, T., Hu, D. & Helms, J. A. Molecular aspects of healing in stabilized and non-stabilized fractures. *Journal of Orthopaedic Research* 19, 78-84 (2001).

50. Okazaki, K. *et al*. Expression of parathyroid hormone-related peptide and insulin-like growth factor I during rat fracture healing. *Journal of Orthopaedic Research* 21, 511-520 (2003).

51. Bostrom, M. P. *et al*. Parathyroid hormone-related protein analog RS-66271 is an effective therapy for impaired bone healing in rabbits on corticosteroid therapy. *Bone* 26, 437-442 (2000).

52. Vickery, B. H. *Fracture healing using pthrp analogs* (2003).

53. Kakar, S. *et al*. Enhanced Chondrogenesis and Wnt Signaling in PTH-Treated Fractures. *Journal of Bone and Mineral Research* 22, 1903-1912 (2007).

54. Komatsubara, S. *et al*. Human parathyroid hormone (1–34) accelerates the fracture healing process of woven to lamellar bone replacement and new cortical shell formation in rat femora. *Bone* 36, 678-687 (2005).

55. Schober, H. -., Westphal, T., Brunnemann, C. & Ganzer, D. PTH as a treatment for long bone fracture nonunion. *Bone* 48, Supplement 2, S164 (2011).

56. Aspenberg, P. *et al*. Teriparatide for acceleration of fracture repair in humans: A prospective, randomized, double-blind study of 102 postmenopausal women with distal radial fractures. *Journal of Bone and Mineral Research* 25, 404-414 (2010).

57. Matsunaga, S., Yamamoto, T. & Fukumura, K. Temporal and spatial expressions of transforming growth factor-betas and their receptors in epiphyseal growth plate. *Int. J. Oncol.* 14, 1063-1067 (1999).

58. Janssens, K., ten Dijke, P., Janssens, S. & Van Hul, W. Transforming Growth Factor-β1 to the Bone. *Endocrine Reviews* 26, 743-774 (2005).

59. Sakou, T. *et al*. Localization of Smads, the TGF-? Family Intracellular Signaling Components During Endochondral Ossification. *Journal of Bone and Mineral Research* 14, 1145-1152 (1999).

60. Rosier, R. N., O'Keefe, R. J., Crabb, I. D. & Puzas, J. E. Transforming growth factor beta: an autocrine regulator of chondrocytes. *Connect. Tissue Res.* 20, 295-301 (1989).

61. Geiser, A. G. *et al*. Decreased bone mass and bone elasticity in mice lacking the transforming growth factor-β1 gene. *Bone* 23, 87-93 (1998).

62. Sanford, L. P. *et al*. TGFbeta2 knockout mice have multiple developmental defects that are non-overlapping with other TGFbeta knockout phenotypes. *Development* 124, 2659-2670 (1997).

63. Serra, R., Karaplis, A. & Sohn, P. Parathyroid Hormone–related Peptide (PTHrP)-dependent and -independent Effects of Transforming Growth Factor β (TGF-β) on Endochondral Bone Formation. *The Journal of Cell Biology* 145, 783-794 (1999).

64. Yang, X. *et al*. TGF-beta/Smad3 signals repress chondrocyte hypertrophic differentiation and are required for maintaining articular cartilage. *J. Cell Biol.* 153, 35-46 (2001).

65. Johnstone, B., Hering, T. M., Caplan, A. I., Goldberg, V. M. & Yoo, J. U. In VitroChondrogenesis of Bone Marrow-Derived Mesenchymal Progenitor Cells. *Exp. Cell Res.* 238, 265-272 (1998).

66. Olney, R. C., Wang, J., Sylvester, J. E. & Mougey, E. B. Growth factor regulation of human growth plate chondrocyte proliferation in vitro. *Biochem. Biophys. Res. Commun.* 317, 1171-1182 (2004).

67. Bostrom, M. P. & Asnis, P. Transforming growth factor beta in fracture repair. *Clin. Orthop. Relat. Res.* (355 Suppl), S124-31 (1998).

68. Zimmermann, G. *et al*. TGF-β1 as a marker of delayed fracture healing. *Bone* 36, 779-785 (2005).

69. Sarahrudi, K. *et al*. Elevated transforming growth factor-beta 1 (TGF-β1) levels in human fracture healing. *Injury* 42, 833-837 (2011).

70. Rosier, R. N., O'Keefe, R. J. & Hicks, D. G. The potential role of transforming growth factor beta in fracture healing. *Clin. Orthop. Relat. Res.* (355 Suppl), S294-300 (1998).

71. Cho, T., Gerstenfeld, L. C. & Einhorn, T. A. Differential Temporal Expression of Members of the Transforming Growth Factor ? Superfamily During Murine Fracture Healing. *Journal of Bone and Mineral Research* 17, 513-520 (2002).

72. Nielsen, H. M., Andreassen, T. T., Ledet, T. & Oxlund, H. Local injection of TGF-β increases the strength of tibial fractures in the rat. *Acta Orthop* 65, 37-41 (1994).

73. Lind, M. *et al*. Transforming growth factor-β enhances fracture healing in rabbit tibiae. *Acta Orthop* 64, 553-556 (1993).

74. He, X. B. *et al*. Effects of bone morphogenetic protein and transforming growth fractor-beta on biomechanical property for fracture healing in rabbit ulna. *Zhongguo Xiu Fu Chong Jian Wai Ke Za Zhi* 17, 185-188 (2003).

75. Critchlow, M. A., Bland, Y. S. & Ashhurst, D. E. The effect of exogenous transforming growth factor-β2 on healing fractures in the rabbit. *Bone* 16, 521-527 (1995).

76. Park, S. H., O'Connor, K. M. & McKellop, H. Interaction between active motion and exogenous transforming growth factor Beta during tibial fracture repair. *J. Orthop. Trauma* 17, 2-10 (2003).

77. Minina, E. *et al*. BMP and Ihh/PTHrP signaling interact to coordinate chondrocyte proliferation and differentiation. *Development* 128, 4523-4534 (2001).

78. Yoon, B. S. *et al*. BMPs regulate multiple aspects of growth-plate chondrogenesis through opposing actions on FGF pathways. *Development* 133, 4667-4678 (2006).

79. Tsuji, K. *et al*. BMP2 activity, although dispensable for bone formation, is required for the initiation of fracture healing. *Nat. Genet.* 38, 1424-1429 (2006).

80. Gautschi, O. P., Frey, S. P. & Zellweger, R. Bone morphogenetic proteins in clinical applications. *ANZ J. Surg.* 77, 626-631 (2007).

81. Shields, L. B. *et al*. Adverse effects associated with high-dose recombinant human bone morphogenetic protein-2 use in anterior cervical spine fusion. *Spine (Phila Pa. 1976)* 31, 542-547 (2006).

82. Carragee, E. J., Hurwitz, E. L. & Weiner, B. K. A critical review of recombinant human bone morphogenetic protein-2 trials in spinal surgery: emerging safety concerns and lessons learned. *The Spine Journal* 11, 471-491 (2011).

83. Argintar, E., Edwards, S. & Delahay, J. Bone morphogenetic proteins in orthopaedic trauma surgery. *Injury* 42, 730-734 (2011).

84. Mikic, B. Multiple effects of GDF-5 deficiency on skeletal tissues: implications for therapeutic bioengineering. *Ann. Biomed. Eng.* 32, 466-476 (2004).

85. Buxton, P., Edwards, C., Archer, C. W. & Francis-West, P. Growth/differentiation factor-5 (GDF-5) and skeletal development. *J. Bone Joint Surg. Am.* 83-A Suppl 1, S23-30 (2001).

86. Chhabra, A. *et al*. BMP-14 deficiency inhibits long bone fracture healing: a biochemical, histologic, and radiographic assessment. *J. Orthop. Trauma* 19, 629-634 (2005).

87. Settle Jr., S. H. *et al*. Multiple joint and skeletal patterning defects caused by single and double mutations in the mouse Gdf6 and Gdf5 genes. *Dev. Biol.* 254, 116-130 (2003).

88. Mikic, B., Ferreira, M. P., Battaglia, T. C. & Hunziker, E. B. Accelerated hypertrophic chondrocyte kinetics in GDF-7 deficient murine tibial growth plates. *Journal of Orthopaedic Research* 26, 986-990 (2008).

89. Kellum, E. *et al*. Myostatin (GDF-8) deficiency increases fracture callus size, Sox-5 expression, and callus bone volume. *Bone* 44, 17-23 (2009).

90. Hamrick, M. W. *et al*. Recombinant myostatin (GDF-8) propeptide enhances the repair and regeneration of both muscle and bone in a model of deep penetrant musculoskeletal injury. *J. Trauma* 69, 579-583 (2010).

91. Rousseau, F. *et al*. Mutations in the gene encoding fibroblast growth factor receptor-3 in achondroplasia. *Nature* 371, 252-254 (1994).

92. Ornitz, D. M. & Marie, P. J. FGF signaling pathways in endochondral and intramembranous bone development and human genetic disease. *Genes Dev.* 16, 1446-1465 (2002).

93. Du, X., Xie, Y., Xian, C. J. & Chen, L. Role of FGFs/FGFRs in skeletal development and bone regeneration. *J. Cell. Physiol.* 227, 3731-3743 (2012).

94. Minina, E., Kreschel, C., Naski, M. C., Ornitz, D. M. & Vortkamp, A. Interaction of FGF, Ihh/Pthlh, and BMP signaling integrates chondrocyte proliferation and hypertrophic differentiation. *Dev. Cell.* 3, 439-449 (2002).

95. Lazarus, J. E., Hegde, A., Andrade, A. C., Nilsson, O. & Baron, J. Fibroblast growth factor expression in the postnatal growth plate. *Bone* 40, 577-586 (2007).

96. Mancilla, E. E., De Luca, F., Uyeda, J. A., Czerwiec, F. S. & Baron, J. Effects of fibroblast growth factor-2 on longitudinal bone growth. *Endocrinology* 139, 2900-2904 (1998).

97. Ohbayashi, N. *et al*. FGF18 is required for normal cell proliferation and differentiation during osteogenesis and chondrogenesis. *Genes Dev.* 16, 870-879 (2002).

98. Parker, H. G. *et al*. An expressed fgf4 retrogene is associated with breed-defining chondrodysplasia in domestic dogs. *Science* 325, 995-998 (2009).

99. Rundle, C. H. *et al*. Expression of the fibroblast growth factor receptor genes in fracture repair. *Clin. Orthop. Relat. Res.* (403), 253-263 (2002).

100. Nakajima, A. *et al*. Spatial and temporal gene expression for fibroblast growth factor type I receptor (FGFR1) during fracture healing in the rat. *Bone* 29, 458-466 (2001).

101. Schmid, G. J., Kobayashi, C., Sandell, L. J. & Ornitz, D. M. Fibroblast growth factor expression during skeletal fracture healing in mice. *Developmental Dynamics* 238, 766-774 (2009).

102. Day, T. F. & Yang, Y. Wnt and hedgehog signaling pathways in bone development. *J. Bone Joint Surg. Am.* 90 Suppl 1, 19-24 (2008).

103. Andrade, A. C., Nilsson, O., Barnes, K. M. & Baron, J. Wnt gene expression in the post-natal growth plate: regulation with chondrocyte differentiation. *Bone* 40, 1361-1369 (2007).

104. Lee, H. H. & Behringer, R. R. Conditional expression of Wnt4 during chondrogenesis leads to dwarfism in mice. *PLoS One* 2, e450 (2007).

105. Silkstone, D., Hong, H. & Alman, B. A. Beta-catenin in the race to fracture repair: in it to Wnt. *Nat. Clin. Pract. Rheumatol.* 4, 413-419 (2008).

106. Hartmann, C. & Tabin, C. J. Dual roles of Wnt signaling during chondrogenesis in the chicken limb. *Development* 127, 3141-3159 (2000).

107. Enomoto-Iwamoto, M. *et al*. The Wnt Antagonist Frzb-1 Regulates Chondrocyte Maturation and Long Bone Development during Limb Skeletogenesis. *Dev. Biol.* 251, 142-156 (2002).

108. Yang, Y., Topol, L., Lee, H. & Wu, J. Wnt5a and Wnt5b exhibit distinct activities in coordinating chondrocyte proliferation and differentiation. *Development* 130, 1003-1015 (2003).

109. Church, V., Nohno, T., Linker, C., Marcelle, C. & Francis-West, P. Wnt regulation of chondrocyte differentiation. *Journal of Cell Science* 115, 4809-4818 (2002).

110. Hadjiargyrou, M. *et al*. Transcriptional Profiling of Bone Regeneration: INSIGHT INTO THE MOLECULAR COMPLEXITY OF WOUND REPAIR , *Journal of Biological Chemistry* 277, 30177-30182 (2002).

111. Chen, Y. *et al*. Beta-catenin signaling plays a disparate role in different phases of fracture repair: implications for therapy to improve bone healing. *PLoS Med.* 4, e249 (2007).

112. Secreto, F. J., Hoeppner, L. H. & Westendorf, J. J. Wnt signaling during fracture repair. *Curr. Osteoporos Rep.* 7, 64-69 (2009).

113. Komatsu, D. E. *et al*. Modulation of Wnt signaling influences fracture repair. *Journal of Orthopaedic Research* 28, 928-936 (2010).

114. Huang, Y. *et al*. Inhibition of ?-catenin signaling in chondrocytes induces delayed fracture healing in mice. *Journal of Orthopaedic Research* 30, 304-310 (2012).

115. Gaur, T. *et al*. Secreted frizzled related protein 1 is a target to improve fracture healing. *J. Cell. Physiol.* 220, 174-181 (2009).

116. Chang, J. *et al*. Noncanonical Wnt-4 Signaling Enhances Bone Regeneration of Mesenchymal Stem Cells in Craniofacial Defects through Activation of p38 MAPK. *Journal of Biological Chemistry* 282, 30938-30948 (2007).

117. Lango Allen, H. *et al*. Hundreds of variants clustered in genomic loci and biological pathways affect human height. *Nature* 467, 832-838 (2010).

118. Lui, J. C. *et al*. Synthesizing genome-wide association studies and expression microarray reveals novel genes that act in the human growth plate to modulate height. *Hum. Mol. Genet.* 21, 5193-5201 (2012).

119. Kember, N. & Sissons, H. Quantitative histology of the human growth plate. *Journal of Bone & Joint Surgery, British Volume* 58-B, 426-435 (1976).

120. Sutter, N. B. & Ostrander, E. A. Dog star rising: the canine genetic system. *Nat. Rev. Genet.* 5, 900-910 (2004).

121. Kilborn, S. H., Trudel, G. & Uhthoff, H. Review of growth plate closure compared with age at sexual maturity and lifespan in laboratory animals. *Contemp. Top. Lab. Anim. Sci.* 41, 21-26 (2002).

122. Tryfonidou, M. A. *et al*. Intraspecies disparity in growth rate is associated with differences in expression of local growth plate regulators. *Am. J. Physiol. Endocrinol. Metab.* 299, E1044-52 (2010).

123. Cooper, K. L. *et al*. Multiple phases of chondrocyte enlargement underlie differences in skeletal proportions. *Nature* 495, 375-378 (2013).

124. Weedon, M. N. *et al*. A common variant of HMGA2 is associated with adult and childhood height in the general population. *Nat. Genet.* 39, 1245-1250 (2007).

125. Vaysse, A. *et al*. Identification of genomic regions associated with phenotypic variation between dog breeds using selection mapping. *PLoS Genet.* 7, e1002316 (2011).

126. Boyko, A. R. *et al*. A simple genetic architecture underlies morphological variation in dogs. *PLoS Biol.* 8, e1000451 (2010).

127. Lynch, S. A. *et al*. The 12q14 microdeletion syndrome: six new cases confirming the role of HMGA2 in growth. *Eur. J. Hum. Genet.* 19, 534-539 (2011).

128. Brants, J. R. *et al*. Differential regulation of the insulin-like growth factor II mRNA-binding protein genes by architectural transcription factor HMGA2. *FEBS Lett.* 569, 277-283 (2004).

129. Weedon, M. N. *et al*. A common variant of HMGA2 is associated with adult and childhood height in the general population. *Nat. Genet.* 39, 1245-1250 (2007).

130. Millar, D. S. *et al*. Novel mutations of the growth hormone 1 (GH1) gene disclosed by modulation of the clinical selection criteria for individuals with short stature. *Hum. Mutat.* 21, 424-440 (2003).

131. Hasegawa, Y. *et al*. Identification of novel human GH-1 gene polymorphisms that are associated with growth hormone secretion and height. *J. Clin. Endocrinol. Metab.* 85, 1290-1295 (2000).

132. Van Heemst, D. *et al*. Reduced insulin/IGF-1 signalling and human longevity. *Aging Cell* 4, 79-85 (2005).

133. Vaessen, N. *et al*. A polymorphism in the gene for IGF-I: functional properties and risk for type 2 diabetes and myocardial infarction. *Diabetes* 50, 637-642 (2001).

134. Schneid, H. *et al*. Insulin-like growth factor-I gene analysis in subjects with constitutionally variant stature. *Pediatr. Res.* 27, 488-491 (1990).

135. Lettre, G., Butler, J. L., Ardlie, K. G. & Hirschhorn, J. N. Common genetic variation in eight genes of the GH/IGF1 axis does not contribute to adult height variation. *Hum. Genet.* 122, 129-139 (2007).

136. Sutter, N. B. *et al*. A single IGF1 allele is a major determinant of small size in dogs. *Science* 316, 112-115 (2007).

137. Hoopes, B. C., Rimbault, M., Liebers, D., Ostrander, E. A. & Sutter, N. B. The insulin-like growth factor 1 receptor (IGF1R) contributes to reduced size in dogs. *Mamm. Genome* 23, 780-790 (2012).

138. Binoux, M. & Gourmelen, M. Statural development parallels IGF I levels in subjects of constitutionally variant stature. *Acta Endocrinol. (Copenh)* 114, 524-530 (1987).

139. Rochiccioli, P., Messina, A., Tauber, M. T. & Enjaume, C. Correlation of the parameters of 24-hour growth hormone secretion with growth velocity in 93 children of varying height. *Horm. Res.* 31, 115-118 (1989).

140. Nap, R., Hazewinkel, H., Voorhout, G., DeBruyne, J. & Mol, J. Prepubertal differences between small- and giant-breed dogs. Clinical, biochemical and endocrine aspects. *Journal of Endocrinological Investigations* 15 (1992).

141. Favier, R. P., Mol, J. A., Kooistra, H. S. & Rijnberk, A. Large body size in the dog is associated with transient GH excess at a young age. *J. Endocrinol.* 170, 479-484 (2001).

142. Tryfonidou, M. A. *et al*. Hormonal regulation of calcium homeostasis in two breeds of dogs during growth at different rates. *Journal of Animal Science* 81, 1568-1580 (2003).

143. Eigenmann, J. E., Amador, A. & Patterson, D. F. Insulin-like growth factor I levels in proportionate dogs, chondrodystrophic dogs and in giant dogs. *Acta Endocrinol. (Copenh)* 118, 105-108 (1988).

144. Eigenmann, J. E., Patterson, D. F. & Froesch, E. R. Body size parallels insulin-like growth factor I levels but not growth hormone secretory capacity. *Acta Endocrinol. (Copenh)* 106, 448-453 (1984).

145. Costin, G., Kaufman, F. R. & Brasel, J. A. Growth hormone secretory dynamics in subjects with normal stature. *J. Pediatr.* 115, 537-544 (1989).

146. Cohen, P. *et al*. Consensus Statement on the Diagnosis and Treatment of Children with Idiopathic Short Stature: A Summary of the Growth Hormone Research Society, the Lawson Wilkins Pediatric Endocrine Society, and the European Society for Paediatric Endocrinology Workshop. *Journal of Clinical Endocrinology & Metabolism* 93, 4210-4217 (2008).

147. Tryfonidou, M. A. *et al*. Growth hormone modulates cholecalciferol metabolism with moderate effects on intestinal mineral absorption and specific effects on bone formation in growing dogs raised on balanced food. *Domest. Anim. Endocrinol.* 25, 155-174 (2003).

148. Kremer, R., Campbell, P. P., Reinhardt, T. & Gilsanz, V. Vitamin D Status and Its Relationship to Body Fat, Final Height, and Peak Bone Mass in Young Women. *Journal of Clinical Endocrinology & Metabolism* 94, 67-73 (2009).

149. Lorentzon, M., Lorentzon, R. & Nordstrom, P. Vitamin D receptor gene polymorphism is associated with birth height, growth to adolescence, and adult stature in healthy caucasian men: a cross-sectional and longitudinal study. *J. Clin. Endocrinol. Metab.* 85, 1666-1670 (2000).

150. Macgregor, S. *et al*. Vitamin D receptor gene polymorphisms have negligible effect on human height. *Twin Res. Hum. Genet.* 11, 488-494 (2008).

151. Xiong, D. H. *et al*. Vitamin D receptor gene polymorphisms are linked to and associated with adult height. *J. Med. Genet.* 42, 228-234 (2005).

152. Scillitani, A., Jang, C., Wong, B. Y., Hendy, G. N. & Cole, D. E. A functional polymorphism in the PTHR1 promoter region is associated with adult height and BMD measured at the femoral neck in a large cohort of young caucasian women. *Hum. Genet.* 119, 416-421 (2006).

153. Minagawa, M. *et al*. Association between AAAG repeat polymorphism in the P3 promoter of the human parathyroid hormone (PTH)/PTH-related peptide receptor gene and adult height, urinary pyridinoline excretion, and promoter activity. *J. Clin. Endocrinol. Metab.* 87, 1791-1796 (2002).

154. Nurminsky, D., Magee, C., Faverman, L. & Nurminskaya, M. Regulation of chondrocyte differentiation by actin-severing protein adseverin. *Dev. Biol.* 302, 427-437 (2007).

155. Tagariello, A. *et al*. Ucma — A novel secreted factor represents a highly specific marker for distal chondrocytes. *Matrix Biology* 27, 3-11 (2008).

156. Vaghjiani, R. J., Talma, S. & Murphy, C. L. Six-transmembrane epithelial antigen of the prostate (STEAP1 and STEAP2)-differentially expressed by murine and human mesenchymal stem cells. *Tissue Eng. Part A.* 15, 2073-2083 (2009).

157. Fuchshofer, R., Stephan, D. A., Russell, P. & Tamm, E. R. Gene expression profiling of TGFβ2- and/or BMP7-treated trabecular meshwork cells: Identification of Smad7 as a critical inhibitor of TGF-β2 signaling. *Exp. Eye Res.* 88, 1020-1032 (2009).

158. Steiglitz, B. M., Keene, D. R. & Greenspan, D. S. PCOLCE2 Encodes a Functional Procollagen C-Proteinase Enhancer (PCPE2) That Is a Collagen-binding Protein Differing in Distribution of Expression and Post-translational Modification from the Previously Described PCPE1. *Journal of Biological Chemistry* 277, 49820-49830 (2002).

159. Tüysüz, B. *et al*. Spondyloepimetaphyseal dysplasia Pakistani type: Expansion of the phenotype. *American Journal of Medical Genetics Part A* 161, 1300-1308 (2013).

160. Brenner, M., Laragione, T. & Gulko, P. S. Arthritis severity locus Cia4 is an early regulator of IL-6, IL-1β, and NF-κB activators' expression in pristane-induced arthritis. *Physiological Genomics* 45, 552-564 (2013).

161. Zreiqat, H., Howlett, C. R., Gronthos, S., Hume, D. & Geczy, C. L. S100A8/S100A9 and their association with cartilage and bone. *J. Mol. Histol.* 38, 381-391 (2007).

162. Tarca, A. L. *et al*. A novel signaling pathway impact analysis. *Bioinformatics* 25, 75-82 (2009).

163. Chuang, P. T. & McMahon, A. P. Vertebrate Hedgehog signalling modulated by induction of a Hedgehog-binding protein. *Nature* 397, 617-621 (1999).

164. Minguell, J. J., Erices, A. & Conget, P. Mesenchymal Stem Cells. *Experimental Biology and Medicine* 226, 507-520 (2001).

165. Beltrami, A. P. *et al*. Multipotent cells can be generated in vitro from several adult human organs (heart, liver, and bone marrow). *Blood* 110, 3438-3446 (2007).

166. Dominici, M. *et al*. Minimal criteria for defining multipotent mesenchymal stromal cells. The International Society for Cellular Therapy position statement. *Cytotherapy* 8, 315-317 (2006).

167. Meirelles, L. d. S., Chagastelles, P. C. & Nardi, N. B. Mesenchymal stem cells reside in virtually all post-natal organs and tissues. *Journal of Cell Science* 119, 2204-2213 (2006).

168. Tateishi-Yuyama, E. *et al*. Therapeutic angiogenesis for patients with limb ischaemia by autologous transplantation of bone-marrow cells: a pilot study and a randomised controlled trial. *The Lancet* 360, 427-435 (2002).

169. Assmus, B. *et al*. Transplantation of Progenitor Cells and Regeneration Enhancement in Acute Myocardial Infarction (TOPCARE-AMI). *Circulation* 106, 3009-3017 (2002).

170. Quarto, R. *et al*. Repair of Large Bone Defects with the Use of Autologous Bone Marrow Stromal Cells. *N. Engl. J. Med.* 344, 385-386 (2001).

171. KRAUS, K. H. & KIRKER-HEAD, C. Mesenchymal Stem Cells and Bone Regeneration. *Veterinary Surgery* 35, 232-242 (2006).

172. Mrugala, D. *et al*. Phenotypic and functional characterisation of ovine mesenchymal stem cells: application to a cartilage defect model. *Annals of the Rheumatic Diseases* 67, 288-295 (2008).

173. Bayati, V., Hashemitabar, M., Gazor, R., Nejatbakhsh, R. & Bijannejad, D. Expression of surface markers and myogenic potential of rat bone marrow- and adipose-derived stem cells: a comparative study. *Anat Cell Biol* 46, 113-121 (2013).

174. Monaco, E. *et al*. Morphological and transcriptomic comparison of adipose and bone marrow derived porcine stem cells. *Open Tissue Eng Regen Med J* 2, 20-33 (2009).

175. Niemeyer, P. *et al*. Comparison of mesenchymal stem cells from bone marrow and adipose tissue for bone regeneration in a critical size defect of the sheep tibia and the influence of platelet-rich plasma. *Biomaterials* 31, 3572-3579 (2010).

176. Takemitsu, H. *et al*. Comparison of bone marrow and adipose tissue-derived canine mesenchymal stem cells. *BMC Vet. Res.* 8, 150-6148-8-150 (2012).

177. Hodgkiss-Geere, H. M. *et al*. Characterisation and differentiation potential of bone marrow derived canine mesenchymal stem cells. *Vet. J.* 194, 361-368 (2012).

178. Spencer, N. D., Chun, R., Vidal, M. A., Gimble, J. M. & Lopez, M. J. In vitro expansion and differentiation of fresh and revitalized adult canine bone marrow-derived and adipose tissue-derived stromal cells. *Vet. J.* 191, 231-239 (2012).

179. Kisiel, A. H. *et al*. Isolation, characterization, and in vitro proliferation of canine mesenchymal stem cells derived from bone marrow, adipose tissue, muscle, and periosteum. *Am. J. Vet. Res.* 73, 1305-1317 (2012).

180. Csaki, C., Matis, U., Mobasheri, A., Ye, H. & Shakibaei, M. Chondrogenesis, osteogenesis and adipogenesis of canine mesenchymal stem cells: a biochemical, morphological and ultrastructural study. *Histochem. Cell Biol.* 128, 507-520 (2007).

181. Hennig, T. *et al*. Reduced chondrogenic potential of adipose tissue derived stromal cells correlates with an altered TGF? receptor and BMP profile and is overcome by BMP-6. *J. Cell. Physiol.* 211, 682-691 (2007).

182. Adamczak, M. & Wiecek, A. The Adipose Tissue as an Endocrine Organ. *Semin. Nephrol.* 33, 2-13 (2013).

183. Rosen, E. D. The transcriptional basis of adipocyte development. *Prostaglandins, Leukotrienes and Essential Fatty Acids* 73, 31-34 (2005).

184. Jundt, G., Berghauser, K. H., Termine, J. D. & Schulz, A. Osteonectin--a differentiation marker of bone cells. *Cell Tissue Res.* 248, 409-415 (1987).

185. Aubin, J. E., Liu, F., Malaval, L. & Gupta, A. K. Osteoblast and chondroblast differentiation. *Bone* 17, S77-S83 (1995).

186. Denhardt, D. T. & Guo, X. Osteopontin: a protein with diverse functions. *The FASEB Journal* 7, 1475-1482 (1993).

187. de Crombrugghe, B. *et al*. Transcriptional mechanisms of chondrocyte differentiation. *Matrix Biology* 19, 389-394 (2000).

188. Solchaga, L. A. *et al*. FGF-2 enhances the mitotic and chondrogenic potentials of human adult bone marrow-derived mesenchymal stem cells. *J. Cell. Physiol.* 203, 398-409 (2005).

189. Reich, C. M. *et al*. Isolation, culture and chondrogenic differentiation of canine adipose tissue-and bone marrow-derived mesenchymal stem cells–a comparative study. *Vet. Res. Commun.* 36, 139-148 (2012).

190. Pittenger, M. F. *et al*. Multilineage Potential of Adult Human Mesenchymal Stem Cells. *Science* 284, 143-147 (1999).

191. Andersen, C. L., Jensen, J. L. & Ørntoft, T. F. Normalization of Real-Time Quantitative Reverse Transcription-PCR Data: A Model-Based Variance Estimation Approach to Identify Genes Suited for Normalization, Applied to Bladder and Colon Cancer Data Sets. *Cancer Research* 64, 5245-5250 (2004).

192. Vandesompele, J. *et al*. Accurate normalization of real-time quantitative RT-PCR data by geometric averaging of multiple internal control genes. *Genome Biol.* 3, RESEARCH0034 (2002).

193. Sekiya, I., Larson, B. L., Vuoristo, J. T., Reger, R. L. & Prockop, D. J. Comparison of effect of BMP-2, -4, and -6 on in vitro cartilage formation of human adult stem cells from bone marrow stroma. *Cell Tissue Res.* 320, 269-276 (2005).

194. Phinney, D. G. *et al*. Donor variation in the growth properties and osteogenic potential of human marrow stromal cells. *J. Cell. Biochem.* 75, 424-436 (1999).

195. Alm, J. J., Heino, T. J., Hentunen, T. A., Vaananen, H. K. & Aro, H. T. Transient 100 nM dexamethasone treatment reduces inter- and

intraindividual variations in osteoblastic differentiation of bone marrow-derived human mesenchymal stem cells. *Tissue Eng. Part C. Methods* 18, 658-666 (2012).

196. Hanada, K., Dennis, J. E. & Caplan, A. I. Stimulatory Effects of Basic Fibroblast Growth Factor and Bone Morphogenetic Protein-2 on Osteogenic Differentiation of Rat Bone Marrow-Derived Mesenchymal Stem Cells. *Journal of Bone and Mineral Research* 12, 1606-1614 (1997).

197. van Gool, S. A. *et al*. Fetal mesenchymal stromal cells differentiating towards chondrocytes acquire a gene expression profile resembling human growth plate cartilage. *PLoS One* 7, e44561 (2012).

198. Petite, H. *et al*. Tissue-engineered bone regeneration. *Nat. Biotechnol.* 18, 959-963 (2000).

199. Jo, C. H., Yoon, P. W., Kim, H., Kang, K. S. & Yoon, K. S. Comparative evaluation of in vivo osteogenic differentiation of fetal and adult mesenchymal stem cell in rat critical-sized femoral defect model. *Cell Tissue Res.* 353, 41-52 (2013).

200. Winter, A. *et al*. Cartilage-like gene expression in differentiated human stem cell spheroids: A comparison of bone marrow?derived and adipose tissue?derived stromal cells. *Arthritis & Rheumatism* 48, 418-429 (2003).

201. Solchaga, L. A. *et al*. FGF-2 enhances the mitotic and chondrogenic potentials of human adult bone marrow-derived mesenchymal stem cells. *J. Cell. Physiol.* 203, 398-409 (2005).